

國立臺灣大學醫學院藥理學研究所

碩士論文

Graduate Institute of Pharmacology

College of Medicine

National Taiwan University

Master Thesis



治療性 H7N9 禽流感病毒人源中和抗體之製作與驗證

Generation and Characterization of
Therapeutic Human Neutralizing Antibodies
Against H7N9 Influenza Virus

陳宜蘊

Yi-Ying Chen

指導教授：曾賢忠 博士

Advisor: Shiang-Jong Tzeng, M. D., Ph. D.

中華民國 104 年 7 月

July, 2015

國立臺灣大學碩士學位論文
口試委員會審定書

治療性 H7N9 禽流感病毒人源中和抗體之製作與驗證

Generation and characterization of therapeutic human
neutralizing antibodies against H7N9 influenza virus

本論文係陳宜蓋君 (r02443014) 在國立臺灣大學醫學院藥理學研究所完成之碩士學位論文，於民國 104 年 07 月 21 日承下列考試委員審查通過及口試及格，特此證明

口試委員：

曾賢忠

(簽名)

(指導教授)

吳仁忠

王為傑

王金和

系主任、所長

林瓊瓏(簽名)

致謝

收穫滿滿的兩年碩士班研究生活即將結束，最要感謝我的指導教授-曾賢忠老師，老師是位嚴厲的好老師，當標準訂在高處時，只有不斷的逼迫自己成長。感謝老師總是能夠耐心的指導，從念書方法、閱讀文獻到上台簡報技巧，甚至做實驗的技術、思考邏輯和如何建立有系統的標準程序，且設立品管確保每個步驟的精確度。因為這樣一路上紮實的訓練，讓我能夠順利完成我的論文及學位口試。另外，要謝謝我的口試委員-中央研究院細胞與個體生物學研究所吳漢忠老師、台大微生物所王萬波老師以及台大獸醫系王金和老師，在百忙之中撥冗參加我的學位口試、修改論文，並且給我許多寶貴的意見，讓整個實驗可以變得更完善。

感謝實驗室的夥伴們-宛諭、峻霈兩年來的互相支持與幫助，這一路因為有你們一起努力，才有辦法一起順利畢業；和惠盈學姊、逸璇在實驗室的相處時光總是非常開心，也謝謝妳們的照顧；兩位未來實驗室的兩大台柱雨璇和琮智，你們為實驗室注入了青春的活力，未來的日子要好好加油。


接著，感謝我的爸媽，對於我的每個決定總是無條件支持與資助，而當我遇到挫折時，也能像朋友一般聆聽，像師長一般指點迷津；感謝我的哥哥，當我電腦壞掉時，毫不吝嗇的借我舊電腦應急；感謝冠任這兩年的持續陪伴與扶持。

此外，感謝我的好同學們，大家經歷了忘年會表演、所遊、畢旅各種美好的回憶，大小 seminar 及各種考試，一起互相加油；要特別感謝宗翰，當我被蜜蜂叮閃過人生跑馬燈時，背我去看醫生，真是我一生的恩人。還有好飯友們，華景、廷濠、姿瑜和米姊，能和你們吃飯聊天就是最好的舒壓。在藥理所的認識每個人，都有值得我學習效仿的優點，相處起來也好自在，你們絕對是我一生的朋友。

進入台大藥理所，是我一生中最正確的決定。兩年充實的學習歷程，除了藥理專業知識、實驗技術之外，也讓自己原本一根腸子通到底的思考模式有了改變，開始習慣以不同的角度、廣度和深度思考；面臨問題時，如何察覺、解決問題的方法學，更是對人生來講，受用無窮。帶著滿滿的能量，往下一個目標繼續前進！

陳宜蓋 謹至於
國立台灣大學 藥理學研究所
中華民國 104 年 7 月

中文摘要



H7N9 新型禽流感病毒在 2013 年春天自中國爆發感染人類病例，並向鄰國蔓延，包括台灣。截至 2015 年 6 月為止，總感染人數累積高達 653 人，其中 227 人死亡，死亡率為 37%。H7N9 屬於 A 型流感病毒，為 RNA 單股病毒，包含了 8 個基因，可轉譯出 11 種病毒蛋白，其中包括了表現在病毒膜上的兩種主要蛋白，即血球凝集素(hemagglutinin)以及神經氨酸酶(neuraminidase)。根據這兩種蛋白的基因序列及其抗原特型不同，可將 A 型流感病毒進一步分成兩大類，而 H7N9 病毒屬於第二群。目前對於 H7N9 的治療方式，仍是在感染初期給予神經氨酸酶抑制劑。而季節性流感疫苗所產生的中和性抗體，對於 H7N9 病毒的中和效果相當有限。此外，病人感染 H7N9 後病情惡化相當迅速，因此需要更有效率的治療方式。目前針對流感病毒最有效且最有潛力的治療方法之一便是人類治療性中和抗體，不僅可以單獨使用，亦可與神經氨酸酶抑制劑併用來達到加成性治療效果，這在感染後尚未產生 H7N9 病毒中和抗體前，尤其重要。

在 2015 年 4 月 9 日，一名感染 H7N9 之 53 歲台灣男性病患，從蘇州返回台灣之後，出現呼吸困難以及發燒的感染症狀。於 4 月 20 日到台大醫院就醫並住院接受治療之後康復出院。台大在與生物技術開發中心合作之下，我們分離此病人血液中的記憶 B 淋巴球和漿細胞，克隆它們的抗體基因和表達純化抗體。在約 80 支克隆的 H7N9 單株抗體中，有三支對於 H7N9 病毒有顯著的中和能力，且各有一支分別對 H1N1 及 H3N2 有交叉中和效果。因此，我的研究目的地是針對這三支抗體的作用和抗原決定位點鑑定做了進一步的分析，以及建立偽病毒系統進行功能性探討。我們首先克隆和表達全長以及三聚體的 H7，轉殖細胞後用流式細胞儀及免疫螢光染色來檢測抗體辨認程度。也表達和純化 H7 全長、片段和三聚體重組蛋白供酵素免疫分析法來判斷抗體對 H7 的抗原辨認位置。另外，建立抗體中和病毒類顆粒試驗，來鑑定抗體廣效中和能力，並希望能應用到動物實驗。總結，我們利用單 B 淋巴球抗體基因克隆方式成功篩選到 H7 中和抗體，可供做流感病毒治療性

中和抗體。這種方法也可應用於其他種類病毒，透過給予抗體被動免疫的方式，提高防疫效果。

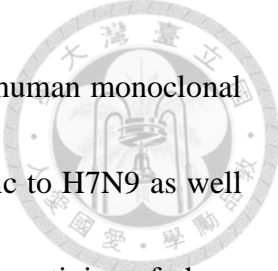


Abstract



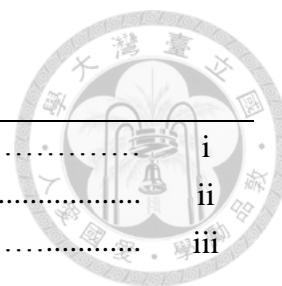
H7N9 is an emerging avian influenza A virus that can infect humans. As of June, a total of 653 human infections, resulting in 227 deaths, have occurred since March 2013.

Influenza A virus is a negative-sense, single-stranded, segmented RNA virus, of which genome encodes 11 viral proteins, including hemagglutinin (HA) and neuraminidase (NA). The influenza A viruses can be further divided into two groups based on their genetic and antigenic differences; accordingly H7N9 belongs to the group 2. As other influenza viruses current recommended anti-H7N9 therapy relies on early treatment with NA inhibitors. In spite of prior seasonal flu vaccination the neutralizing antibodies (Abs) elicited in people offer little cross-protection against H7N9. Moreover, the often fast and deleterious clinical course of patients warrants more effective therapeutics against H7N9. One potentially effective therapy is to utilize therapeutic human neutralizing Abs, which can not only synergize the efficacy of NA inhibitors but surrogate the needed humoral immunity during the window when the host has not yet developed anti-influenza neutralizing Abs. For this, in collaboration with the Development Center for Biotechnology we have generated human anti-H7N9 neutralizing Abs by single B-cell cloning of Ab genes from the circulating plasmablasts of an infected 53-year-old male. He returned from Suchow, Jiangsu Province on April 9 in 2013 and later admitted to NTUH on April 20 due to progressive dyspnea for four



days and prior fever for three days. So far we have cloned some 80 human monoclonal Abs, at least three of which showed significant neutralization specific to H7N9 as well as cross-reactive to H1N1 and H3N2 viruses, respectively. The reactivity of these neutralizing Abs was further investigated using full-length and trimeric H7-transfected cells by flow cytometry and immunofluorescence. To identify the residues where these human neutralizing Abs recognized on HA, we performed epitope mapping using the full-length and domain-specific recombinant proteins of H7 by ELISA. Moreover, we developed a WSN (A/WSN/1933) strain-based pseudovirus and reassortant assay to examine the functionality of strain-specific vs. broadly neutralizing H7 mAb using cytopathic plaque detection and reporter gene activity as readouts. Future directions include Ab engineering of H7 mAb for optimization and *in vivo* experiments for evaluation of Ab efficacy. In summary, our results demonstrate a feasible approach to develop an effective therapeutic against the emerging zoonotic influenza virus and perhaps other viruses through passive immunity.

Contents



口試委員會審定書	i
致謝	ii
中文摘要	iii
Abstract	v
List of Figures	ix
List of Tables	x
List of Abbreviations	xi
List of Appendix	xiii
<hr/>	
Chapter 1. Introduction	1
1.1 Antibody	2
1.1.1 The classes and structure of antibodies	2
1.1.2 The functions of antibodies	6
1.1.3 Monoclonal antibody-based therapeutics in the clinic	7
1.2 Influenza virus	8
1.2.1 The genome composition of influenza virus	8
1.2.2 The epidemics of influenza virus	10
1.2.3 Antiviral strategy of influenza virus by inhibition of entry	11
1.2.4 Antiviral strategy of influenza virus by inhibition of replication	12
1.2.5 Antiviral strategy of influenza virus by inhibition of releasing	13
1.2.6 The prevention of influenza virus	14
1.3 Anti-viral therapeutic neutralizing antibody	15
1.3.1 The effect of anti-viral therapeutic neutralizing antibody	15
1.3.2 The production of therapeutic neutralizing antibody against viral infection	16
1.3.3 Therapeutic neutralizing antibodies against influenza virus	18
1.4 Characterization of the H7N9 viruses	22
1.4.1 Three waves of H7N9 outbreak	22
1.4.2 Characterization of the H7N9 viruses	23
1.4.3 Clinical presentations and therapeutic effects	23
1.5 Motivation	25
<hr/>	
Chapter 2. Materials and Methods	27
2.1 Reagents and antibodies	28



2.2 Viruses and cells.....	28
2.2.1 HEK293T cells.....	28
2.2.2 A549 cells.....	29
2.2.3 MDCK cells.....	29
2.2.4 WSN-based reassortant influenza virus.....	29
2.3 Lymphocyte sorting from peripheral blood of the NTUH H7N9 patient.....	30
2.4 Single B-cell RT-PCR cloning of Ig genes.....	30
2.5 Construction of plasmids.....	31
2.5.1 pSecTag2-H1, H3, H5, H7 constructs.....	31
2.5.2 pFlu-HA-KpnI-XhoI.....	32
2.6 Cell transfection.....	32
2.7 Western Blot.....	33
2.8 ELISA.....	34
2.9 Antibody staining and flow cytometric analysis.....	35
2.10 Immunofluorescence staining.....	36
2.11 Plaque assay.....	36
Chapter 3. Results.....	38
3.1 Cloning of H7N9 neutralizing antibody genes from the patient's plasmablasts.....	39
3.2 H7N9 neutralizing mAbs were able to bind to H7 on HEK293T and A549 cells transfected with monomeric H7.....	39
3.3 Expression of trimeric H7 hemagglutinin in HEK293T cells and A549 cells respectively for binding assays of human anti-H7 monoclonal antibodies.....	41
3.4 Conversion of the whole IgG1 human anti-H7 monoclonal antibody to scFv-Fc format.....	42
3.5 H7 domain-specific constructs for epitope mapping.....	43
3.6 Generation of equivalent HA domain constructs of other subtypes.....	45
3.7 Generation of WSN-based reassortant influenza viruses.....	46
Chapter 4. Discussions.....	49
Figures.....	61
Appendix.....	86
References.....	109



List of Figures

Figure 1. Sorting memory B cells and plasmablasts from the H7N9 patient's blood for single B-cell expression cloning of its antibody gene	62
Figure 2. A representation of three human anti-H7 mAbs that were able to bind H7 on HEK293T cells transfected with full-length H7	64
Figure 3. The P3C1 clone of human anti-H7 mAb was able to bind to surface H7 on A549 cells transfected with the full-length H7 cDNA	66
Figure 4. Anti-H7 mAbs were able to bind to H7 trimers expressed on HEK 293T cells.....	68
Figure 5. Human anti-H7 mAbs were able to bind to trimeric H7 proteins expressed on A549 cells	70
Figure 6. Development and characterization of scFv-Fc anti-H7 monoclonal antibodies.....	72
Figure 7. Generation of domain-specific of H7 recombinant proteins for epitope mapping.....	74
Figure 8. Generation of full-length and domain-specific H1 recombinant proteins for epitope mapping.....	78
Figure 9. Generation of full-length and domain-specific H3 recombinant proteins for epitope mapping.....	80
Figure10. Generation of full-length and domain-specific H5 recombinant proteins for epitope mapping.....	82
Figure11. Plaque reduction assay of WSN-based reassortant influenza virus.....	84

List of Tables



Table 1.	Properties of recombinant multimeric antibodies	4
Table 2.	Broadly neutralizing antibodies	20
Table 3.	Primers for cloning	108

List of Abbreviations



ADCC	Antibody-dependent cell-mediated cytotoxicity
Ab	Antibody
Ag	Antigen
AID	Activation-induced cytidine deaminase
CDR	Complementarity determining region
CMC	Complement-mediated cytotoxicity
EBV	Epstein–Barr virus
Fab	Fragment antigen-binding
Fc	Fragment crystalline
Fc γ R	Fc gamma receptor
FcRn	Neonatal Fc receptor
HA	Hemagglutinin
HI	Inhibition of hemagglutination
HPAI	Highly pathogenic avian influenza
Ig	Immunoglobulin
IVA	Influenza virus A
ITAM	Immunoreceptor tyrosine-based activation motifs

IIV	Inactivated influenza vaccine
LAIV	Live attenuated influenza vaccines
LPAI	Low pathogenic avian influenza
mAb	Monoclonal antibody
NA	Neuraminidase
NP	Nucleoprotein
NS1, NS2	Non-structural protein 1 and 2
RdRp	RNA-dependent RNA polymerase
RPV	Recombinant protein vaccines
scFv	Single-chain fragment variable
SHM	Somatic hypermutation
TRIM21	Tripartite motif-containing 21
vRNPs	Viral ribonucleoprotein complexes



List of Appendix



Appendix 1.	pSecTag2A-H7-1	87
Appendix 2.	pSecTag2A-H7-2	88
Appendix 3.	pSecTag2A-H7-3	89
Appendix 4.	pSecTag2A-H7-4	90
Appendix 5.	pSecTag2A-H7-5	91
Appendix 6.	pSecTag2A-H7-6.....	92
Appendix 7.	pcDNA3.1-H7-Foldon	93
Appendix 8.	pSecTag2A-3H	94
Appendix 9.	pSecTag2A-H1-1.....	95
Appendix 10.	pSecTag2A-H1-2	96
Appendix 11.	pSecTag2A-H1-3	97
Appendix 12.	pSecTag2A-H3-1.....	98
Appendix 13.	pSecTag2A-H3-2	99
Appendix 14.	pSecTag2A-H3-3	100
Appendix 15.	pSecTag2A-H5-1	101
Appendix 16.	pSecTag2A-H5-2	102
Appendix 17.	pSecTag2A-H5-3	103
Appendix 18.	pFISE-hIgG1-Fc2-HNP4 A4.....	104
Appendix 19.	pFISE-hIgG1-Fc2-HNP4 C3	105
Appendix 20.	pFISE-hIgG1-Fc2-HNP4 H3	106
Appendix 21.	pFlu BsmBI HA-KpnI XhoI M	107



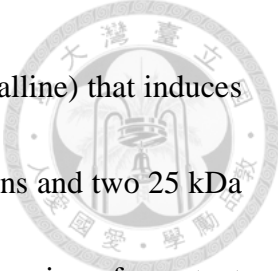
Chapter 1. Introduction



1.1 Antibody

1.1.1 The classes and structure of antibodies

There are five major classes of immunoglobulin (Ig) which are pentamer immunoglobulin M (IgM), dimer immunoglobulin A (IgA) and monomer immunoglobulin E (IgE), immunoglobulin D (IgD), immunoglobulin G (IgG). Among all Igs, IgG is most abundant and it can be further classified into four isotypes IgG1, IgG2, IgG3, and IgG4 in humans. The Fc domain of IgG interacts with Fc γ receptors on immune effector cells. IgG isoforms can exert different levels of effector functions with the increase in the order of IgG4<IgG2<IgG1 \leq IgG3. There are several subtypes of human IgG receptor family, including activating Fc γ RI, Fc γ RIIa, Fc γ RIIIa, Fc γ RIIIb and inhibitory Fc γ RIIb, all of which are distinct from their affinities for the IgG subclasses. FcRn (neonatal Fc receptor) is also an Fc receptor for IgG, but it is predominantly expressed in epithelial tissues, e.g. trophoblasts and intestinal epithelium. FcRn is known to be able to prevent IgG from intracellular catabolic degradation and improve the half-life of Abs in serum through pinocytosis, which depends on the physiological pH for ligand dissociation while acidic pH for IgG association with receptor (Roopenian and Akilesh, 2007). As for the aspect of structure, IgG can be divided into two regions: the Fab (fragment-antigen binding) that contains the variable



domain responsible for the Ab specificity, and the Fc (fragment crystalline) that induces immune response. In addition, they consist of two 50 kDa heavy chains and two 25 kDa light chains. There are one domain of variable region and three domains of constant region in a heavy chain. The two heavy chains are linked to each other with disulfide bonds termed as the hinge region. Each heavy chain is linked to a light chain comprising one domain of variable region and constant region by a disulfide bond. A heavy chain encoded by V, D, J gene and a light chain encoded by V, J gene contain three respective complementarity determining regions (CDRs) that determines the final antigen-binding site known as the epitope. There are two types of light chain, lambda (λ) and kappa (κ), found in antibodies with no functional difference (Kenneth, 2011).

Due to the advanced recombinant technology, there are a variety of novel mAb formats that have improved the affinity, avidity, tissue penetration, and tissue half-life of Abs. The engineered Abs can generally be separated into two types, orthodox (IgG-like structures) and heterodox (non-IgG-like structures). Some antibodies are developed to contain multiple binding sites, allowing improved avidity (**Table 1**) (Cuesta *et al.*, 2010).

Table1. Properties of recombinant multimeric antibodies (Cuesta *et al.*, 2010)

Antibody	Molecular weight (kDa)	Antibody Format	Associated Functional effect	Serum stability	Ref.
Monovalent					
V _{HH}	10~15	-	-	-	1
scFv	30	-	-	-	2
scFab	50	-	-	-	3
Bivalent					
Diabody	55	heterodox	-	+/-	4
Single-chain(sc)-diabody	55	heterodox	-	+	5
(scFv) ₂	55	heterodox	-	+	6
Miniantibody	64	heterodox	-	+/-	7
Minibody	80	orthodox	-	+	8
Barnase-barstar	85	heterodox	+	+	9
scFv-Fc	100-105	orthodox	+	+	10
sc(Fab') ₂	110	heterodox	-	+/-	11
Trivalent					
Triabody	80	orthodox	-	+	12
Trimerbody	110	heterodox	-	NP	13
Tribody	115	heterodox	-	+	14
Collabody	125	heterodox	-	+	15
Barnase-barstar	130	heterodox	+	+	9
(scFv-TNF α) ₃	150	heterodox	+++	+	16
(Fab) ₃ /DNL	160	heterodox	-	+	17

- **Parameter:** high (+++); intermediate (++); low (+); negative (-); inconclusive (+/-)
- **Antibody Format:** orthodox (IgG-like) or heterodox (non-IgG-like)
- **Associated Functional effects:** Functionality derived from structural components.
- **Serum stability:** Protein integrity following incubation in serum.
- **Abbreviation:** NP, not published.
- **Ref :**
 1. (Harmsen and De Haard, 2007)
 2. (Sanz *et al.*, 2004)
 3. (Hust *et al.*, 2007)
 4. (Holliger *et al.*, 1993)

5. (Kipriyanov *et al.*, 1999)
6. (Kontermann, 2005)
7. (Huhlov and Chester, 2004)
8. (Hu *et al.*, 1996)
9. (Deyev *et al.*, 2003)
10. (Li *et al.*, 2000)
11. (Tahtis *et al.*, 2001)
12. (Dolezal *et al.*, 2000)
13. (Cuesta *et al.*, 2009)
14. (Schoonjans *et al.*, 2000)
15. (Fan *et al.*, 2008)
16. (Bauer *et al.*, 2006)
17. (Goldenberg *et al.*, 2008)





1.1.2 The functions of antibodies

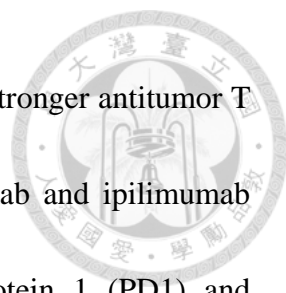
Abs are secreted by the B lymphocytes, possessing a wide range of effector functions in immune system. First, Abs can cross-react with receptors inducing the agonistic or antagonistic effects through natural ligand mimicry or allosteric modulation (Chodorge *et al.*, 2012). Second, Abs bind to pathogens and thereby block their access to cells known as neutralization, which is important for protection against viruses from entering cells and replicating, and against bacterial toxins. Third, antigens (Ags) on the surface of pathogens can be recognized by Abs whose Fc region binds to the receptor of macrophages and neutrophils leading to Ab-dependent cell phagocytosis. The Abs-coating-pathogens and foreign particles in this way is known as opsonization. Fourth, the Abs activate the complement system comprising classical, alternative, and lectin three pathways that converge at the activation of the C3 and C5 convertase forming the membrane attack complex to kill the pathogen by complement-mediated cytotoxicity (CMC). Fifth, immune effector cell that express immunoreceptor tyrosine-based activation motifs (ITAMs) such as natural killer cells, monocytes, macrophages or granulocytes that have activating Fc γ RIII receptors on their surface bind to pathogen or infected cell coated with Abs and eliminate them rapidly through the perforin and granzymes secretion in Ab-dependent cell-mediated cytotoxicity (ADCC). Sixth, Abs can cause receptor internalization altering Ag density on the cell

surface (Kenneth, 2011).



1.1.3 Monoclonal antibody-based therapeutics in the clinic

The natural human Ab response is a self-tolerant therapeutic reagent with highly recognizing specificity and widely used in the treatment of a variety of human diseases, including cancer, autoimmune disease and pathogenic infection. To target the cancer cells, there are several monoclonal Ab-based therapeutic strategies, resulting in cancer cell death. In general, direct effects of the Ab execute blockade of agonistic receptor activity, induction of apoptosis, or delivery of a drug or cytotoxic agent to kill tumor cells. Cetuximab that is an EGFR mAb used for the treatment of metastatic colorectal cancers, metastatic non-small cell lung cancers and head and neck cancers that carry wild-type EGFR (van Cutsem *et al.*, 2009). Trastuzumab targets HER2/neu receptor to trigger ADCC for the treatment of certain breast cancers. Both of them are examples of the effect abrogating of tumor cell signaling (Hudis, 2007). Bevacizumab is classified as a mAb and anti-angiogenesis drug. It is designed to block VEGF-A to interrupt the activation of VEGF receptor to deprive a growing tumor of nutrients and oxygen provided by the new blood vessels growing in the tumor (Lima *et al.*, 2011). For mAbs that require immune cells to act, target ablation of cancer cells can be achieved by induction of phagocytosis, complement activation and ADCC. For example, all three effects are achieved by rituximab, a mAb specific for CD20, which is widely expressed

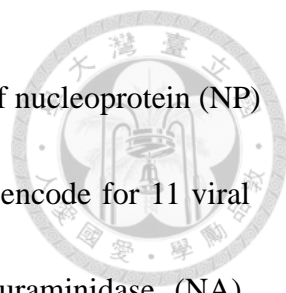


on B-cell lymphoma and leukemia (Braster *et al.*, 2014). To obtain stronger antitumor T cell response, immune checkpoint blockade Abs, such as nivolumab and ipilimumab that inhibit the inhibitory receptors, programmed cell death protein 1 (PD1) and cytotoxic T lymphocyte-associated antigen 4 (CTLA4), respectively can efficiently prevent T cells from exhaustion and rejuvenate tumor-specific T cells (Brahmer *et al.*, 2012; Hodi *et al.*, 2010). In addition, Abs that recognize cancer cells with one variable chain while the other one bind to the activating receptors on immune effector cells are known as bispecific mAbs, which are emerging popular Ab drugs. For instance, blinatumomab (AMG103), a bi-specific T-cell engager (BiTE), specifically re-direct T cells to target the CD19 antigen expressing on B cells for the treatment of acute lymphoblastic leukemia (ALL) (Topp *et al.*, 2015). Recently, chimeric antigen receptor (CAR) T cells, which are genetically modified to target cancer cells expressing a specific antigen, through the variable regions of mAb linked to a T cell-activating motif, have shown significant, promising therapeutic efficacy (Barrett *et al.*, 2014)

1.2 Influenza virus

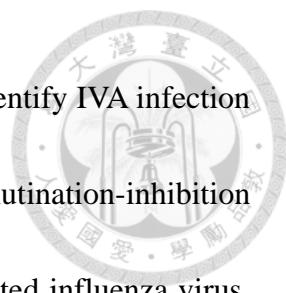
1.2.1 The genome composition of influenza virus

The influenza virus belongs to the family of *Orthomyxoviridae*. It is an enveloped virus containing eight negative-sense, single-stranded RNA. There are three types of



influenza viruses: A, B and C on the basis of their internal proteins of nucleoprotein (NP) and matrix (M) protein. The eight segments of influenza A viruses encode for 11 viral genes, including three surface protein: hemagglutinin (HA), neuraminidase (NA), matrix 2 (M2) ion channel, whereas the M1 molecules (M) keep viral ribonucleoprotein complexes (vRNPs) attached to the inner layer of envelope; nucleoprotein (NP); non-structural protein (NS1, NS2: also known as nuclear export protein, NEP); the three subunits (PB1, PB2, and PA) of the RNA polymerase complex coated with nucleoproteins (NPs) to form the vRNPs (Bogusław *et al.*, 2014). All the genomes of influenza virus perform high frequency of point mutations because the RNA polymerase of influenza viruses lacks the ability of exonuclease to proofreading the mismatched 3' nucleotides resulting in antigen drift. In addition, they undergo gene segment reassortments resulting in antigenic shift. Notably, influenza virus exploits antigen drift and antigen shift to gain evolutionary advantages during hypermutation and gene exchange (Domingo and Holland, 1997). Influenza A virus is sub-classified into several subtypes by two surface proteins, the virus-entry-related hemagglutinin (HA), which binds to sialic acid receptors of host cells and the virus-releasing-related NA that cleaves off sialic acid from glycans on the host cell surface.

The classification of influenza A viruses is based on serology-based assays, such as hemagglutination inhibition (Francis *et al.*, 1944) and microneutralization (Rowe *et al.*,

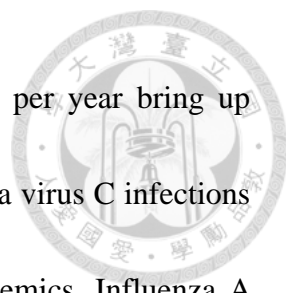


1999), both of which are classical laboratory experiments used to identify IVA infection through the detection of IVA-specific antibodies in serum. Hemagglutination-inhibition (HI) assay are used to identify the HA subtype of an unknown isolated influenza virus. Based on the ability of the viral HA protein binding to and agglutinating red blood cells (RBCs) from different species, a positive hemagglutination assay indicates that the viral HA protein were not neutralized by specific subtype HA Abs forming agglutination and showing a cloudy appearance, whereas a negative result shows a point of cells at the bottom of plate. Another method of specific IVA identification by RT-PCR and sequence analysis is more reliable (Fouchier *et al.*, 2000).

There are 18 HA subtypes and 11 NA subtypes that have been identified as a result of antigen shift. Among these, H17N10 and H18N11 had been isolated from bats recently. On the basis of their primary sequences, these HA molecules can be divided into two groups: group 1 (H1, H2, H5, H6, H8, H9, H11, H12, H13, H16, H17, and H18) and group 2 (H3, H4, H7, H10, H14, and H15). All the known NA molecule can also be grouped into two groups: group 1 (N1, N4, N5, N8) and group 2 (N2, N3, N6, N7, N9). The bat-derived N10 and N11 belonging to neither group1 nor group2 were proposed to be influenza A-like group 3 (Wu *et al.*, 2014)

1.2.2 The epidemics of influenza virus


Influenza virus type A and B causing seasonal epidemics estimated to cause 2 to 5



million cases of severe illness and up to 250,000–500,000 deaths per year bring up pandemics at irregular intervals all over the world, whereas influenza virus C infections leading to a slight respiratory disease have less risk to cause epidemics. Influenza A viruses can be further divided into different subtypes due to reassorted combination from the animal reservoir. Current subtypes of influenza A viruses found in people are H1N1, H3N2 viruses and the highly pathogenic avian influenza (HPAI) infections with H5N1 and the recent H7N9 in 2013. However, Influenza B viruses are not partitioned into subtypes, but able to be further subdivided into lineages and strains. There are two currently circulating influenza B virus lineages: B/Yamagata and B/Victoria (Kanegae *et al.*, 1990).

1.2.3 Antiviral strategy of influenza virus by inhibition of entry

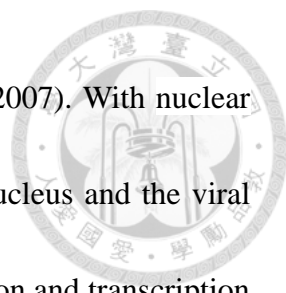
According to the steps of influenza virus replication cycle, there are several antiviral strategies that can be categorized to inhibit the virus infection. Infection can be inhibited either by blocking the binding to cellular receptors or interfering with the fusion machinery between influenza virus and host cell. The first step of influenza virus infection is that HA, in trimeric form, binds to sialic acid receptors on the surface of target cells. Influenza viruses primarily bind to $\alpha 2, 3$ -linked sialic acid receptors of avian and to $\alpha 2, 6$ -linked sialic acid receptors of human (Rogers *et al.*, 1983). Once the receptors are endocytosed into endosomes where a low pH-induced conformational



change occurs, rendering hemagglutinin (HA0) becomes sensitive to trypsin-like protease to be digested into the receptor-binding-related HA1 and the membrane-fusion-related HA2. The HA1 contains a globular head domain, which is variable owing to evolving with a high mutation rate. The HA2 domain comprises mostly the conserved stalk region is otherwise much more conserved. The trimeric HA stalk domain undergoes a conformational change to fuse with the endosomal membrane of infected cells, leading to membrane fusion and endocytosis. To inhibit virus entry, there are at least two pharmacological inhibitors to disrupt virus attachment and to block protease activity. Attachment inhibitors include mAbs against the globular head or stalk domain of HA as well as compounds that block either HA or sialic acid receptors. Atropnin is a protease inhibitor that can prevent the cleavage of HA for activation and this is one of the host-targeted antiviral strategies (Zhirnov *et al.*, 2011).

1.2.4 Antiviral strategy of influenza virus by inhibition of replication

After entry, the second step of virus infection is that M2 ion channel opens and creates a proton flow from the endosome into the virion leading to the vRNPs dissociated from M1 matrix and to the virus uncoating in the acidification endosome. Differ from most RNA viruses replicating in the cytoplasm, influenza virus is one of the very few RNA viruses replicating in the nucleus. The reasons are that the mRNA of two IVA gene, M and NS, are required of being splicing and translating into M1 matrix and



M2 ion channel, NS1 and NS2 protein, respectively (Boulo *et al.*, 2007). With nuclear localization signals (NLSs), the vRNPs of IVA transport into the nucleus and the viral RNA-dependent RNA polymerase (RdRP) initiates genome replication and transcription into mRNAs that are then transported to the cytoplasm. The polymerase of the host cells further translates the spliced mRNA into viral proteins for viral replication. On the other hand, the nuclear export protein, NEP (a.k.a. NP), is responsible for the exportation of the newly synthesized viral genome. Therefore, at this step M2 ion channel inhibitors, RNA-dependent RNA polymerase (RdRP) inhibitors and NP inhibitors are options to disturb the replication of influenza virus (Loregian *et al.*, 2014). Inhibitors of inosine 5'-monophosphate (IMP) dehydrogenase or viral RNA polymerase can also block the process of virus replication.

1.2.5 Antiviral strategy of influenza virus by inhibition of releasing

After viral replication, the final step of virus infection is that the newly synthesized viral genome and proteins package together in the cytoplasm. The packaged virus will bud out of the membrane with the aid of NA to cleave the binding between the sialic acid and HA allowing the virus to leave the host cell. Zanamivir and oseltamivir are NA inhibitors that block influenza virus replication by restraining the release of the newly formed viruses at the final step.



1.2.6 The prevention of influenza virus

World Health Organization (WHO) recommends that vaccination is the most effective way to protect the public from influenza virus infection and needs to be updated annually. To date, there are three types of influenza vaccines are licensed by the Food and Drug Administration (FDA) and two of them are produced by egg-based production system. One is the intramuscular inactivated influenza vaccine (IIV), which is chemically inactivated by formaldehyde or β -propiolactone, and the viral envelope is destroyed with detergents. The other one is intranasal live attenuated influenza vaccines (LAIV) produced through genetic reassortment between the HA and NA from currently epidemic strain of influenza virus and attenuated donor virus with remaining internal segments. It takes six to eight months for egg-based production system to manufacture these vaccines, thereby decreasing the protection efficiency. Instead of egg-based production processes, recombinant protein vaccines (RIV) were generated by cell-based production technology in a shorter amount of time without involving eggs or any infectious virus during the process. The advantage of not using eggs for vaccine production is the avoidance of egg components that might induce allergic reactions. In 2007, the European Union approved Optaflu, a vaccine produced by Novartis using a mammalian cell line. In 2013, the recombinant HA vaccine (Flublok) manufactured in insect cells by Protein Sciences was also licensed in the United States (Krammer and

Palese, 2015).




1.3 Anti-viral therapeutic neutralizing antibody

1.3.1 The effect of anti-viral therapeutic neutralizing antibody

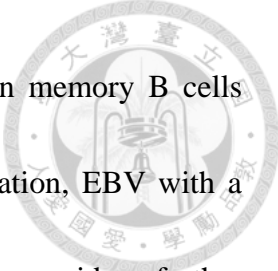
The neutralization toward virus by Abs contributes three effects to restrict the infectivity. Generally, neutralizing Abs bind to viral glycoproteins that mediate the fusion of the viral and host membranes of enveloped viruses or to the protein shell of non-enveloped virus that penetrates into host cytoplasm. The Ag-binding phenomenon causes the envelope glycoprotein to lose function, thereby protecting host cells from viral infectivity (Klasse and Sattentau, 2002). Additionally, the antigenic recognition also activates effector cells, which can contribute to viral clearance through complement-dependent virolysis or phagocytosis (Burton, 2002). Moreover, when Ab-coated-viruses get into the cytoplasm, Abs may also neutralize infectivity through a intracellular cytosolic protein called tripartite motif-containing 21 (TRIM21), which is a high-affinity and specific intracellular IgG receptor and is able to engage with a proteasome mechanism for targeting virus for ubiquitin-dependent degradation. The processed Ags are further presented to CD4 and CD8 T cells through MHCI/MHCII leading to elicitation of the adaptive immune response (Mallery *et al.*, 2010).

1.3.2 The production of therapeutic neutralizing antibody against viral infection




Human mAbs also have been developed to serve as potent therapeutic tools against a range of viral infection such as influenza virus and HIV. It is crucial to choose the potential case with a wider breadth or higher potency of serum neutralizing ability such as HIV long-term non-progressors, influenza pandemic survivors, currently or recently infected individuals, vaccinated individuals to enhance the chances of cloning human mAbs with both potent and broad reactivity against particular virus or pathogen. Generally speaking, three different strategies have been used to generate the therapeutic neutralizing mAbs. First, panning of phage display libraries, which was the most classical method constructed from random variable gene immunized or infected individuals and has been used widely to identify and clone single-chain variable antibody fragments (scFvs) mAbs with high affinities. This approach is considered as a high-throughput way to search for Abs produced by B cells responding to a specific pathogen. For example, it has been useful in obtaining neutralizing Abs specific for West Nile virus, rabies virus, severe acute respiratory syndrome (SARS) virus, hepatitis A virus, HIV, Ebola virus, hepatitis C virus, measles virus and human and avian influenza virus strains (Marasco and Sui, 2007).

The second approach is B cell immortalization. The hybridoma technology is inefficient in human B cell compared with mouse B cell. Alternatively, Epstein–Barr



virus (EBV)-mediated transformation is used to immortalize human memory B cells from the recovered, infected patients. In the process of immortalization, EBV with a TLR9 ligand and/or allogeneic irradiated mononuclear cells provides further co-stimulatory signals to facilitate B cells to differentiate and secrete Abs. After 7 to 14 days of incubation, the Ag binding affinity and/or viral neutralization are tested from the Ab-secreted supernatants. The Ab-secreting cells of interest are limiting diluted to the single-cell level and further screened for the ideal reactivity (Traggiai *et al.*, 2004). To stably produce high quality and quantity of Abs, EBV-transformed B cell clones are further fused with myeloma cells to generate hybridomas (Smith *et al.*, 2012). Nonetheless, there is another approach used to immortalize B cells by genetic programming. Transducing memory B cells obtained from peripheral blood with anti-apoptotic factors B cell lymphoma 6 (BCL-6) and BCL-xL as well as culturing with interleukin-21 (IL-21) and CD40 ligand stimulates the transduced B cells to differentiate into long-lived Ab-secreting cells. In the presence of activation-induced cytidine deaminase (AID), the B cells undergo V(D)J recombination and increase the repertoire of Abs (Kwakkenbos *et al.*, 2010).

The third approach is single B cell RT-PCR cloning. The Ag-specific B cells from the immunized or infected subjects are sorted with the surface markers of the Ab-secreting cell such as CD19, CD27 and CD38 and with the fluorescently labelled



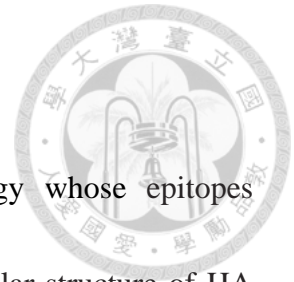
Ags by flow cytometry into a single cell per well in plates. Single B-cell reverse transcription PCR from extracted RNA of sorted Ab-secreting cells allows cloning of the Ig heavy and light chains of the variable gene. These genes could further be cloned into vectors containing constant region gene of Ig and expressed in eukaryotic cell lines for the mAb production, purification and assay for binding and neutralization (Smith *et al.*, 2009).

1.3.3 Therapeutic neutralizing antibodies against influenza virus

There are three glycoproteins expressed on the surface of influenza virus including HA, NA and M2 ion channel, which are considered as the potent targets of therapeutic neutralizing Ab against influenza virus. Abs specific to surface NA prevent the release of new-synthesized influenza virions from the infected cell surface, whereas Abs binding to M2 ion channel prevent the release of viral genome into the cytosol. In addition, Abs against HA will inhibit the viral entrance through sialic acid of host cells to reach the neutralizing effect. More specifically, when targeted the globular head domain of HA glycoprotein, the Abs block the binding of virus to sialic acid and protect the host cells from infections. Abs specific for globular head domains are known as subtype-specific Abs due to the extensive variable characteristic of this domain among different subtypes. While binding to the group-conserved stalk domain, the Abs named as group-specific antibodies inhibit its low-pH triggered fusion between viral envelope

and membrane of host cells. (Subbarao and Joseph, 2007)

Broadly neutralizing antibody is a new therapeutic strategy whose epitopes recognize conserved domain on certain subtypes, groups or particular structure of HA and provides cross-subtypes protection (**Table 2**).



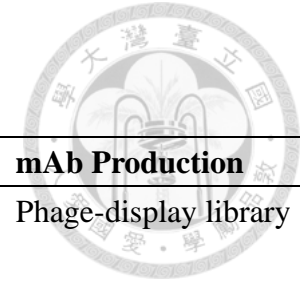
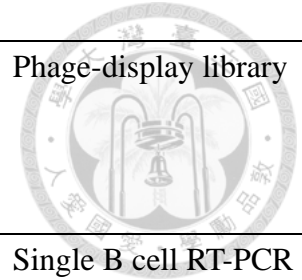


Table2. Broadly neutralizing antibody

Monoclonal Antibody	Group	Epitope	mAb Production
A06 (Kashyap <i>et al.</i> , 2010)	1 (H1, H5)	Stalk domain HA2: V18, D19, G20, W21, S40, T41, Q42, N43, A44, I45, D46, E47, I48, 49T, N50, K51, V52, N53, S54, V55, I56 (H1 numbering)	Phage-display library
C05 (Ekiert <i>et al.</i> , 2012)	1&2 (H1, H2, H3, H9, H12)	Globular head domain Y98, T131, N133, G134, T135, S136, S137, N145, W153, T155, K156, A189, E190, T192, S193, L194, Q226 (H1 numbering)	Phage-display library
CR6261 (Ekiert <i>et al.</i> , 2009)	1 (H1, H2, H5, H6, H8, H9, H11, H13, H16)	The interface of HA1 and HA2 H25, H45, V46, N47, L496, S306, L307, P308, T333, D363, G364, W365, Q382, T385, Q386, I389, D390, T393, V396, N397, I400 (H1 numbering)	Phage-display library
CR8020 (Ekiert <i>et al.</i> , 2011)	2 (H3, H4, H7, H10, H14, H15)	The base of the Stalk domain E341, E360, G361, I363, D364, R370, E375, T377, G378, Q379, A380, A381, L383, N491, E495 (H3 numbering)	Single B cell RT-PCR cloning
CR8043 (Friesen <i>et al.</i> , 2014)	2 (H3, H10)	The base of the Stalk domain P37, E341, K342, E360, G361, I363, D364, R370, T377, Q379, L383 (H3 numbering)	B cell immortalization
CR9114 (Dreyfus <i>et al.</i> , 2012)	1&2&B (H1, H3, H5, H7, H9)	Stalk domain HA1: H38, Q40, D41, I42, S291, M292, P293; HA2: V18, D19, G20, W21, A36, K38, T41, Q42, I45, D46, V48, T49, V52, I56 (H5 numbering)	Phage-display library

F10 (Sui <i>et al.</i> , 2009)	1 (H1, H2, H5, H6, H8,H9, H11, H13, H16)	The interface of HA1 and HA2 A: H24, H44, Q46, S304, M305; B: V364, D365, G366, W367, K384, T387, Q388, I391, T395, V398, N399, I402 (H5 numbering)	Phage-display library
FI6v3 (Corti <i>et al.</i> , 2011)	1&2 (H1, H2, H5, H6, H8, H9, H13, H3, H4, H7, H10)	A shallow groove on the F subdomain of the HA trimer HA1: N38, C277, I278, T318; HA2: I18, D19, G20, W21, L38, K39, T41, Q42, A43, I45, D46, I48, N49, N53, I56, E57 (H5 numbering)	Single B cell RT-PCR cloning

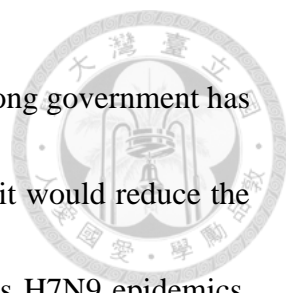




1.4 Characterization of the H7N9 viruses

1.4.1 Three waves of H7N9 outbreak

In March 2013, the first outbreak of a novel low pathogenic avian influenza (LPAI) A virus, H7N9 whose natural hosts are still under debate emerged in Eastern China. A first human case of H7N9 virus infection crossed the species barrier was reported in Shanghai through the exposure to infected poultry and caused the infected patient severe lower respiratory tract disease and fatal complications (Gao *et al.*, 2013). There were 133 H7N9-confirmed cases, including 45 deceases centralized in the Eastern Chinese provinces of Shanghai, Zhejiang, and Jiangsu during the first wave of H7N9 started from March to May 2013 (Li *et al.*, 2014). While the H7N9 virus continued reassortment in the avian species, the pathogenicity and the ability for human-to-human transmission of H7N9 virus were gaining strength (Mok *et al.*, 2014). Several months later the H7N9 induced the second wave of human infection that brings about 266 cases during 2013 to 2014 winter season with a geographic spread to the Southern Chinese province (Lu *et al.*, 2014). Following this, the Guangdong province had the largest amount of infected cases during the third wave infection of this year due to the business of poultry industry with Eastern China Province. Until June 2015, the total laboratory-identified cases of human infection with H7N9 virus are 653 and results in




227 deaths since February 2013 (Millman *et al.*, 2015). The Guangdong government has made a restriction of live poultry merchandising with the hope that it would reduce the zoonotic transmission. There seems a tendency of these three waves H7N9 epidemics, that is the virus is spreading southward and likely to recur in cooler seasons from winter to spring of next year (Liu *et al.*, 2015).

1.4.2 Characterization of the H7N9 viruses

The whole genomic virus genes isolated from the first three H7N9 virus infected cases in China were shown that the three viruses had greatest feature with genes of avian influenza viruses that circulated in China (Shi *et al.*, 2013). The HA genes originated from LPIA H7N3 avian viruses have been detected recently in poultry isolated in 2011 in Zhejiang province. The NA genes belongs to N9 NA genes from viruses circulating recently in domestic ducks in LPIA H11N9 viruses isolated in 2010 in the Czech Republic with a distinct 15 nucleotide deletion (amino acids 69-73) at the position 215. The remaining six viral genes (PB2, PB1, PA, NP, M and NS) are closely related to H9N2 poultry viruses that have been in circulation in China since 1994 (Kageyama *et al.*, 2013).

1.4.3 Clinical presentations and therapeutic effects

The most common symptoms of patients, who infected H7N9, were typical acute respiratory infection, such as fever, cough, and shortness of breath. Following by



rapidly developing severe pneumonia, many patients suffered from fatal complications, including acute respiratory distress syndrome, septic shock and multi-organ failure, demand intensive nursing care and mechanical ventilation equipment. For the anti-viral treatments, the H7N9 virus was resistant to M2 protein inhibitors, amantadine and rimantadine, due to the S31N mutation, which interrupts drug binding to the lipid-facing pocket in transmembrane region allosterically (Pielak *et al.*, 2009). It was found that NA inhibitors, oseltamovir and zanamivir, are sensitive against A/Anhui/1/2013 virus infection in reducing severe illness and deaths when they were given in the early stage of virus infection (Yen *et al.*, 2014). However, A/Shanghai/1/2013 virus revealed a polymorphism of NA genes encoding N9-294R or -294K, indicating that oseltamivir-therapeutic effect might be compromised through interfering with the binding of oseltamivir carboxylate (Wu *et al.*, 2013). For the prevention, it is necessary to develop the vaccine, which is a key defensive means against pandemics. Recombinant H7N9 virus-like-particle combining the HA and NA of A/Anhui/1/13 virus with the M1 of A/Indonesia/5/05 virus have been approved in phase 1 clinical trial (Fries *et al.*, 2013).



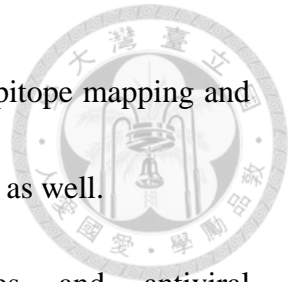
1.5 Motivation

H7N9 is an emerging avian influenza A virus that can infect humans since February, 2013. Until June 2015, World Health Organization (WHO) has reported that the laboratory-identified cases of human infection with H7N9 virus are 653 and the death toll is 227. As other influenza viruses, current recommended anti-H7N9 therapy relies on early treatment with NA inhibitors. However, A/Shanghai/1/2013 virus reveals a polymorphism of NA genes (N9-294R or -294K) and this indicates that oseltamivir-therapeutic effect might be compromised through interfering with the binding of oseltamivir carboxylate (Wu *et al.*, 2013).

In Taiwan, a 53-year-old male traveling from Suchow, Jiangsu province and later admitted to NTUH due to progressive dyspnea and fever. The patient was successfully cured after receiving a daily dose of 150 mg oseltamivir and extracorporeal membrane oxygenation (ECMO) application. Because the patient recovered we thought he might have circulating B cells producing H7N9-specific Abs. Before discharge from NTUH about one month after infection and one week without viremia, his blood was drawn for sorting memory B cells and plasmablasts for Ab gene cloning with an aim to develop therapeutic human neutralizing Abs. The therapeutic Abs can not only synergize the efficacy of NA inhibitors but surrogate the needed humoral immunity during the

window before the host develops anti-influenza neutralizing Abs. Epitope mapping and functional assays for the cloned Abs will be developed in this project as well.

Moreover, influenza viruses evade immune responses and antiviral chemotherapeutics through genetic drift and gene reassortment almost every year. It is essential to demonstrate a feasible approach to develop effective therapeutic neutralizing Abs against the emerging zoonotic influenza virus. The ultimate goal is to obtain and engineer the broadly neutralizing Abs against most, if not all HA subtypes of influenza A viruses.





Chapter 2. Materials and Methods



2.1 Reagents and antibodies

Influenza A virus hemagglutinin cDNA Clone, H7N9 (A/Anhui/1/2013), H1N1 (A/California/07/2009), H3N2 (A/Brisbane/10/2007), H5N1 (A/Vietnam/1194/2004) were all purchased from Sino Biological Inc. (Beijing, P.R. China). The pFlu-BsmBI eight-plasmid reverse genetics system was kindly provided by Dr. King-Song Jeng (Institute of Molecular Biology, Academia Sinica, Taiwan). Mouse mAbs to H7N9 HA (11056-MM05-50), H3N2 HA (11082-MM04) and H5N1 HA (11048-MM01-50) as well as rabbit mAbs to H7N9 HA (11082-R002) and H1N1 HA (11055-RM10) were acquired from Sino Biological Inc. (Beijing, P.R. China). Anti-myc Ab was purchased from Abcam (Cambridge, MA, U.S.A.). The Alexa Fluor® 488 conjugated anti-rabbit IgG (H+L) (#4412) was obtained from Cell Signaling. Alexa Fluor® 647 AffiniPure F(ab')₂ fragment anti-human IgG (-606-098) was purchased from Jackson ImmunoResearch (West Grove, PA, U.S.A.).

2.2 Viruses and cells

2.2.1 HEK293T cells

HEK293T cells were grown in RPMI1640 medium supplemented with 10% fetal bovine serum containing L-glutamate (HyClone, Thermo Scientific, Waltham, MA, U.S.A.) and penicillin/streptomycin at 37°C in a 5% CO₂ incubator.



2.2.2 A549 cells

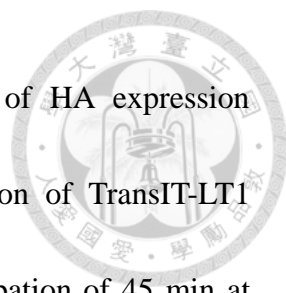
A549 cells, an alveolar basal epithelial cell line derived from human adenocarcinoma, were grown in Kaighn's modification of Ham's F-12 medium supplemented with 10% fetal bovine serum containing L-glutamate (HyClone, Thermo Scientific, Waltham, MA, U.S.A.) and penicillin/streptomycin at 37°C in a 5% CO₂ incubator.

2.2.3 MDCK cells

MDCK (Madin-Darby canine kidney) cells were grown in Dulbecco's modified Eagle's medium (DMEM, Gibco, Life Technologies, Pitam Pura, Delhi, India) supplemented with 10% fetal bovine serum containing L-glutamate (HyClone, Thermo Scientific, Waltham, MA, U.S.A.) and penicillin/streptomycin at 37°C in a 5% CO₂ incubator.

2.2.4 WSN-based reassortant influenza virus

Six-well plate was seeded with a mixture of 3.5×10^5 /ml HEK293T cells and 5×10^5 /ml MDCK cells in 2 ml OPTI-MEM per well and then incubated in CO₂ incubator overnight, followed by addition of 16 µl of TransIT-LT1 (Mirus, Madison, WI, U.S.A.) mixed with 125 µl OPTI-MEM for 5 min at ambient temperature. One µg of each expression plasmid of A/WSN/33/H1N1 (pFlu-PB2, pFlu-PB1, pFlu-PA, pFlu-HA, pFlu-NP, pFlu-NA, pFlu-M, and pFlu-NS) was added into 125 µl of OPTI-MEM. The




pFlu-HA of A/WSN/33/H1N1 was replaced by other subtypes of HA expression constructs for HA-specific broadly neutralizing test. After addition of TransIT-LT1 reagent into the diluted plasmid mixture above, an additional incubation of 45 min at room temperature was performed. The mixture of TransIT-LT1 reagent/DNA complexes was then added onto different regions of the well drop by drop, followed by culture in CO₂ incubator overnight. After 24 hr, the medium was replaced with 2 ml fresh OPTI-MEM containing 0.5 µg/ml TPCK-trypsin. After a 3-day incubation, supernatants were collected, titrated, and frozen at -80 °C until use.

2.3 Lymphocyte sorting from peripheral blood of the NTUH H7N9 patient

The first H7N9 Taiwanese patient, who traveled from Suchow to Taiwan, had medical treatment in NTUH. After the viremia subsided, the patient's blood was drawn and the leukocytes were purified. The memory B cells and plasma cells are sorted according to surface markers of CD19⁺CD27⁺CD38^{hi} by fluorescence-activated cell sorting (FACS) Aria (BD Biosciences, Franklin Lakes, NJ, U.S.A.).

2.4 Single B-cell RT-PCR cloning of Ig genes

The sorted antibody-secreting cells were seeded into 96 well-plates containing 100 µl of lysis buffer and immediately frozen until use. To perform reverse transcription (RT), an aliquot of thawed lysis buffer was taken from each well, followed by PCR



using a cocktail of primers specific for all human V_H and V_L genes for amplification. PCR products of V_H and V_L genes were then cloned into a vector containing the backbone of Herceptin with a leader peptide sequence of κ chain for expression and purification from culture medium.

2.5 Construction of plasmids

2.5.1 pSecTag2-H1, H3, H5, H7 constructs

The pSecTag2A plasmid (Invitrogen, Waltham, MA, U.S.A.) comprises a c-myc tag for protein detection and six tandem histidine residues for protein purification at the C terminus. At the N terminus, the addition of a leader peptide sequence from murine Ig κ chain makes the myc-His fusion protein able to be secreted. Various cDNAs of HA domains from H1N1, H3N2, H5N1 and H7N9, respectively were amplified by PCR with primers containing flanking KpnI and XhoI sites and a high-fidelity DNA polymerase (Thermo Fisher Scientific, Waltham, MA, U.S.A.). After clean-up of PCR products (Geneaid, New Taipei City, Taiwan) and enzyme digestion, the purified DNA fragments was subcloned into the KpnI and XhoI sites of pSecTag2A plasmid by T4 ligase at room temperature overnight.




2.5.2 pFlu-HA-KpnI-XhoI

pFlu plasmid is a pol I/pol II bidirectional plasmid system, which comprises RNA polymerase II and CMV promoters and a polyadenylation signal from a bovine gene encoding growth hormone (BGH pA). In addition, human RNA polymerase I promoter (PolIp) and murine terminator (terminator) were inserted between CMV promoter and BGH pA. The insertion of IVA cDNA between the PolII promoter and murine terminator enables synthesis of the virus mRNA, from which viral proteins are translated, as well as the negative sense of virus RNA for virus replication. In order to retain the packaging sequence of Influenza A virus HA, site-directed mutagenesis was performed to create two restriction enzyme sites between the coding region of A/WSN/33/H1N1 HA. At the end of the 5' packaging region (45 nucleotides of coding sequence), a KpnI restriction site was created with TSJ498 and TSJ499 primers for PCR cloning using Pfu-X DNA polymerase (SolGent, Daejeon, Korea). Likewise, an XhoI restriction site was generated with TSJ500 and TSJ509 primers at the end of the 3' packaging region (80 nucleotides of coding sequence) (Marsh *et al.*, 2007).

2.6 Cell transfection


The HEK293T and A549 cells were seeded 24 hours before transfection. DNA plasmids were diluted in serum-free medium and mixed with TurboFect transfection



reagent (Thermo Fisher Scientific, Waltham, MA, U.S.A.) at the ratio of 1:2 in for 20 to 30 min at room temperature, followed by transfer of the transfection reagent/DNA mixture onto the cells drop by drop with gently shaking of the plate to achieve even distribution of the mixture. After incubation at 37 °C in a 5% CO₂ incubator for 24 to 48 hr, the efficiency of transfection in cells was analyzed by western blotting, ELISA, flow cytometry, and immunofluorescence staining, respectively.

2.7 Western Blotting analysis


After 24~48 hr post-transfection, HEK293T cells were rinsed in PBS and lysed in RIPA buffer containing a cocktail of protease inhibitors. The cells were lysed for 30 min on ice followed by centrifugation at 12,500 rpm for 15 min. The supernatants and cell lysates were separately collected and their protein concentration was determined by the Coomassie protein assay kit (Thermo Fisher Scientific, Waltham, MA, U.S.A.) according to the manufacturer's instructions. Lysates of 50 µg were boiled in reducing sample buffer before loading into a SDS-PAGE gel to resolve in Tris-HCl/Glycine running buffer. After the gel running was completed, the gel was transferred onto PVDF membrane (Millipore, Billerica, MA, U.S.A.) at a condition of 90V (~450mA) at 4 °C for 2.5 hr. After blocking with 0.5% non-fat milk in TBS for 1 hour at room temperature, the membrane was incubated with primary antibodies specific for HA of H1N1, H3N2,



H5N1, H7N9, respectively at 4 °C overnight, followed by 5 serial washes with TBST for 10 min each at room temperature. Membranes were then incubated with secondary Abs of horseradish peroxidase (HRP)-conjugated goat anti-mouse (1:5,000), goat anti-rabbit (1:5,000), (Fab')₂ fragment of anti-human (1:1,000) separately for 1.5 hr at room temperature. The membranes were washed 5 times with TBST for 10 min each time. An ECL kit was used to detect specific protein binding on the membrane by UVP system for image display.

2.8 ELISA

Recombinant HA proteins secreted into culture medium were coated onto 96-well nickel-coated plates (Thermo Fisher Scientific, Waltham, MA, U.S.A.) with gentle shaking at 4 °C overnight. After washes with TBS containing 0.05% Tween-20 (TBST) three times, HA-specific Abs were incubated (1 µg/ml) with shaking for 1.5 hr at room temperature. After washing plates with TBST three times, the plates were blocked with BlockPRO™ blocking buffer (Visual Protein). HRP-conjugated anti-human IgG Ab (1:1,000) (Jackson Immuno Research, West Grove, PA, U.S.A.), HRP-conjugated anti-rabbit (1:1,000) (Sigma-Aldrich, St. Louis, MO, U.S.A.) or HRP-labeled anti-mouse (1:1000) (Santa Cruz Biotechnology, Dallas, TX, U.S.A.) or HRP-conjugated anti-human (Fab')₂ (1:1,000) (Jackson Immuno Research, West Grove,



PA, U.S.A.) was used to detect binding after 1-hr incubation at room temperature before development with TMB substrate reagent set (BD Biosciences, Franklin Lakes, NJ, U.S.A.). The substrate developing reaction was terminated by 2N H₂SO₄ and the absorbance of protein was measured at 450 nm (OD₄₅₀) on a microplate spectrophotometer (BioTek, Winooski, VT, U.S.A.).

2.9 Antibody staining and flow cytometric analysis

In order to assess the expression level of various HA proteins at the cell surface, we transfected HEK293T and A549 cells with each HA plasmid by using TurboFect transfection reagent (Thermo Fisher Scientific, Waltham, MA, U.S.A.) following the manufacturer's instructions. After 48 hr of transfection, the cells were first washed with 800 μ l of PBS and then incubated in 100 μ l of staining solution, PBS containing 1% BSA. Samples were stained by commercial HA Abs or cloned human neutralizing Abs in dark for 30 min at 4 °C followed by washes with PBS. Rabbit IgG1 and human IgG1 were used as isotype controls. As a control of Ab specificity, cells were also stained with only the secondary Abs, anti-rabbit-IgG conjugated with Alexa 488 and anti-human IgG conjugated with Alexa 647, respectively for 30 min at 4 °C. After serial washes with PBS, the pellets were quickly resuspended in 300 μ l of PBS containing 1% of paraformaldehyde. The samples were analyzed by a flow cytometer (FACSCalibur,

BD Biosciences, Franklin Lakes, NJ, U.S.A.). Samples with higher mean fluorescent intensity (MFI) value than unstained and controls were considered as positive.




2.10 Immunofluorescence staining

A549 cells (2.4×10^5 /ml) were seeded on the coverslip in the 6- well plate 24 hr before transfection. After plasmid transfection, cells were fixed with 99% methanol (-20 °C) for 5 min at room temperature and then rinsed in PBS twice, followed by blocking with BlockPRO™ blocking buffer (Visual Protein) for 30 min at room temperature. Primary Abs against HA were diluted to 1 µg/ml in blocking buffer and incubated at 4 °C overnight. Rabbit and human IgG were used as isotype control Abs. Either Alexa Fluor 647–conjugated goat anti-human IgG Ab (Jackson Immuno Research, West Grove, PA, U.S.A.) or Alexa Fluor 488–conjugated goat anti-rabbit IgG Ab (Cell Signaling Technology, Danvers, MA, U.S.A.) was used as a secondary Ab for detection. Finally, cells were counterstained with DAPI for nucleus for 5 min at room temperature. Specific binding was visualized using a Zeiss AxioImager A1 fluorescence microscope.

2.11 Plaque assay

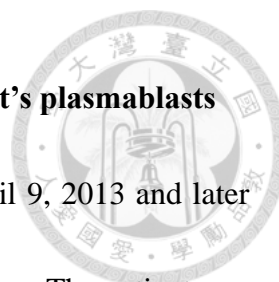
MDCK cells were seeded in 6-well plates at a density of 1×10^6 /well. On the next day, cells were washed with PBS, followed by addition of 100 µl of 10-fold diluted medium containing virus to each well and then incubated at 37°C for 1 hr with gentle



mixing every 15 min. During the period of infection, serum-free DMEM medium supplemented with antibiotics (100 U/ml penicillin and 100 mg/ml streptomycin) and TPCK-trypsin (2 μ g/ml) (BioScience) was warmed up at 37 °C, and 3% agarose was heated at 56 °C (Seakem, Lonza, Basel, Switzerland). Cells were then first washed with PBS before addition of agarose overlay medium, a mixture of 1.8 ml DMEM and 200 μ l 3% of melted agarose (final concentration: 0.3%), into each well carefully while it was still in liquid form. After solidification of the agarose overlay medium, cells were incubated for additional 48 hr and fixed with 10% paraformaldehyde for 2 hr. Agarose plugs formed in each well was carefully removed and cells were stained with 0.1% crystal violet in 25% ethanol for 5 min. After removal from the crystal violet solution, plates were washed with H₂O and allowed air dried at room temperature.



Chapter 3. Results

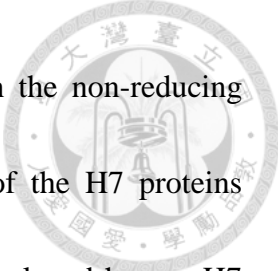


3.1 Cloning of H7N9 neutralizing antibody genes from the patient's plasmablasts

A 53-year-old male Taiwanese returned from Suchow on April 9, 2013 and later admitted to NTUH due to progressive dyspnea and fever for three days. The patient was successfully cured and discharged on May 24. One week after the viremia completely subsided, we took 10 ml of patient's venous blood to isolate B cells that are potentially secretors of virus-specific Abs. The RBCs in the blood were lysed first and a Ficoll gradient was performed at centrifugation of 2,000 rpm for 15 min to isolate the buffy coat. Purified leukocytes were stained with a cocktail of lineage-specific fluorescent Abs to sort CD19⁺CD27⁺CD38^{+/high} B cells. Approximately 4.5% of B cells were subjected to sorting for single B-cell cloning of Ab genes (**Figure. 1**). We cloned ~80 human mAbs and 9 of them have the various degrees of H7N9 virus neutralization activity (data not shown).

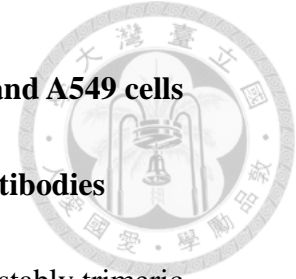
3.2 H7N9 neutralizing mAbs were able to bind to H7 on HEK293T and A549 cells transfected with monomeric H7

The expression of HA gene of H7N9 (A/Anhui/1/2013) was driven by the CMV promoter to induce HA over-expression on the plasma membrane of HEK293T cells. To test whether the construct expressed correctly, we used anti-H7 HA Ab (11082-MM04) (11082-R002) for western blotting and flow cytometry, respectively (**Figure 2**). The results of western blotting showed that H7 proteins expressed and formed not only



monomers but also oligomeric structures, e.g. dimer and trimer in the non-reducing protein gel (**Figure 2A**). Consistently, flow cytometric analyses of the H7 proteins indicated correct surface expression (**Figure 2B**). We then used the cloned human H7 mAbs to examine their binding ability to the H7 over-expressed on cell membrane of HEK293T cells using flow cytometry. The results showed that some of human anti-H7 mAb clones indeed could bind to the H7 protein and three of them, designated as P2F7, P3C1 and P4C3, showed greatest binding affinities (**Figure 2C**). Since lung epithelial cells are trophic to influenza virus, we investigated these human anti-H7 mAbs for their binding on A549 cells, a lung adenocarcinoma cell line. Since HA is known to be heavily glycosylated, the use of A549 cells might be more relevant for glycosylation may affect the conformation of HA protein (Guo *et al.*, 2009). It appeared that H7 proteins could be expressed and detected in A549 cells by western blotting but the commercial H7 Ab (11082-R002) did not bind the H7 expressed on the surface of A549 cells using flow cytometry (**Figure 3A**). However, the P3C1 and P4C3 clones of anti-H7 mAbs could bind substantially to the surface H7 expressed on A549 cells by immunofluorescence (**Figure 3C**). In this experiment a commercial anti-H7 mAb (11082-R002) was used as a positive control (**Figure 3B**).

3.3 Expression of trimeric H7 hemagglutinin in HEK293T cells and A549 cells respectively for binding assays of human anti-H7 monoclonal antibodies



The HA proteins on the viral envelope are normally formed in a stably trimeric conformation. The trimeric HA –stalk domain recombinant proteins with the foldon domain have been reported to elicit the broadly neutralizing antibodies and provide cross protection toward different subtypes of IVAs (Mallajosyula *et al.*, 2014). In order to generate the trimeric form of HA proteins in expressing cells, we replaced the transmembrane domain of H7 with fibrin foldon from T4 bacteriophage to the C terminus of the H7 stalk domain to induce trimer formation (**Figure 4A**). Unexpectedly, no appreciable binding by the anti-H7 mAb (11082-R002) was observed using flow cytometry (**Figure 4B**). It is likely the epitope of this mAb was masked or embedded in the H7 trimer proteins. Consistent with this notion, the trimeric H7 proteins could be readily recognized in both reducing and non-reducing SDS-PAGE gels (**Figure 4C**). We next examined whether the human anti-H7 mAbs could bind to the engineered trimeric H7 proteins using flow cytometry. The data revealed that the P2F7 clone of human anti-H7 mAb could bind to the surface trimeric H7 proteins weaker than that of full-length H7 transfectants. In contrast, both P3C1 and P4C3 clones of human anti-H7 mAbs bound surface trimeric and monomeric H7 proteins comparably (**Figure 4D**). Lastly, we performed immunofluorescence experiments on trimeric H7-transfected


A549 cells and found that the commercial anti-H7 mAb as well as the P3C1 clone of human anti-H7 mAb exhibited marked binding (**Figure 5A and 5B**).



3.4 Conversion of the whole IgG1 human anti-H7 monoclonal antibody to scFv-Fc format

Based on the data from flow cytometry and immunofluorescence described early on, some of the human IgG1 mAbs specific for H7 could bind both monomeric and trimeric forms of H7 proteins. Due to patent issue of the backbone of IgG1 plasmid, we decided to convert the Ab format from whole IgG1 to scFv-Fc. It is regarded that the scFv Abs are generally less thermally stable, have a shorter half-life and tend to degrade or aggregate under the conditions of practical uses. Thus, the applications of the scFvs might be limited and need to engineer to stabilize the structure (Wang and Duan, 2011).


With this in mind and the need to generate a more specific, more stable and longer half-life neutralizing mAb, we cloned the variable regions of heavy and light chain genes of selected anti-H7 mAbs in scFv format into pFUSE-hIgG1-Fc2 plasmid, which contains the CH2 and CH3 domains of the human IgG heavy chain and the hinge region to form a scFv-Fc, which is a small IgG-like recombinant protein. In addition, the IL-2 signal peptide was included to allow for secretion of scFv-Fc mAbs when expressed in cells (**Figure 6A**). The scFv gene sequences are approximately 750 bp consisting of a



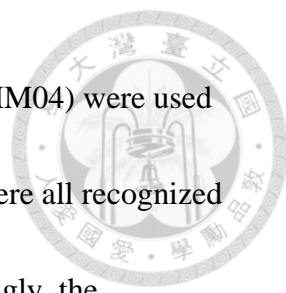
light chain, a linker (GGGGS)₃ and a heavy chain (**Figure 6B**). After transient transfection of scFv-Fc plasmid in HEK293T cells, cell lysate was analyzed by SDS-PAGE, transferred and immunoblotted with HRP-conjugated anti-human (Fab')₂ Ab. The result showed that the molecular weight of scFv-Fc Abs was ~55 kDa when reduced in gel. A minor band of ~110 kDa was detected, suggesting dimer formation or insufficient denaturing of proteins. Under non-reducing conditions, a high molecular weight band was observed, indicating that the inter-chain disulfide bond in the hinge region was obtained (**Figure 6C**). Next, we examined the supernatant collected from transfected cells to detect the secretion of the scFv-Fc Abs using ELISA assays. Compared with the un-transfected supernatant, the H7 scFv-Fc transfected supernatant exhibited a significant binding to HRP-conjugated (Fab')₂ anti-human secondary Ab (**Figure 6D**).

3.5 H7 domain-specific constructs for epitope mapping

Since some the human anti-H7 mAb clones were able to bind recombinant H7 proteins by ELISA assay and/or native H7 proteins expressed on mammalian cell surface, we next wanted to identify the epitopes of these human anti-H7 Abs. In order to be able to purify the domain-specific recombinant proteins, we subcloned various H7 domains into pSecTag2 constructs that contain a leader peptide sequence of Igk chain at the N terminus of H7 for secretion and replaced the transmembrane domain with the




c-myc and histidine tags in tandem for protein identification and purification. In total six domain-specific constructs of H7 gene (A/Anhui/1/2013) were designed. As shown in **Figure 7**, the first construct generated full-length extracellular domain of H7 proteins since it lacked sequences of transmembrane (starting at position I525) and cytoplasmic domains and this construct was designated as H7-1, which contained 1,575 base pairs of nucleic acids. Two disulfide-linked glycosylated polypeptides, HA1 and HA2, were predicted from the conserved proteolytic cleavage site (R339). We subcloned the HA1 domain of H7, designated as H7-2 and HA2 domain, designated as H7-6 into pSecTag2 vector, respectively. Based on the blast search, a highly conserved region with a disulfide bond (Cys52-Cys277 [H3 numbering]) was known to be the starting site of the variable globular head domain. The H7-3 construct contained the sequence of the globular head domain of H7 (Cys60-Cys286) while the H7-4 construct comprised the conserved stalk domain. The H7-5 construct was composed of several important epitopes of the well-known broadly neutralizing Abs, such as CR9114 and CR8020 Abs (**Figure 7A**). The cDNA inserts of H7 domains of constructs were resolved by agarose gel electrophoresis (**Figure 7B**). To determine whether these H7 domain-specific constructs could be properly expressed, we transiently transfected these constructs individually into HEK293T cells for 48 hr and cell lysates were harvested for identification of H7 domain proteins using SDS-PAGE. After transfer onto PVDF



membrane, anti-myc Ab and the commercial anti-H7 mAb (11082-MM04) were used for probing. As illustrated, proteins expressed from each construct were all recognized by anti-myc mAb with correct estimated molecular weight. Interestingly, the commercial anti-H7 mAb bound readily to H7-1, H7-4, H7-5 and H7-6 domains, all of which contained the common stalk domain, indicating that the epitope the commercial anti-H7 mAb recognized was located in the stalk domain (**Figure 7C and 7D**). In addition, we collected the supernatants from transfected cells by plasmids containing each H7 domain cDNA and used ELISA to detect secreted recombinant H7 domain proteins. We found that the results of ELISA were consistent with those of western blotting. We included another commercial anti-H7 (11082-R002) mAb, which was inefficient for western blotting, and found that the epitope of this anti-H7 mAb was likely located at the HA1 domain for its significant bindings to recombinant H7-1, H7-2 and H7 trimeric proteins, all of which contained the globular head domain.

3.6 Generation of equivalent HA domain constructs of other subtypes

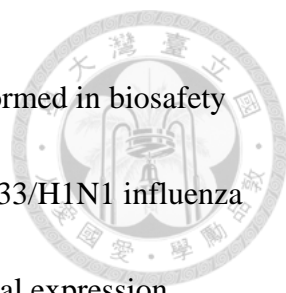
In order to be able to examine and compare the effect of neutralization by human scFv-Fc anti-H7 mAbs and to determine their strain specificity, we selected HAs of H1 (group 1), H5 (group1) and H3 (group2) for generation of domain specific constructs. The full-length HAs without transmembrane domain were designed as H1-1, H3-1, H5-1. From the sequence alignment of these full-length cDNAs without transmembrane



domain, we could roughly divide each HA into two domains at the conserved proteolytic cleavage site. Accordingly, the HA1 domains of each HA were designated as H1-2, H3-2 and H5-2, respectively. As for the HA2 domain, constructs were designated as H1-3, H3-3 and H5-3, respectively (**Figures 8A, 9A and 10A**). Various insert cDNAs of these HA domains were demonstrated by agarose gel electrophoresis (**Figure 8B, 9B and 10B**). After transient transfection, the cell lysates of the recombinant H1, H3, H5 proteins were analyzed by SDS-PAGE and transferred onto PVDF membranes, followed by probing with anti-myc Ab (**Figure 8C, 9C and 10C**) or commercial anti-H1, anti-H3, and anti-H5 mAbs (**Figure 8D, 9D and 10D**). As shown in western blotting, the epitopes of all three commercial anti-HA Abs were located in their corresponding HA1 domain. The supernatant from transfected cells by these domain-specific constructs were investigated by ELISA assay using anti-myc and anti-HA Abs for detection. The results showed the same findings in terms of epitope locations of these three respective commercial mAbs as western blotting (**Figures 8E, 9E and 10E**).

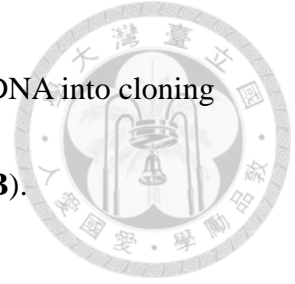
3.7 Generation of WSN-based reassortant influenza viruses

In order to test the binding and neutralization of human scFv-Fc mAbs to influenza virus in a safe and convenient way, we used a bidirectional plasmid to subclone the HA gene for transfection along with expression constructs of other 7 core proteins to



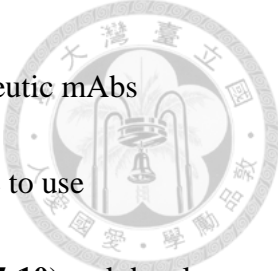
generate low pathogenic influenza reassortants, which could be performed in biosafety level 2 laboratory. This system was based on ‘rescue’ of the A/WSN/33/H1N1 influenza virus from transient transfection of eight plasmids. In this bidirectional expression system, the insertion of IVA cDNA between PolII promoter and murine terminator results in the synthesis of antisense viral RNA and sense mRNA from one viral cDNA template, allowing production of virus to infect cells to form plaques. We first used the 8 plasmids derived from WSN influenza strain that expresses H1 to test this system. The plaque formation in the MDCK cells with ~10-fold dilution of supernatant, i.e. 10^{-2} , 10^{-3} , 10^{-4} , 10^{-5} of virus stock, of transfected cells induced a dilution-dependent lysis of MDCK cells. The titer of the WSN-based reassortant virus was $\sim 2.5 \times 10^6$ PFU. More importantly, if the same amount of virus was pre-incubated with commercial anti-H1 mAb ($10 \mu\text{g/ml}$), the plaque area was greatly reduced (**Figure 11A**). These results indicated feasibility to assess neutralization effects of commercial anti-H1 mAb using this plaque assay. The next experiment would be to utilize this WSN-based reassortant virus system to replace H1 with H7 as well as other HAs, respectively, to examine whether the commercial anti-H7 mAbs and our scFv-Fc mAbs could demonstrate strain-specific or broad neutralization to the reassortant virus. We replaced the H1 with H7 and maintained the packaging sequence of H1. Taking H7 as an example, since the packaging sequence was located in the non-coding region of H1 as well as the first 45

and the last 80 nucleotides of H1 coding region, we subcloned H7 cDNA into cloning sites, KpnI and XhoI between these two regions by PCR (**Figure 11B**).






Chapter 4. Discussions

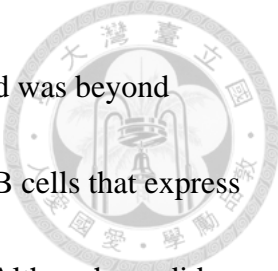


Our findings demonstrate a feasible approach to generate therapeutic mAbs through single B-cell Ig cloning (**Figure 1**). In addition, we were able to use domain-specific recombinant proteins for epitope mapping (**Figures 7-10**) and develop a WSN reassortant virus-based functional assay for evaluation of neutralization using H1 virus as an example (**Figure 11**). Once the epitopes of human anti-H7 mAbs are identified, the WSN-based reassortant virus containing mutant epitopes of H7 can be confirmed by the absence of functional block in comparison to the wild-type H7 protein containing virus. In this regard, we plan to compare human anti-H7 scFv-Fc mAbs (**Figure 6**) with IgG1 mAbs. Our microneutralization assay using attenuated reassortants in conjunction with the traditional HA inhibition assay are proper surrogates for evaluation of the neutralization efficiency of the therapeutic neutralizing mAbs, in particular when the target virus is highly pathogenic to humans. From the aspect of pharmacology, the affinity between the HA of virus and the neutralizing mAb is important for a therapeutic neutralizing Ab. We plan to perform surface plasmon resonance (SPR) analysis in the future. The functional assay we have developed can be utilized as a method to screening compounds for anti-viral agents as well for enhancement of host immunity.

The timing for blood collection from the infected H7N9 patient is critical. Since we used the single B-cell cloning method and attempted to isolate the high-affinity




virus-specific B cells that express Ig with potent virus neutralization, a rule of thumb to collect blood for B cell isolation at right time is when viremia subsides with a concomitant appearance of anti-viral Abs. In our case, the H7N9 patient's blood was drawn one week after no viremia, which was accompanied by a low level of virus-specific Abs detected by ELISA. In general, B-cell mediated immune response requires naïve B cells to undergo germinal center reaction in the secondary lymphoid tissues, e.g. spleen, lymph nodes and tonsil. After one to three days viral infection, B cells undergo somatic hypermutation (SHM) followed by affinity maturation to generate high-affinity virus-specific Abs in the dark zone and subsequently the light zone of germinal center, respectively. With the assistance of CD4⁺ follicular helper T cells (T_{FH} cells) that secrete IL-21, selected high-affinity virus-specific B cells then differentiate to form antibody-secreting plasma cells and memory B cells in the light zone of germinal center within 10 days post-infection. These B cells further undergo class switching from IgM to IgG or IgA, followed by the secretion of large numbers of these high-affinity Abs that can neutralize virus directly, block the entrance of the virus, activate complement system, promote phagocytosis and allow antibody-dependent cellular cytotoxicity to diminish the virus in about 2 weeks after infection. Once the virus or antigen is cleared, a subset of plasma cells differentiate into a long-lived phenotype and virus-specific memory B cells become quiescent (Chiu and Openshaw, 2015). Since we



collected the blood sample from the patient after the virus in the blood was beyond detection at one month after infection, the plasmablasts and memory B cells that express high-affinity virus-specific Ig genes had exited GCs into circulation. Although we did not include virus or HA antigen in cell sorting, the frequency of CD19⁺CD27⁺CD^{38+/high} B cells, i.e. plasmablasts and memory B cells was approximately 4.5%, a reasonable number in the ballpark for cloning the variable genes of these B cells.

As mentioned early on in Introduction, there are three common strategies to generate therapeutic antibodies, including the single B-cell cloning we used. Recently the humanized mice have emerged as a unique, novel tool to speed up the production of human antibodies. The transgenic mice were engineered to insert the full complement of variable genes from all three human Ig loci into precise locations in the corresponding loci of mouse and silenced the endogenous mouse variable genes using a large chromosomal inversion. With antigen challenges, the mice produce high-affinity chimeric antibodies with human variable domains and mouse constant domains. For usage of clinical therapy, the mouse constant region can be substituted with a human constant region without loss of affinity or potency (Lee *et al.*, 2014). The essence of this technique is to make the development of therapeutic Abs with the antigen more feasible. For instance, the necessity of *in vitro* affinity maturation to optimize affinity of human mAbs to antigen out of the described three means can be waived.



In our research, the neutralizing Abs were converted to the scFv-Fc format with an approximate molecular weight of 100 kDa and IgG-like properties such as advantages of dimerization and effector functions, complement reaction, provided by the fused Fc domain. Although the half-life of scFv-Fc Abs is shorter than whole IgG Abs *in vitro* and *in vivo*, scFv-Fc Abs have been reported with greater tumor-targeting and penetrating ability than the whole IgG Abs due to the smaller size (Wang *et al.*, 2011). Also, scFv-Fc Abs are able to provide the protective and therapeutic capacity against West Nile viral challenge in mouse model (Gould *et al.*, 2005). Therefore, it is worth trying for us to purify the scFv-Fc Abs and test the neutralizing ability both *in vitro* and *in vivo*.

As for epitope mapping, our way is conventional so that it is labor-intensive and time-consuming. With the advance of proteomics, epitope mapping can become fast, accurate and high throughput in the near future. For now we generate and purify domain-specific recombinant HA proteins for mapping. Once we pinpoint the antigenic epitope region to perhaps ~50 to 100 amino acids, a series of overlapping peptides flanking the epitope region will need to be synthesized in order to perform ELISA assays for mapping. In this way the epitope of H7 can be further narrowed down to ~10-20 residues. Although there is a lack of epitope information in the public influenza database, there are ample literatures on anti-influenza Abs to provide some important




insights into the epitope of neutralizing Abs either strain-specific or cross-reactive between subtypes. For example, the epitope of CR9114 Ab that has broad neutralizing effects to the group 2 influenza A virus, was identified as AADYKSTQSAIDQITGKLNRLIE, which resides in the conserved stalk domain of H7 protein (at positions 375 to 395) (Dreyfus *et al.*, 2012). One common epitope conserved in all H7 viruses has been characterized as RSGSSFYAEMK (at positions 149 to 159) termed Uni-H7 epitope, which is located in the globular head domain and highly conserved in all influenza A virus (Gravel *et al.*, 2015). With the knowledge of such peptides, we can synthesize them as competitors in our functional assay for neutralization of mAbs to determine their strain specificity and cross-reactivity. Moreover, there are several HA mutant residues that have been reported for reference. For instance, I384 of H7 is a crucial site for CR9114 Ab. Moreover, the I384T of H7 is an escape mutant for interfere binding to CR9114. In addition, G63E and G234D are also found in escape mutants and they are located in the globular head domain of H7 (Dunand *et al.*, 2015). It is worth checking whether our human anti-H7 mAbs and scFv-Fc mAbs can bind to and neutralize these H7 mutants by our functional assay. It is conceivable that the neutralizing Abs' epitope(s) locating on the globular head domain of HA that are able to protect the host cells from viral infection since they could block the virus entry completely compared with Abs targeting the stalk domain of HA. Our

priority is to obtain the Abs targeting the globular head domain of HA, followed by *in vitro* affinity maturation assay to enhance the diversity of Abs for selection of high-affinity Abs.



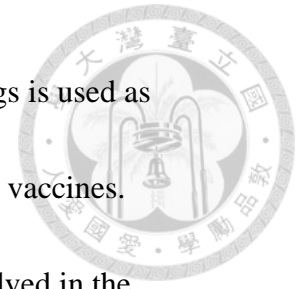
The *in vivo* mechanism of affinity maturation is SHM of variable region depending on the activation-induced cytidine deaminase (AID) at the dark zone of germinal center and followed by clonal selection of B-cells at the light zone of germinal center. In order to improve the antigen-binding affinity of Abs, several *in vitro* affinity maturation assay have been developed. One approach involves the polymerase chain reaction (PCR) with an error-prone DNA polymerase to point-mutate the variable region of Abs. Another approach is generating mutations on residues of Ab CDRs with synthetic oligonucleotides, i.e. CDR-shuffling. The library of V-gene mutants is then displayed on phage, and mutant antibodies with improved affinities are selected by repeated panning (Fujii, 2004). With these approaches to mimic the *in vivo* affinity maturation, one can enhance the binding specificity of selected Abs.

In vitro pseudotype virus-related functional assays can be performed without the requirement of a biosafety-3 laboratory and thereby are commonly used. Furthermore, we can mutate the gene sequences of IAV proteins, HA and NA, easily for more functional application. There are at least three ways to exploit this system. First, the lentiviral pseudotyped viruses expressing different subtypes of HA and NA are



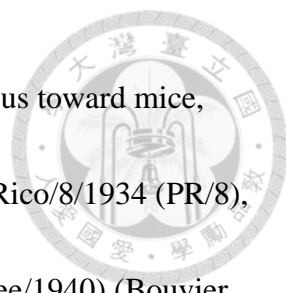
composed of HIV- type 1 (HIV-1) gag-pol construct (pCMV-Δ8.91), a reporter plasmid expressing firefly luciferase and the required envelope glycoprotein constructs (HA and/or NA) in a ratio of 1:1:1.5 but this method yields limited generation of virus. The virus titer can be determined by virus itself or by the reporter gene activity but the latter is more common for its sensitivity. The virus collected from the supernatant can be used for infectivity assessment quantitatively and qualitatively by measurement of relative luciferase unit (RLU), e.g. in HEK293 cells (Molesti *et al.*, 2013). Second, the HIV-1–based pseudotyping assay comprising plasmids that encode HA/NA and Env-defective, luciferase-expressing HIV-1 (pNL4-3.Luc.R⁻.E⁻) can be applied for safe and high throughput screening of neutralizing mAbs and anti-viral agents targeting HA or NA of IVAs. The titer of the pseudovirus is expressed as RLU as well (Du *et al.*, 2010). Third, a bidirectional DNA transfection system for the rescue of infectious influenza A virus from eight plasmids of IVAs similar to what used in this study (Hoffmann *et al.*, 2000). The virus titers are usually determined by cytopathic effects in plaque assay. Another bidirectional DNA transfection system involved in the use of reporter gene is that one of eight plasmids (mostly HA) is selected to stably express in the MDCK cells. The coding region of the HA in the construct is usually replaced by a reporter gene such as EGFP or luciferase for the virus to pack in. The reporter genes make it more convenient to evaluate the infection and neutralization in assay. In

addition, the reassortant virus propagated in embryonated chicken eggs is used as candidate vaccine virus, which is known as live attenuated influenza vaccines.



As for the prevention of IVAs, the vaccine development is involved in the immunization test in animal models. There are several candidates that can be used as antigens such as recombinant proteins, domain-specific peptides of HA, the reassortant virus and the M2e strain. The trimeric HA recombinant proteins with the foldon domain have been reported to elicit broadly neutralizing Abs and provide cross protection toward different subtypes of IVAs (Mallajosyula *et al.*, 2014). The reassortant virus incubated in 10-day-old embryonated chicken eggs protected mice from normally lethal virus challenge (Duan *et al.*, 2014). The M2e vaccine, matrix protein 2 ectodomain tetrameric peptide vaccine, is highly conserved in all human influenza A virus strains and confers cross-protection against lethal infection (Leung *et al.*, 2015). After the immunization, the lethal infection dose and morbidity of the virus-challenged animals are assessed to evaluate the protective effects of the vaccine antigen.

For the *in vivo* neutralization assay, mice are used most frequently for animal experiments of influenza virus research. BALB/c and C57BL/6 are the most widely used mouse strains due to their advantages of low cost, small size, ease of handling and housing. Additionally, a variety of transgenic, knockout, and knock-in mice allow specific infection-related gene to be studied in depth with influenza virus infection.



However, there are specific strains of influenza virus that are infectious toward mice, including two influenza A/H1N1 isolates from the 1930s : A/Puerto Rico/8/1934 (PR/8), A/WSN/1933 (WSN) and an influenza B virus isolated in 1940 (B/Lee/1940) (Bouvier and Lowen, 2010). As a result, research targeting other subtype of influenza virus often implement with the reassortant virus comprising a backbone of the six internal genes of PR/8 or WSN and two target subtypes of the HA and NA genes. There are two methods to infect mice with the influenza virus, intranasally (IN) or by aerosol, which is more susceptible to mice (Smith *et al.*, 2011). The timing of the administration of neutralizing Abs allows for evaluation of different effects of the Ab. With the neutralizing Abs administered before viral infection, the neutralizing effect can be validated by observing the 50% infectious (ID₅₀) and 50% lethal doses (LD₅₀), whereas the body weight loss and survival rate of infected mice allow assessing the therapeutic effects of neutralizing Abs administered after the viral infection. Furthermore, the effects of neutralizing Ab treatment in combination with NA inhibitors or M2 ion channel inhibitors are likely to be synergistic since both entrance and replication of virus are blocked at the same time. This combination treatment is a potential strategy for further clinical evaluation and human use. If the *in vivo* experiment to evaluate the neutralization efficacy of therapeutic Abs to influenza A virus is restricted by high pathogenicity of virus, the WSN-based reassortant influenza viruses can be utilized as an appropriate surrogate to

assess the neutralizing ability of a series of Abs using plaque assay as the functional readout.



Recently rapamycin given during influenza A infection has been shown to alter germinal center reaction toward a propensity to generate broadly neutralizing Abs. In light of this, pharmacological modulation in humanized transgenic mice in the generation of human therapeutic neutralizing Abs might extend its power. Such maneuver might be of great usefulness in vaccinology as well. Since influenza A virus is one of the vigorously studied areas for the generation of protective broadly neutralizing Abs, it is of great importance to develop novel strategies to advance the current methods in the generation of therapeutic neutralizing Abs as well as better vaccines.



This Page Intentionally Left Blank



Figures

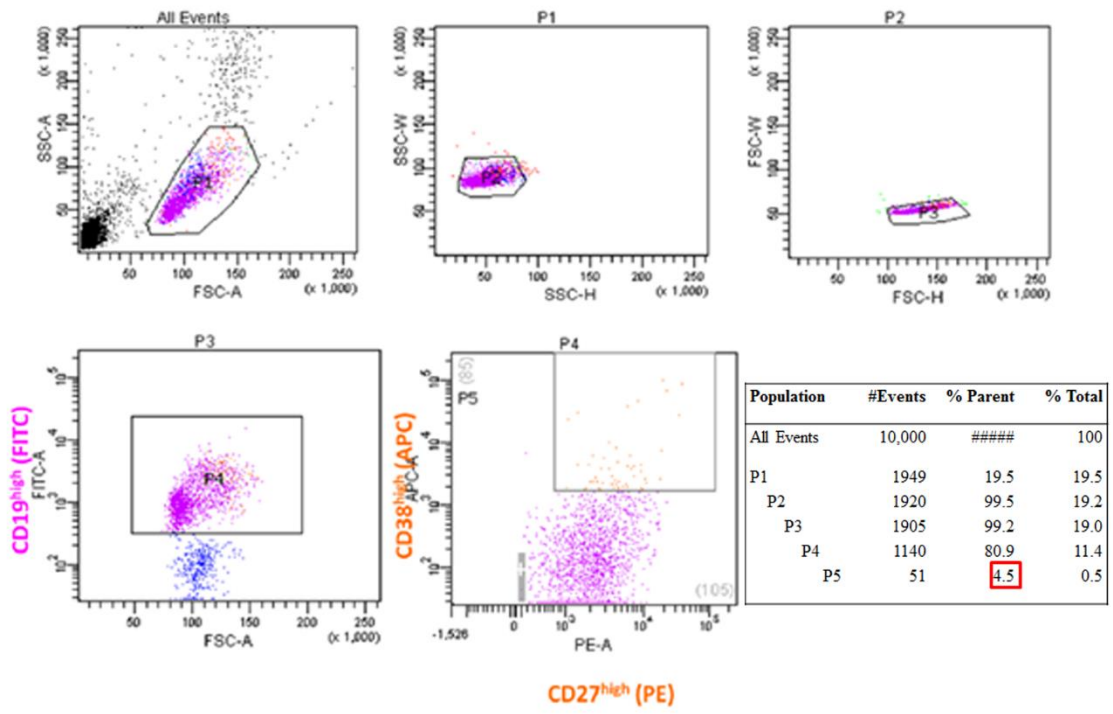
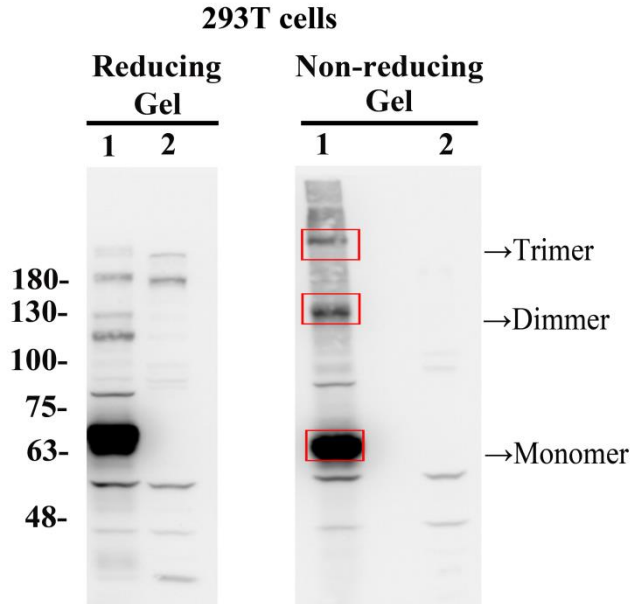


Figure 1. Sorting memory B cells and plasmablasts from the H7N9 patient's blood for single B-cell expression cloning of its antibody gene.



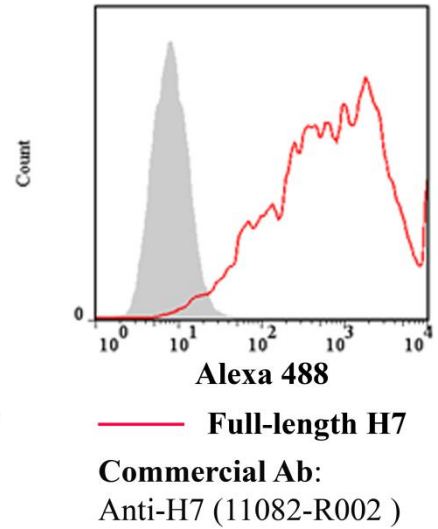
About 10 ml blood of the first Taiwanese H7N9 patient was drawn. Red blood cells were lysed, followed by a Ficoll gradient for isolation of the buffy coat, which contains most leukocytes. Leukocytes were then stained with CD19-FITC, CD27-PE, CD38-APC as well as CD45, IgG, IgM on ice for 30 min. After washes with PBS, the CD19⁺CD27⁺CD38^{+high} population of B cells were sorted one by one into each single well of 96-well plates, which were pre-loaded with ~100 μ l of lysis buffer for RNA extraction, using a FACSAria sorter. Plates were immediately frozen and sealed until use for cloning. Roughly about 4.5% of CD19⁺CD27⁺CD38^{+high} B cells were identified in the gated lymphocytes. A total of 20 plates of sorted B cells were collected and the remaining lymphocytes were lysed in Trizol and stored for further use.

A



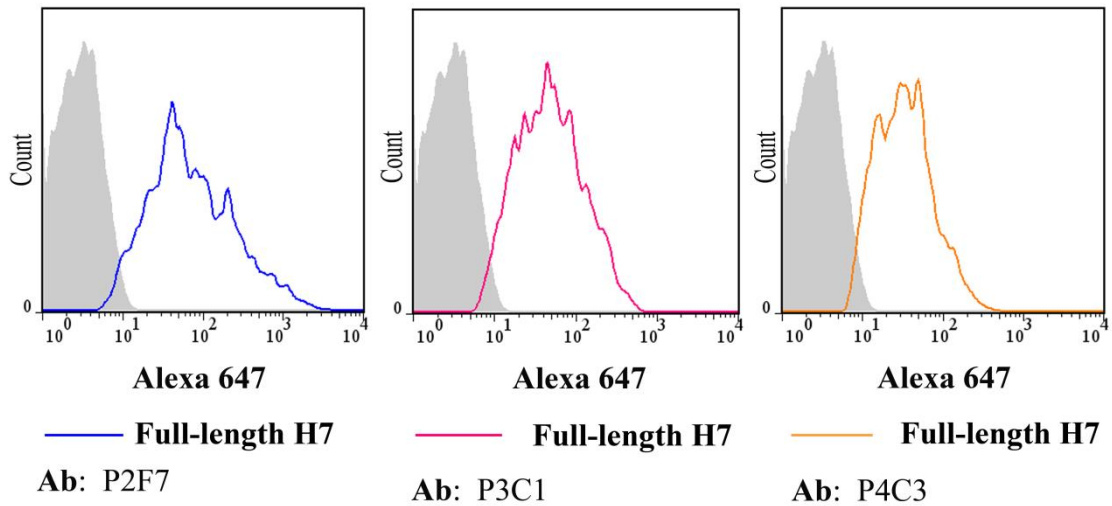
1. Full-length H7
2. Untransfected

B



	Sample	Geom Mean.
—	Full length H7 (11082-R002)	612
—	Unstained	7.97

C



	Sample	Geom Mean.
—	Full length H7 (P2F7)	72
—	Unstained	2.86

	Sample	Geom Mean.
—	Full length H7 (P3C1)	47.6
—	Unstained	2.86

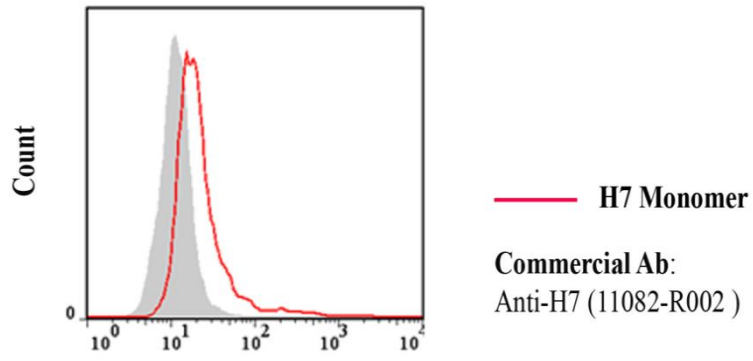
	Sample	Geom Mean.
—	Full length H7 (P4C3)	33
—	Unstained	2.86



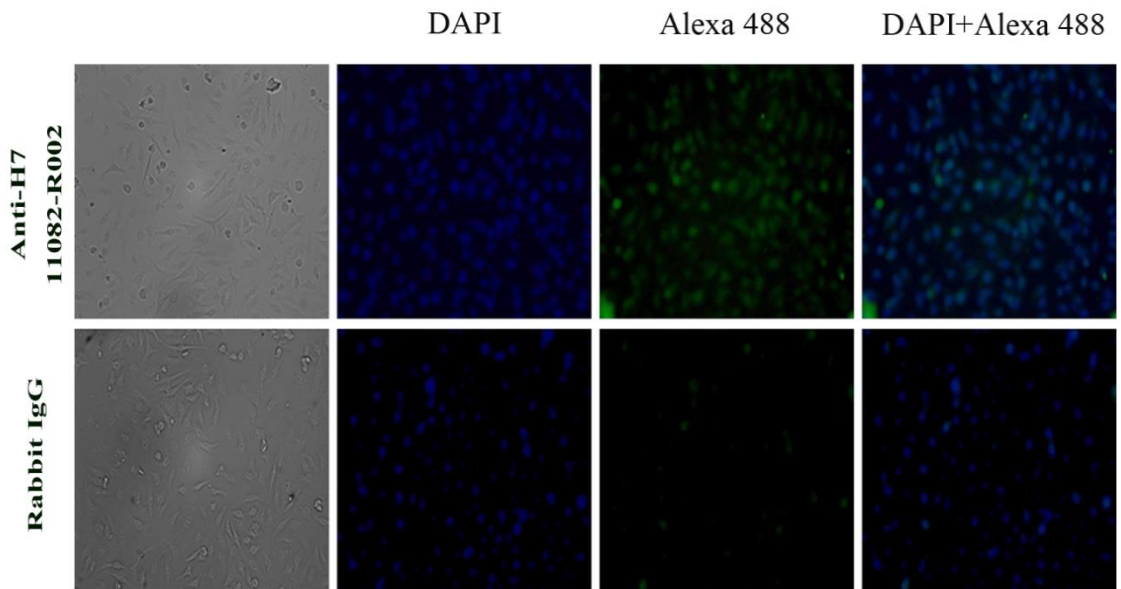
Figure 2. A representation of three human anti-H7 mAbs that were able to bind H7 on HEK293T cells transfected with full-length H7.

- A.** HEK293T cells (2.4×10^5 /ml) were transiently transfected with the full-length H7 plasmid in a 6-well plate. Cell lysates were prepared using RIPA lysis buffer and ~50 μ g of proteins were resolved in reducing and non-reducing protein gels, respectively. After gel transfer onto PVDF membrane, anti-H7 specific Abs (11082-MM04) (1 μ g/ml) was used for immunoblotting to identify H7 proteins.
- B.** The surface expression of H7 by introduction of the full-length H7 plasmids was evaluated in transiently transfected HEK293T cells. After 48 h of transfection, HEK293T cells were harvested and stained with 1 μ g of commercial anti-H7 Abs (11082-R002) followed by incubation with Alexa 488-conjugated anti-rabbit IgG (1 μ g/ml) to evaluate the expression level of H7 proteins on the cell surface by flow cytometry.
- C.** HEK293T cells were transfected as in (B). Cells were harvested for flow cytometric analysis and incubated with 1 μ g each of P2F7, P3C1 and P4C3 clones of human anti-H7 mAb, followed by Alexa 647-conjugated anti-human IgG (1 μ g/ml).

A



B



C

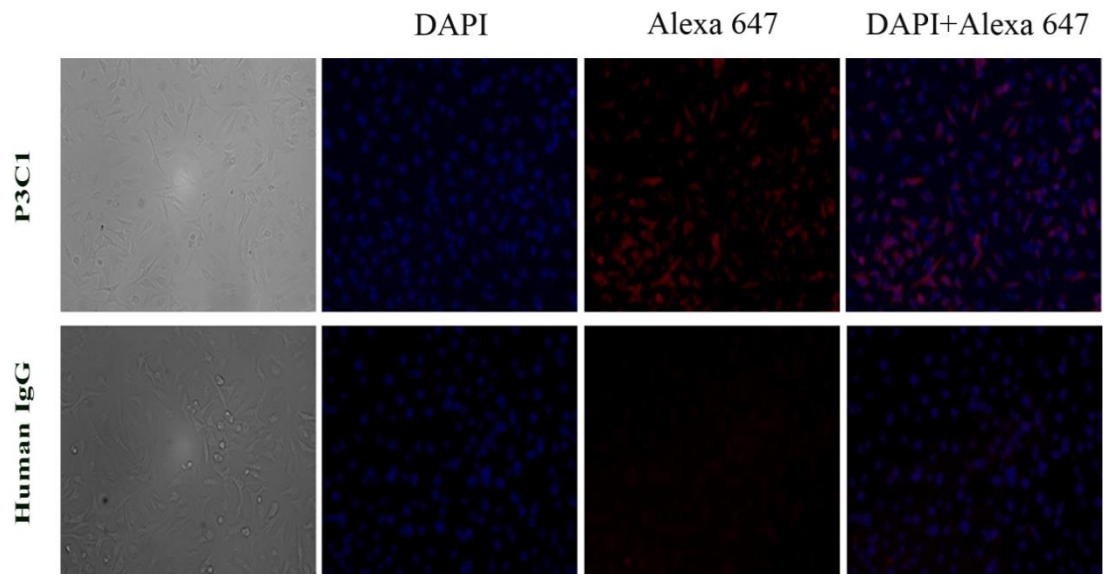
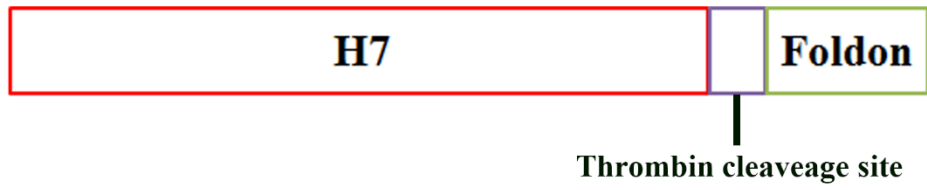


Figure 3. The P3C1 clone of human anti-H7 mAb was able to bind to surface H7 on A549 cells transfected with the full-length H7 cDNA.

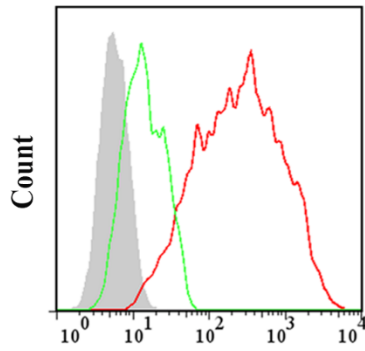


- A. A549 cells were transiently transfected with full-length H7 as done in HEK293T cells in **Figure 2A**. The surface expression of H7 proteins was examined 48 hr later by flow cytometry. Anti-H7 mAb (1 $\mu\text{g}/\text{test}$, #11082-R002) followed by Alexa 488-conjugated anti-rabbit IgG (1 $\mu\text{g}/\text{ml}$) was used for determination of specific binding.
- B. A549 cells were transfected as in (A). Anti-H7 mAb (11082-R002) (1 $\mu\text{g}/\text{ml}$) and isotype control Ab, i.e. rabbit IgG, were incubated separately followed by washes and then addition of Alexa 488-conjugated anti-rabbit IgG (1 $\mu\text{g}/\text{ml}$) for detection.
- C. A549 cells were treated as in (B) for immunofluorescence study of binding specificity of P3C1 human anti-H7 mAb (1 $\mu\text{g}/\text{ml}$) and then addition of Alexa 647-conjugated anti-human IgG (1 $\mu\text{g}/\text{ml}$). The P3C1 human anti-H7 Ab binding to H7 was shown in red.

A



B

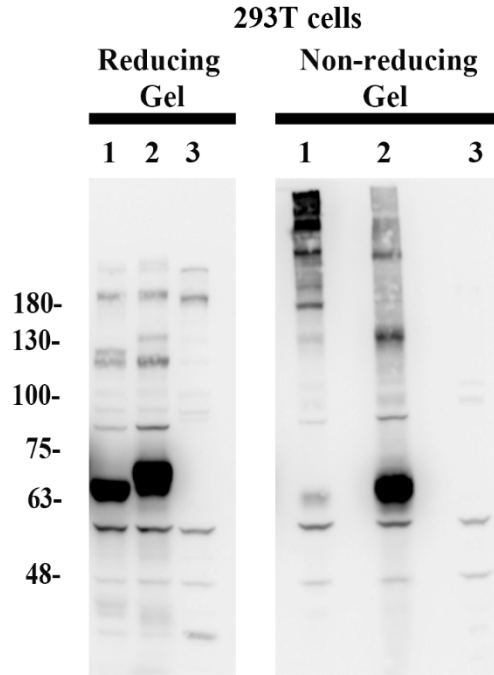


FL1-H: Alexa 488-H7

	Sample	Geom Mean.
—	Engineer H7 trimer	14
—	Full length H7	240
—	Unstained	5.72

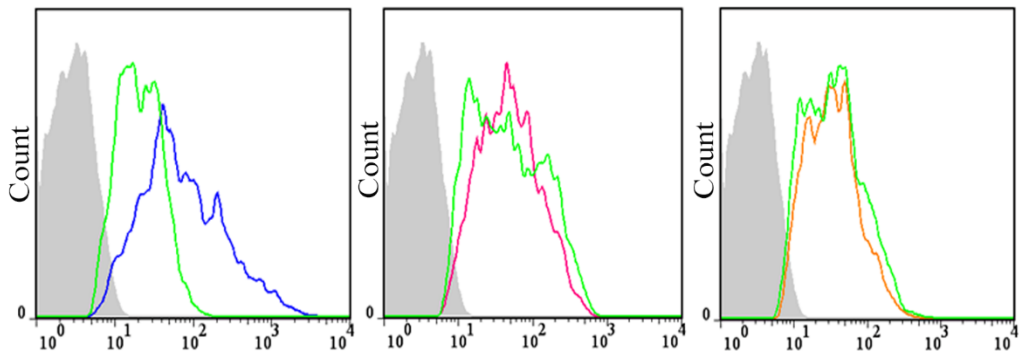
Commercial Ab:
Anti-H7 (11082-R002)

C



1. Enginee H7 Trimer
2. Full-length H7
3. Untransfected

D



FL4-H: Alexa 647-H7

	Sample	Geom Mean.
—	Engineer H7 trimer	14
—	Full length H7	72
—	Unstained	2.82

Ab: P2F7

FL4-H: Alexa 647-H7

	Sample	Geom Mean.
—	Engineer H7 trimer	46.1
—	Full length H7	47.6
—	Unstained	5.72

Ab: P3C1

FL4-H: Alexa 647-H7

	Sample	Geom Mean.
—	Engineer H7 trimer	34.4
—	Full length H7	33
—	Unstained	2.8

Ab: P4C3

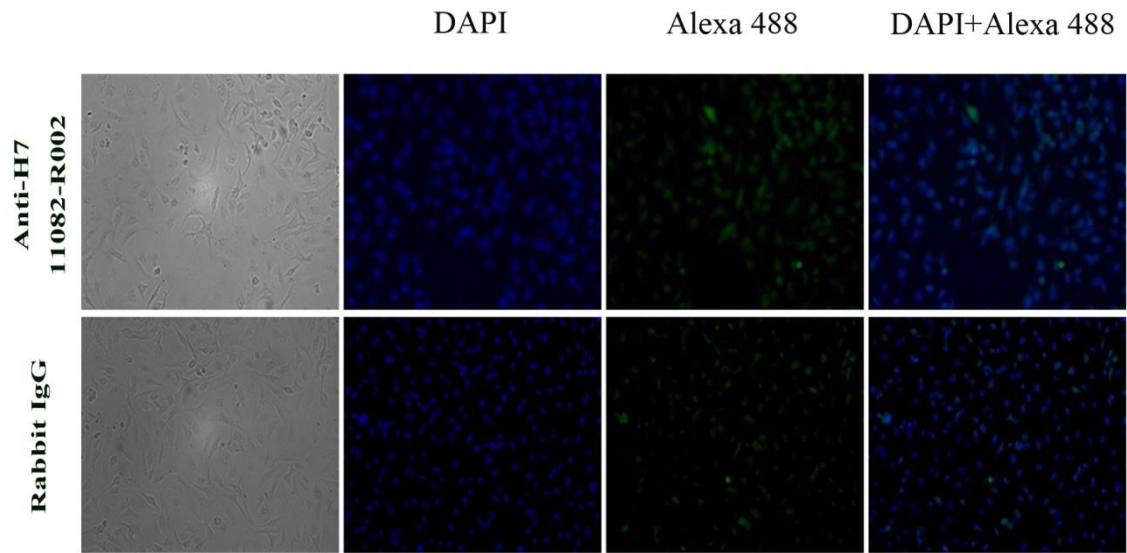


Figure 4. Anti-H7 mAbs were able to bind to H7 trimers expressed on HEK 293T cells.

- A. Schematic diagram of the thrombin cleavage site of H7 cDNA and the location of replacement of fibrin foldon from T4 bacteriophage with transmembrane and cytoplasmic domains of H7. The inclusion of foldon domain enables H7 proteins to form trimers on cell surface.
- B. HEK293T cells were transfected with H7 trimer constructs as described above. Forty-eight hr after transfection, HEK293T cells were analyzed by flow cytometry using 1 μ g of anti-H7 mAb (11082-R002) to evaluate the expression of trimeric H7 proteins on the cell surface.
- C. Western blot analysis of the expression of H7 trimer constructs in transfected HEK293T cells. Cells were harvested 48 hr later for cell lysates and an aliquot of ~50 μ g proteins was subjected to running reducing and non-reducing gels separately. After transfer the PVDF membrane was incubated with anti-H7 mAb (1 μ g/ml) (11082-MM04) overnight before addition of secondary Abs.
- D. Plasmids containing trimeric H7 cDNAs were transfected into HEK293T cells for 48 hr. Three human anti-H7 mAbs, designated as P2F7, P3C1 and P4C3, were examined for specific binding to trimeric H7 proteins expressed on cells using flow cytometry. The secondary Ab was conjugated with Alexa 647.



A



B

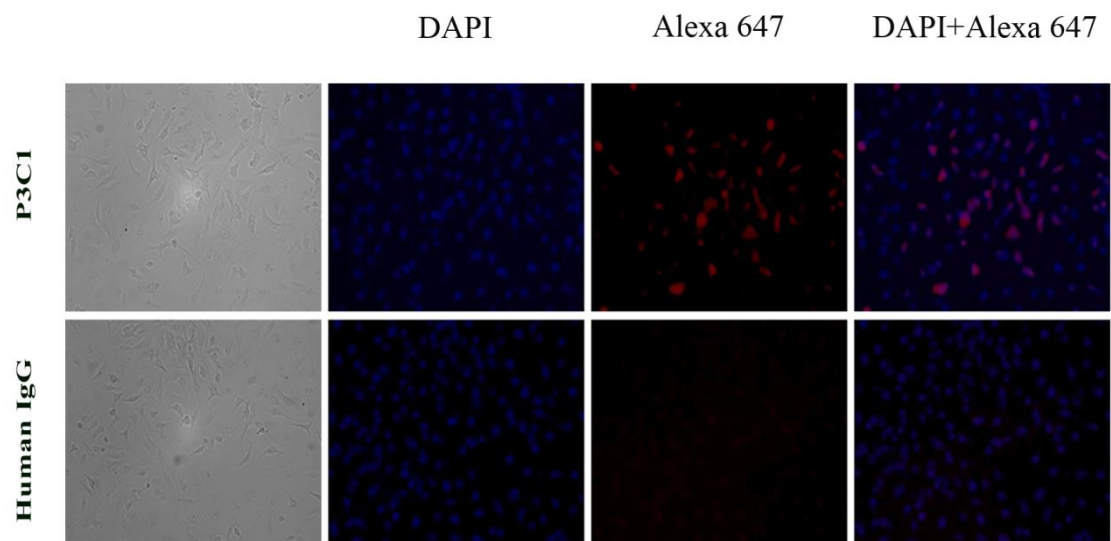
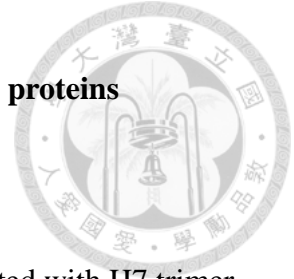
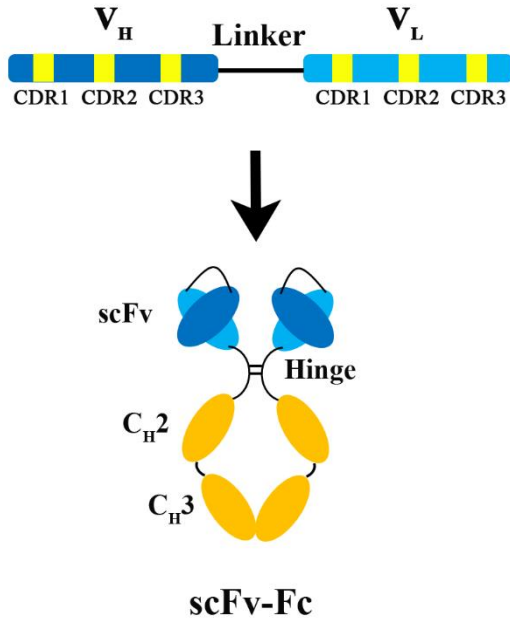


Figure 5. Human anti-H7 mAbs were able to bind to trimeric H7 proteins expressed on A549 cells.

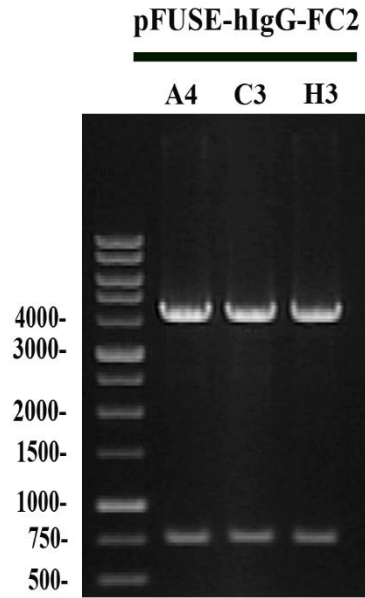


- A. Immunofluorescence images of the A549 cells that were transfected with H7 trimer constructs for 48 hr. Cells were then fixed for staining with 1 $\mu\text{g/ml}$ of anti-H7 Ab (11082-R002) at 4 $^{\circ}\text{C}$ overnight followed by Alexa 488-conjugated anti-rabbit Ab (1 $\mu\text{g/ml}$). Rabbit IgG served as an isotype control.
- B. A549 cells were transfected as in (A). Cells were stained with human anti-H7 mAb, P3C1 clone, followed by Alexa 647-conjugated anti-human Ab (1 $\mu\text{g/ml}$) to visualize specific binding to trimeric H7 proteins in comparison to isotype control, human IgG.

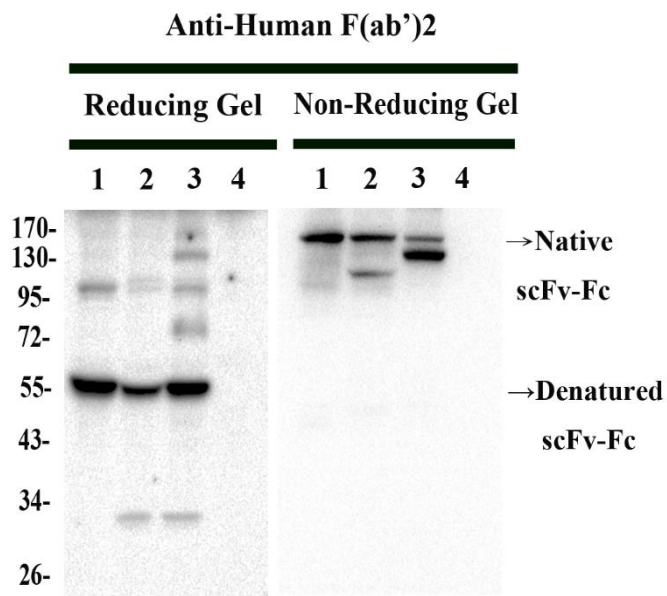
A



B



C



D

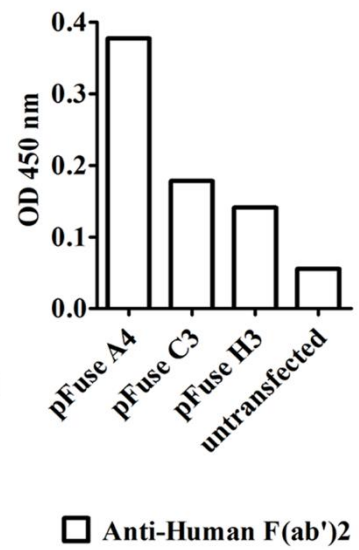
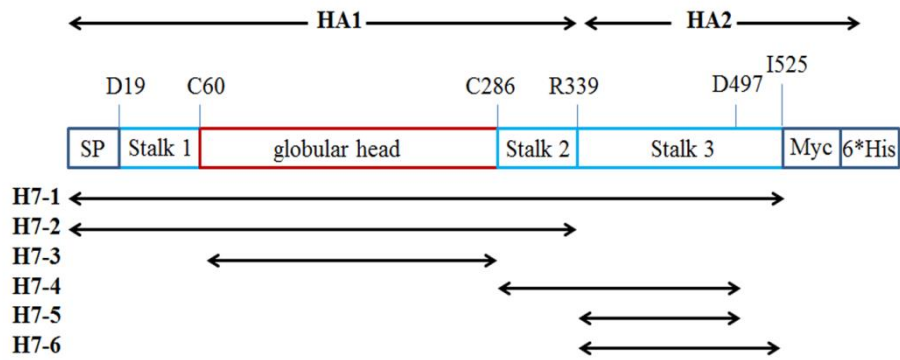


Figure 6. Development and characterization of scFv-Fc anti-H7 monoclonal antibodies.

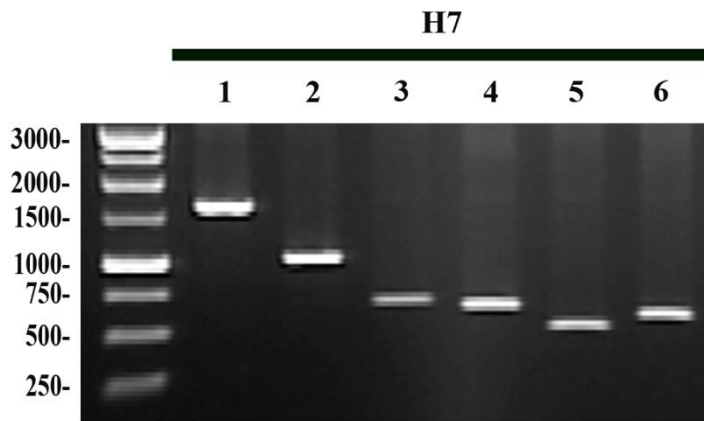


- A. The schematic of human anti-H7 scFv-Fc mAb. The variable gene regions of heavy and light chains of selected human anti-H7 mAbs were engineered to generate scFv-Fc version of neutralizing Abs. The scFv cDNA of human anti-H7 was PCR cloned into pFUSE-hIgG1-Fc2 plasmid, which contains CH2 and CH3 domains and hinge region of human IgG heavy chain to form a scFv-Fc. The resultant scFv-Fc Ab was a smaller IgG-like recombinant protein with addition of the IL-2 signal peptide at the N terminus to allow for secretion into culture medium for purification.
- B. The cDNA of scFv is approximately 750 bp and the pFUSE-hIgG1-Fc2 plasmid is 4,000 bp as shown in agarose gel electrophoresis.
- C. HEK293T cells were transfected with the scFv-Fc expression constructs for 48 hr before harvesting cell lysates for fractionation in reducing and non-reducing gels. After transfer proteins in the gel onto PVDF membrane the HRP-conjugated anti-human F(ab')₂ Ab (1 µg/ml) was incubated for detection using an ECL kit. Three anti-H7 scFc-Fc mAbs were analyzed. Note: Lane 1: pFUSE-A4, Lane 2: pFUSE-C3, Lane 3: pFUSE-H3, Lane 4: untransfected cells.
- D. The secretion of human anti-H7 scFv-Fc Abs into the culture medium was examined by an ELISA assay with the HRP-conjugated anti-human F(ab')₂ Ab (1 µg/ml).

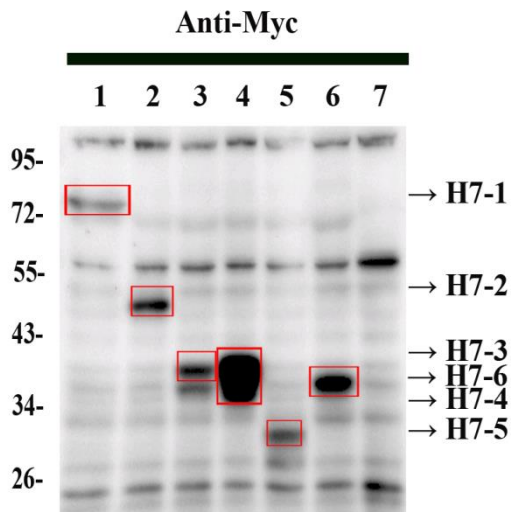
A



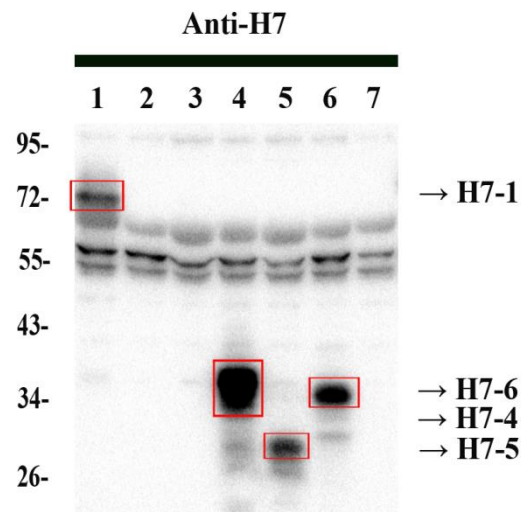
B

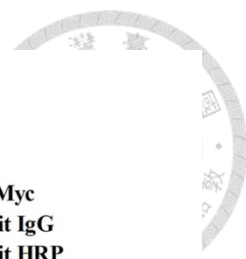


C

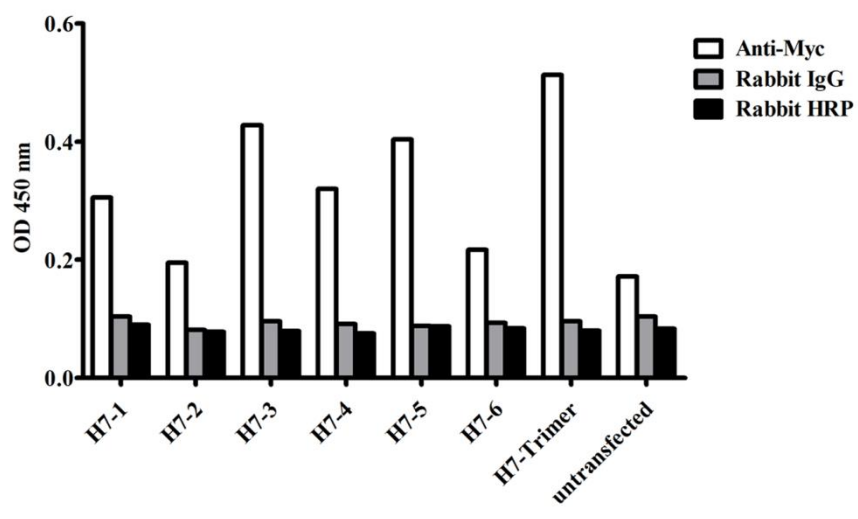


D

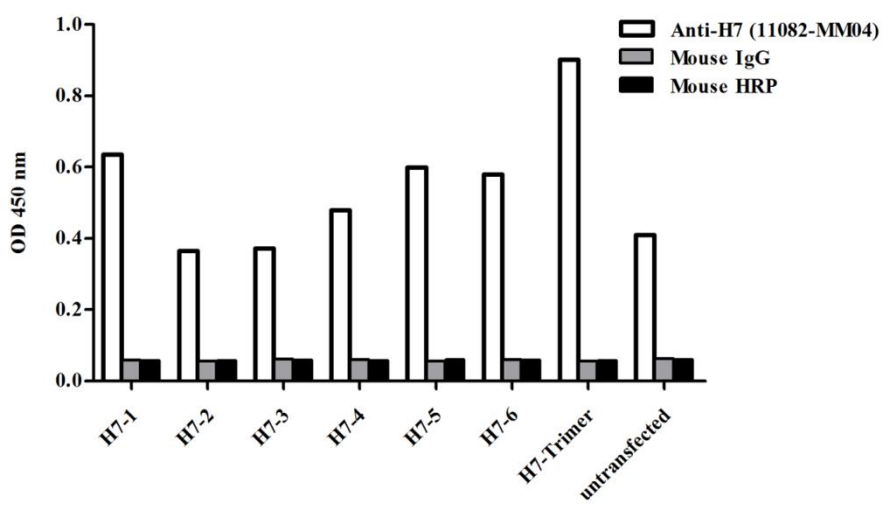




E



F



G

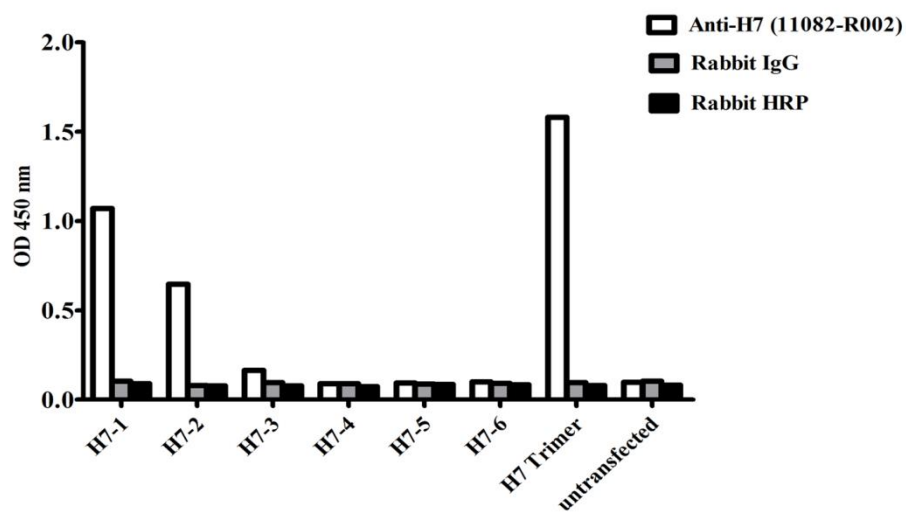
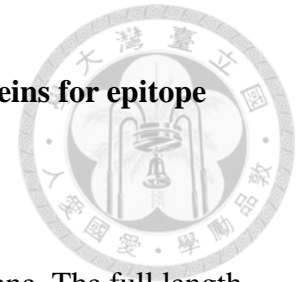



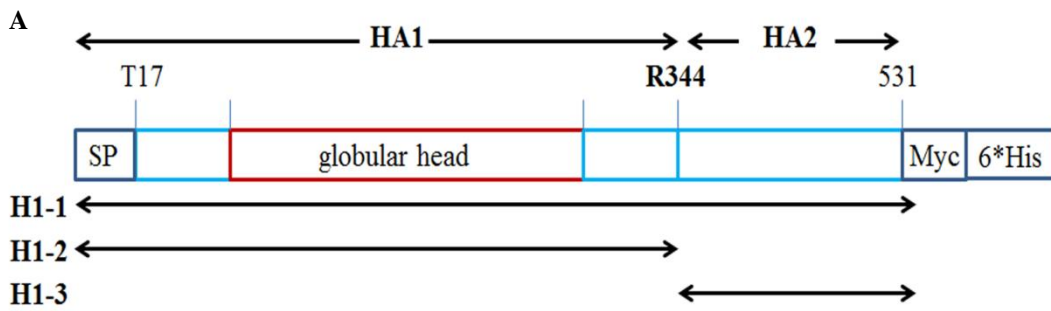
Figure 7. Generation of domain-specific of H7 recombinant proteins for epitope mapping.



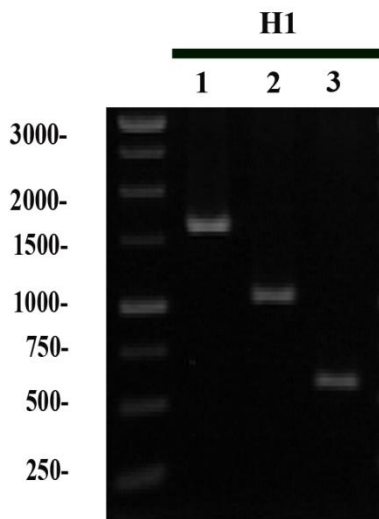
- A. Schematic diagram of the domain-specific construct of the H7 gene. The full length of H7 gene without transmembrane domain (truncated at position I525) was designated as H7-1 with a length of 1,575 bp. From the predicted proteolytic cleavage site at R339, we defined the N-terminal fragment to this site as HA1 domain, which was designated as H7-2 while the C-terminal domain of HA2 domain was designated as H7-6. For determination of strain specificity, the H7-3 construct was designed to contain the globular head domain alone, while the H7-5 construct included the stalk domain on the HA2. H7-5 comprised the epitopes of importance for some well-known broadly neutralizing Abs.
- B. The cDNA inserts of these H7 fragments described in (A) were examined by agarose gel electrophoresis after cloning.
- C. Each of the H7 DNA fragments was transiently expressed in HEK293T cells. Cell lysates were analyzed by SDS-PAGE for western blotting. Since a myc tag was included at the C terminus of each construct, anti-myc mAb (1:5,000) was used to determine the proper expression and specificity of all seven constructs.
- D. Anti-H7 mAb (11082-MM04) (1 μ g/ml) was utilized to examine the correct expression of these constructs. The results were compared with (C).

- 
- E. Due to the inclusion of leader peptide of Ig κ chain, the various domain-specific H7 proteins were rendered to secrete into culture medium. The medium was collected and the amount of secreted H7 proteins was examined by ELISA assays using 1 $\mu\text{g/ml}$ of anti-myc Abs for detection.
- F. Culture media of full-length, domain, or trimeric H7 cDNA transfected HEK293T cells were collected separately and the secreted H7 proteins was examined by ELISA. H7 mAb (11082-MM04) (1 $\mu\text{g/ml}$) was used as a detection Ab.
- G. Culture media were collected and ELISA assay was performed as (F) except that anti-H7 (11082-R002) (1 $\mu\text{g/ml}$) mAb was used as the detection Ab.

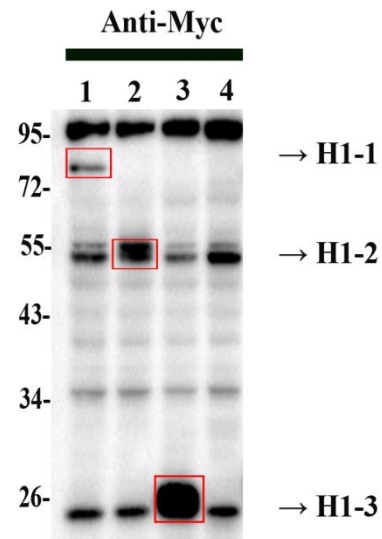
A



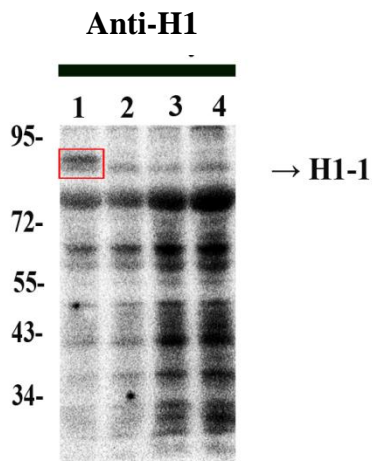
B



C



D



E

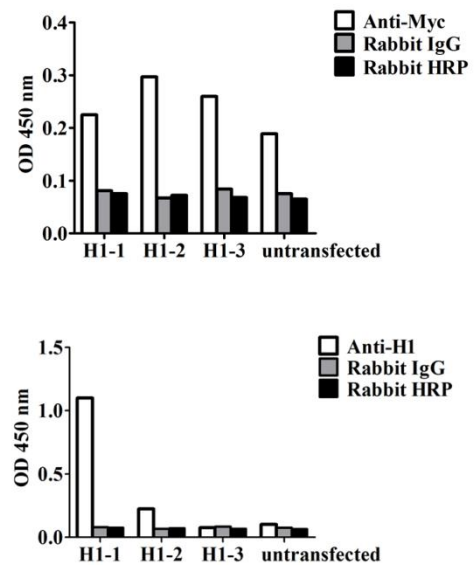


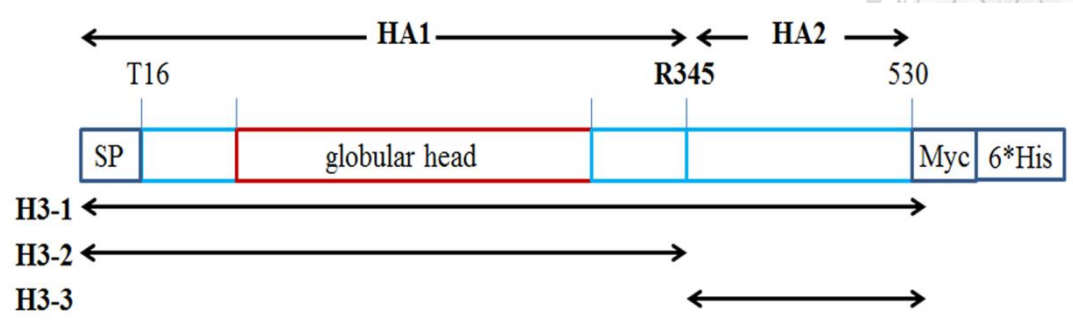


Figure 8. Generation of full-length and domain-specific H1 recombinant proteins for epitope mapping.

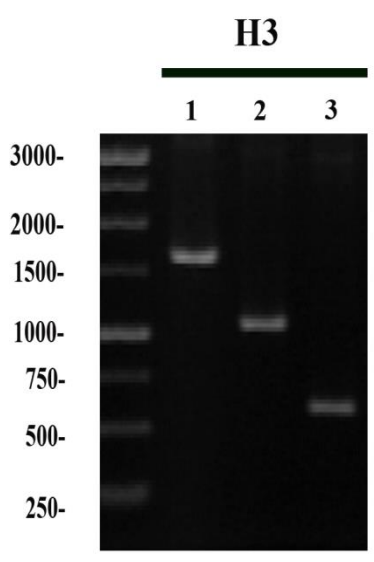
- A. The schematic diagram of H1 domain-specific constructs. The full-length H1 HA protein without transmembrane domain was divided into two domains at the trypsin-cleavage position R344. The N-terminal H1-2 domain contained the receptor-binding-site, i.e. globular head domain, whereas the C-terminal H1-3 included the conserved stalk domain. All the cDNAs of full-length or domains of the H1 gene were individually subcloned into pSecTag2A vector, which allowed inclusion of c-myc and 6 histidine tags at the C-terminal of H1 gene.
- B. The full-length and domain-specific DNA fragments of H1 gene were resolved by agarose gel electrophoresis.
- C. HEK293T cells were transiently transfected with vectors containing each piece of DNA fragments of H1 gene. Cell lysates were collected and analyzed by western blotting. The anti-myc mAb (1 $\mu\text{g/ml}$) was used to detect the C-terminal myc tag.
- D. Anti-H1 mAb (11055-RM10) (1 $\mu\text{g/ml}$) was utilized to confirm the correct expression of the constructs.
- E. Cells were transfected and culture media were collected as in **Figure 7** for ELISA assay. Anti-myc and anti-H1 mAbs were used for detection, respectively.



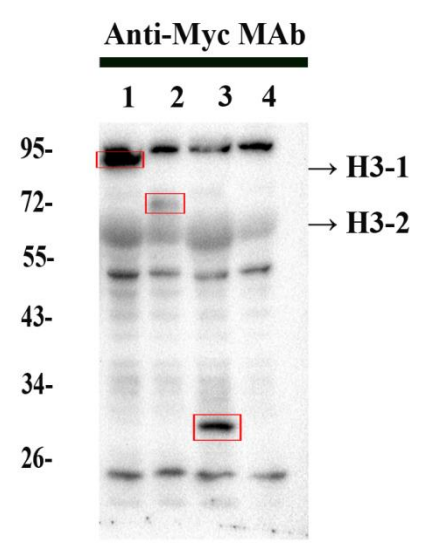
A



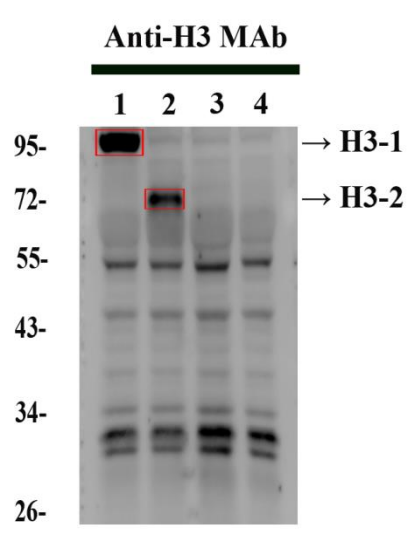
B



C



D



E

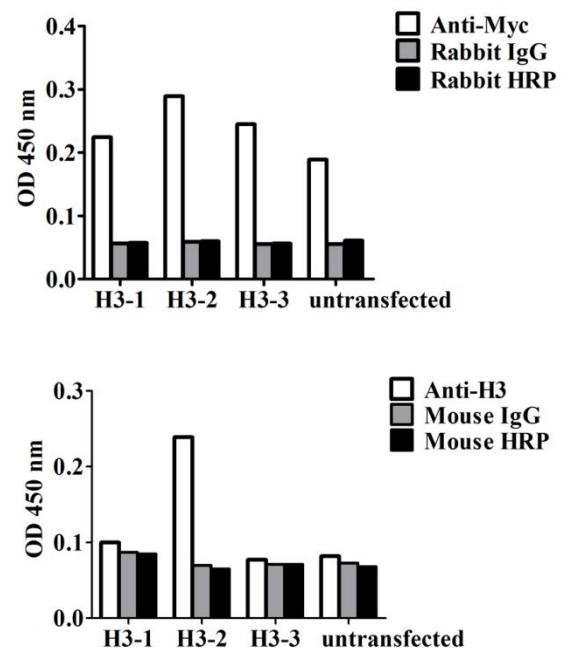
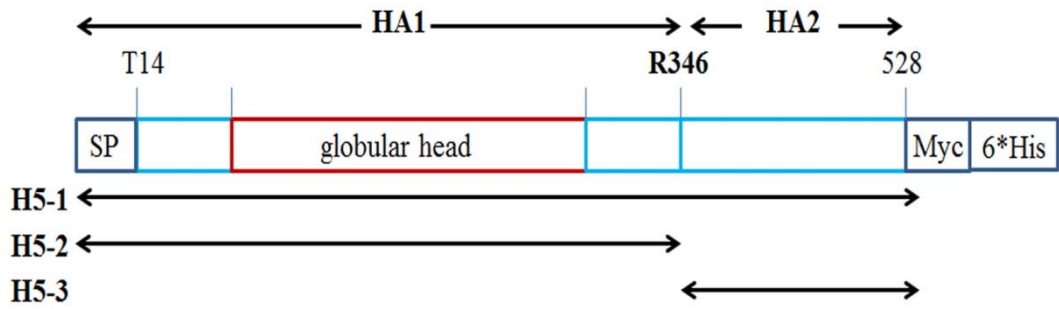




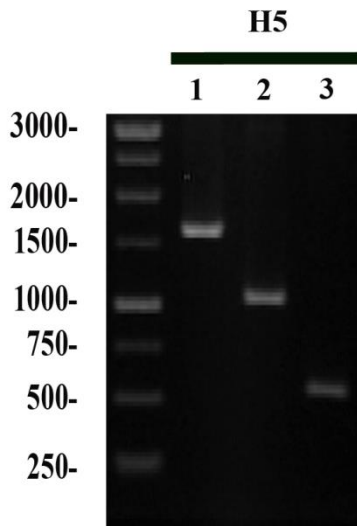
Figure 9. Generation of full-length and domain-specific H3 recombinant proteins for epitope mapping.

- A. Schematic diagram of H3 domain-specific constructs. The H3 full-length protein without transmembrane domain was divided into two domains at the trypsin-cleavage position R345. The N-terminal H3-2 domain contained the globular head domain for receptor binding while the C-terminal H3-3 included the conserved stalk domain. The cDNAs of these H3 domains were subcloned into the pSecTag2A vector.
- B. The DNA fragments of H3 gene were analyzed by running an agarose gel.
- C. HEK293T cells were transfected with constructs containing either full-length or each domain fragment of H3 gene. Cell lysates were analyzed by SDS-PAGE and western blotting. The anti-myc mAb (1 $\mu\text{g/ml}$) was used to detect the C-terminal myc tag fused to the full-length and domain H3 proteins, respectively.
- D. Anti-H3 mAb (11056-MM05-50) (1 $\mu\text{g/ml}$) was utilized to confirm the correct expression of the constructs.
- E. Cells were transfected and culture media were collected as in **Figure 7** for ELISA assays. Anti-myc and anti-H3 (11056-MM05-50) mAbs were used for detection.

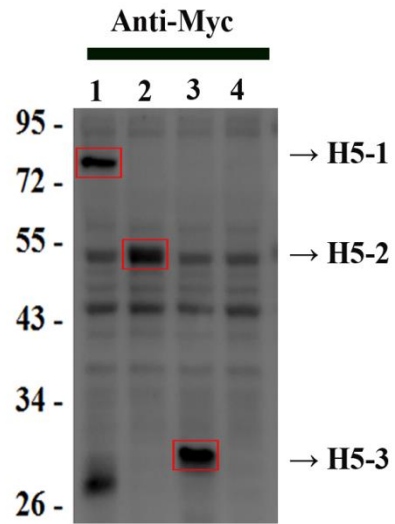
A



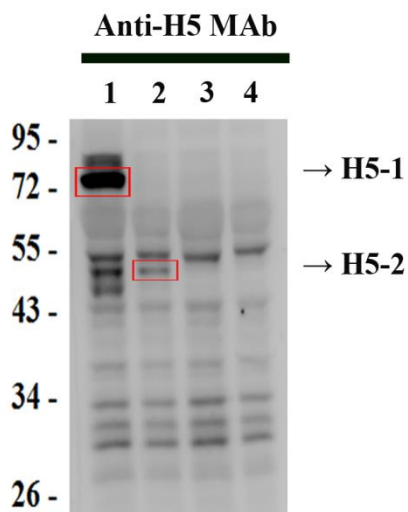
B



C



D



E

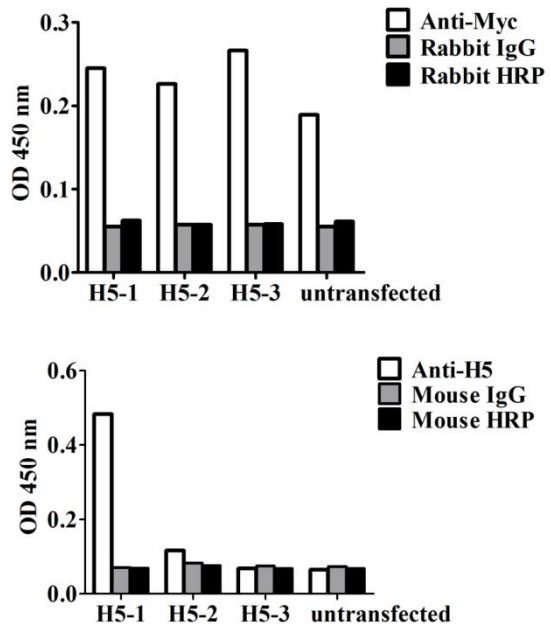




Figure 10. Generation of full-length and domain-specific H5 recombinant proteins for epitope mapping.

A. Schematic diagram of H5 full-length and domain-specific constructs. H5 full-length without transmembrane domain was divided into HA1 and HA2 domains at the trypsin-cleavage position R346. The N-terminal H5-2 domain contained the receptor-binding globular head domain, while the C-terminal H5-3 included the conserved stalk domain. All H5 cDNAs were PCR cloned into the pSecTag2A vector.

B. The cDNAs of H5 domain fragments were examined by agarose gel electrophoresis.

C. HEK293T cells transfected with each H5 construct separately and their cell lysates were analyzed by SDS-PAGE and western blotting. The anti-myc mAb (1 $\mu\text{g/ml}$) was used to detect the C-terminal myc tag fused to every H5 construct.

D. Anti-H5 mAb (11048-MM01-50) (1 $\mu\text{g/ml}$) was utilized to confirm the correct expression and specificity of each H5 construct.

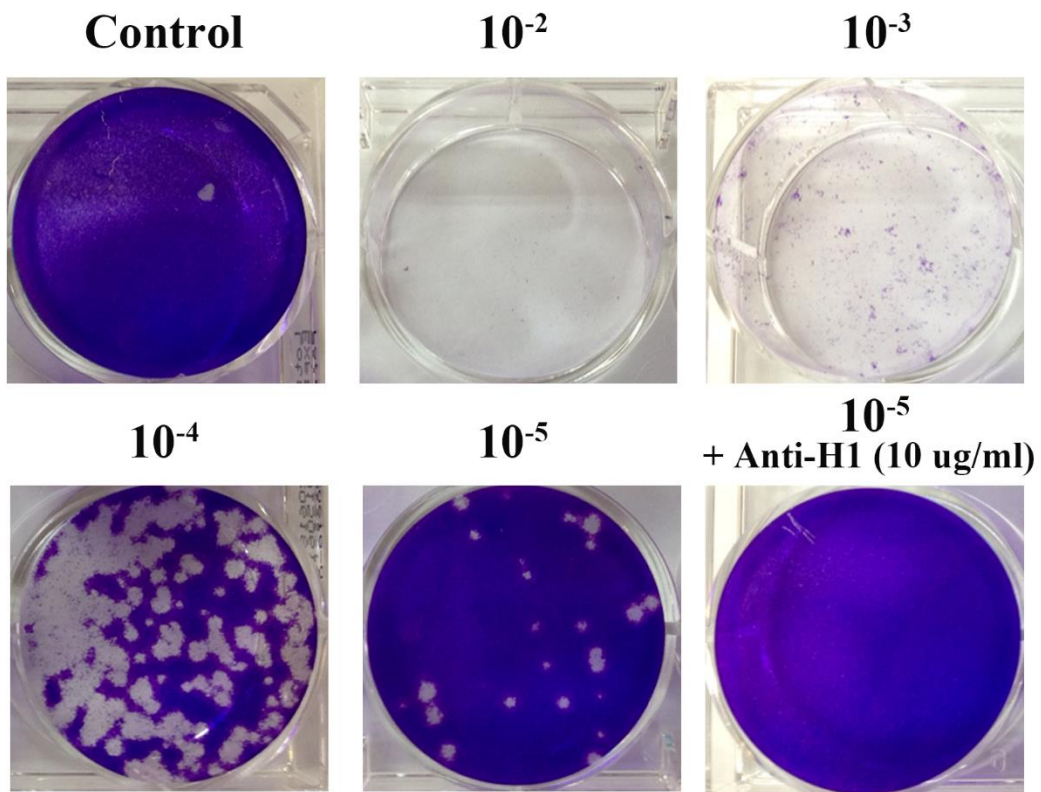
E. HEK293T cells were transfected and culture media were collected as described in

Figure 7. The secreted full-length and domain-specific H5 recombinant proteins

were examined by ELISA assays using either anti-myc or anti-H5 (11048-MM01-50) mAb for detection.

A

A/WSN/1933 H1N1 (PFU=2.5x10⁶)



B

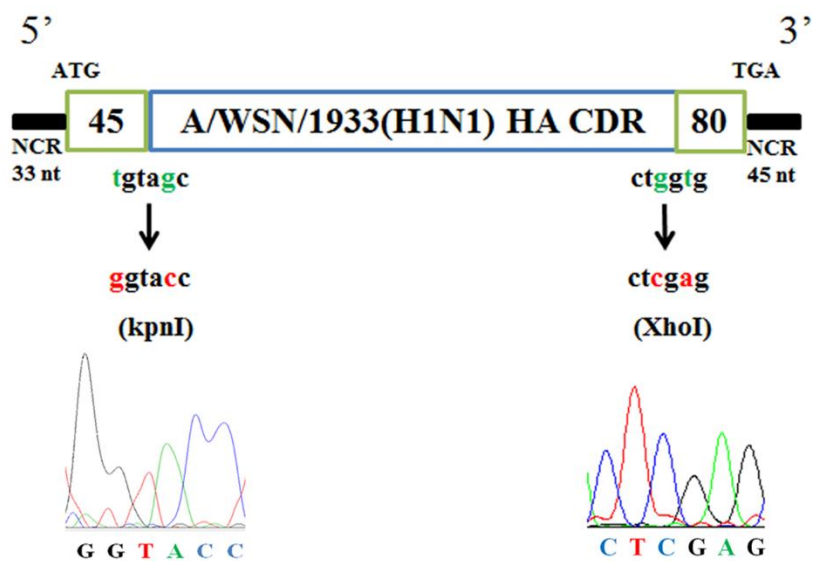




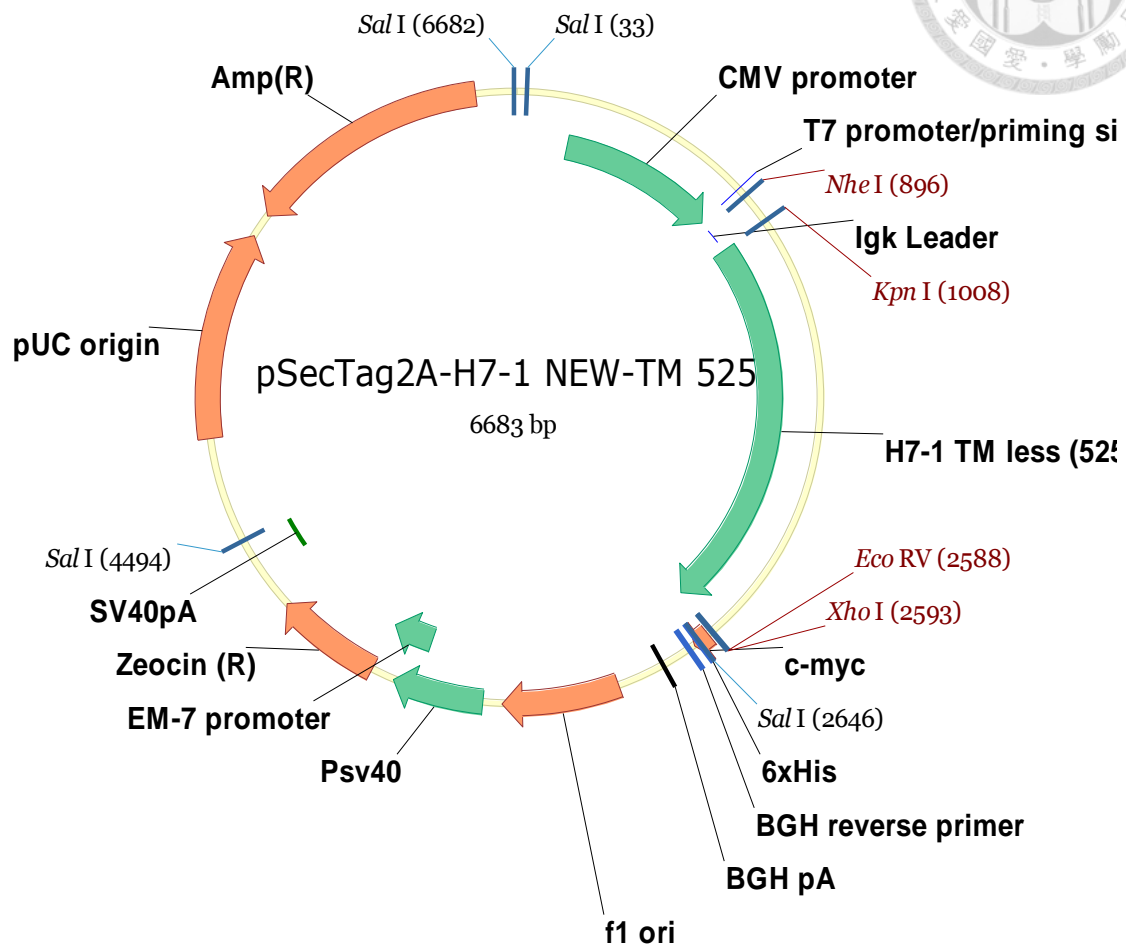
Figure 11. Plaque reduction assay of WSN-based reassortant influenza virus.

- A. WSN-based reassortant influenza virus expressing H1 proteins were examined by a plaque assay, which used MDCK cells for infection. About 1.8 ml of supernatant was collected as a virus stock. One μl from it was taken for titrating by 10-fold serial dilutions, i.e. 10^{-2} , 10^{-3} , 10^{-4} and 10^{-5} of the original, followed by infection of MDCK cells. The calculated virus titer was 2.5×10^6 PFU/ml. Virus from stock with a dilution factor of 10^5 was pre-incubated with anti-H1 Ab ($10 \mu\text{g/ml}$) before addition onto MDCK cells. No virus addition was used as a negative control.
- B. Two restriction enzyme sites, KpnI and XhoI, were generated between first 45 and the last 80 nucleotides of coding region of A/WSN/33/H1N1 HA gene by site-directed mutagenesis to retain the packaging sequence of H1 for replacement of the coding region of H1 with different subtypes of HA.



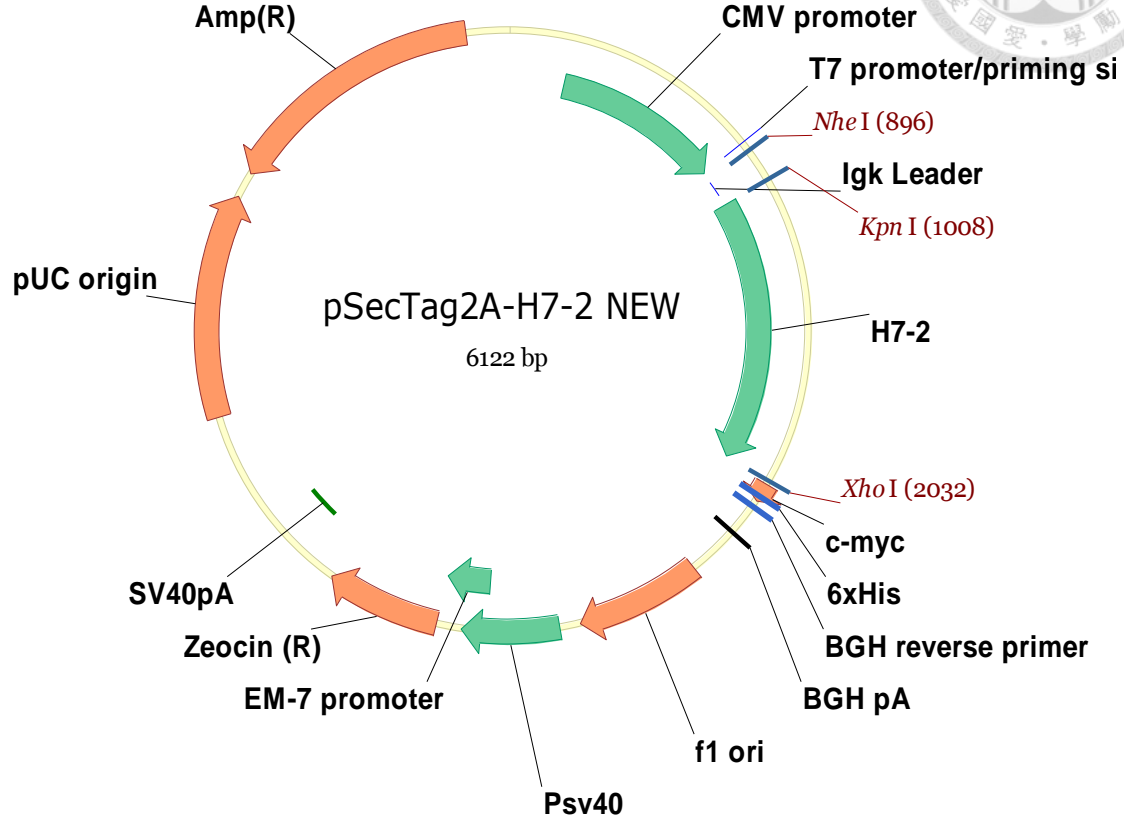
Appendix

Appendix 1. pSecTag2A-H7-1



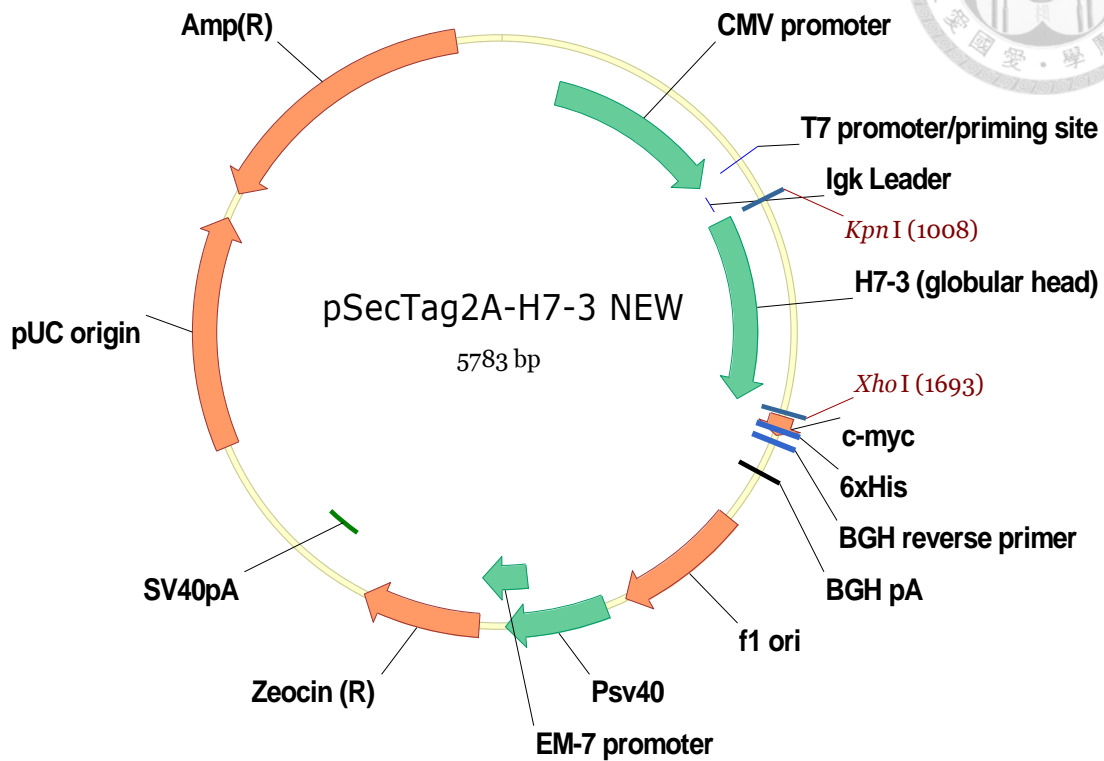
H7-1, which includes 525 amino acids without transmembrane domain were amplified by DNA polymerase (Phusion) using TSJ429 and TSJ507 primers, which contained KpnI and XhoI sites for cloning. PCR cycle was set for annealing temperature at 57 °C for 40 cycle using the pCMV-H7 vector (Sino Biological Inc.) as template. After digestion, the H7-1 (525) was flanked by KpnI and XhoI sites was subcloned into cloning sites 3' to the leader peptide sequence of pSecTag2A by T4 ligase for ligation.

Appendix 2. pSecTag2A-H7-2



H7-2, which included HA1 domain of H7 were amplified by PCR with TSJ429 and TSJ431 primers containing KpnI and XhoI sites. PCR was performed with DNA polymerase (Phusion) for 40 cycles at the condition of annealing temperature 60 °C. The pCMV-H7 plasmid containing the H7 cDNA (Sino Biological Inc.) was the template. After digested with both the two restriction enzymes, the H7-2 cDNA was subcloned into the KpnI and XhoI cloning sites 3' to the sequence of leader peptide of pSecTag2A vector.

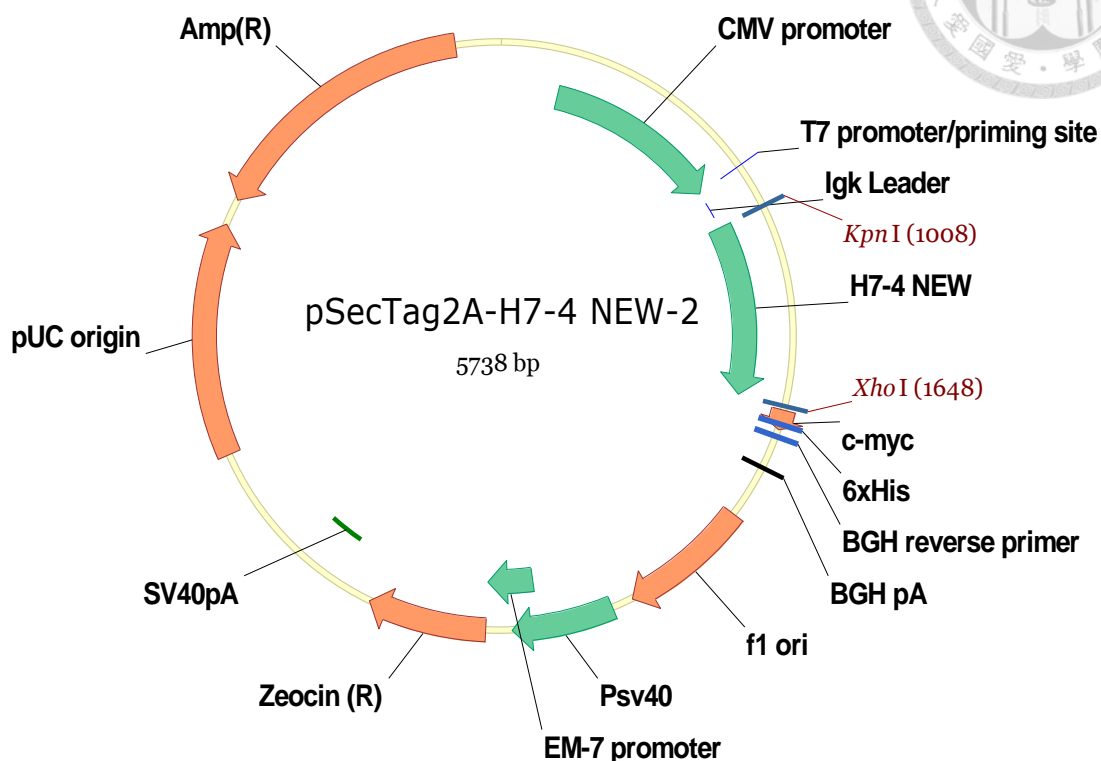
Appendix 3. pSecTag2A-H7-3



H7-3, which includes the globular head domain of H7 was amplified by PCR with TSJ432 and TSJ433 primers containing KpnI and XhoI sites for 40 cycles at the condition of annealing temperature 62 °C and pCMV-H7 (Sino Biological Inc.) was included as the template. After digestion with KpnI and XhoI, the H7-3 cDNA were subcloned into these sites in frame following the sequences of leader peptide in the pSecTag2A vector.

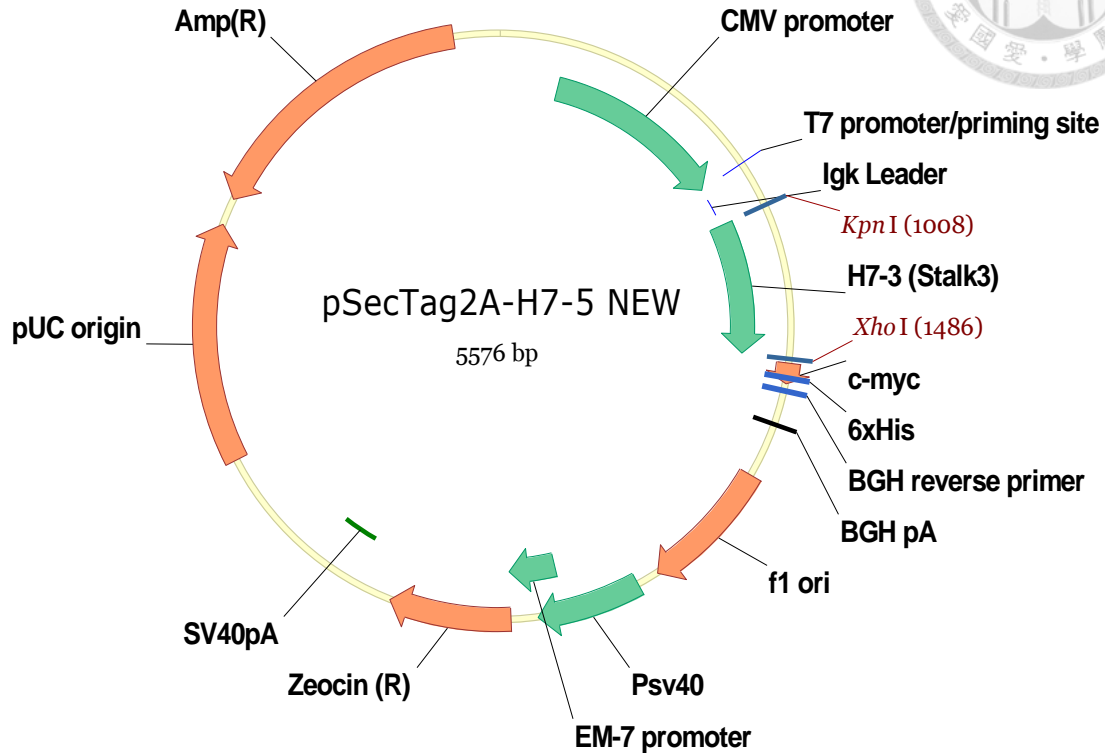


Appendix 4. pSecTag2A-H7-4



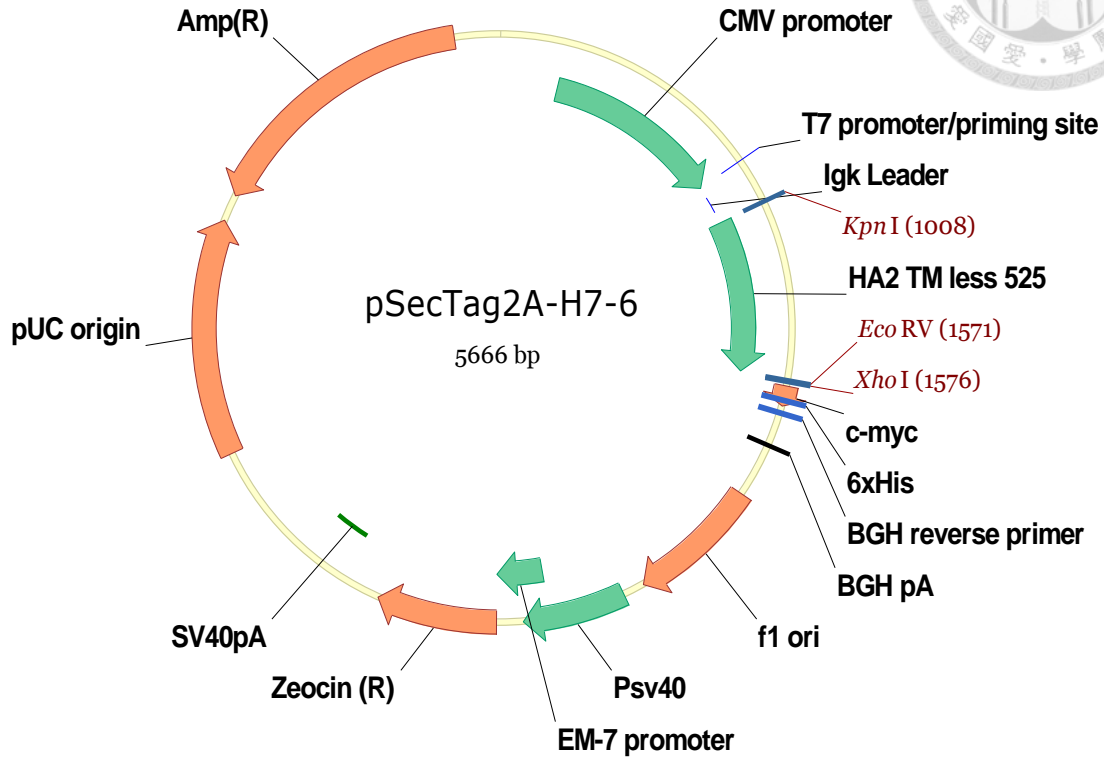
H7-4, which included the stalk domain of H7, was amplified by PCR with TSJ434 and TSJ430 primers and pCMV-H7 (Sino Biological Inc.) template using DNA polymerase (Phusion) at annealing temperature 62 °C for 40 cycles. After digestion with KpnI and XhoI, the H7-4 cDNA was subcloned into the corresponding cloning sites of the pSecTag2A vector.

Appendix 5. pSecTag2A-H7-5



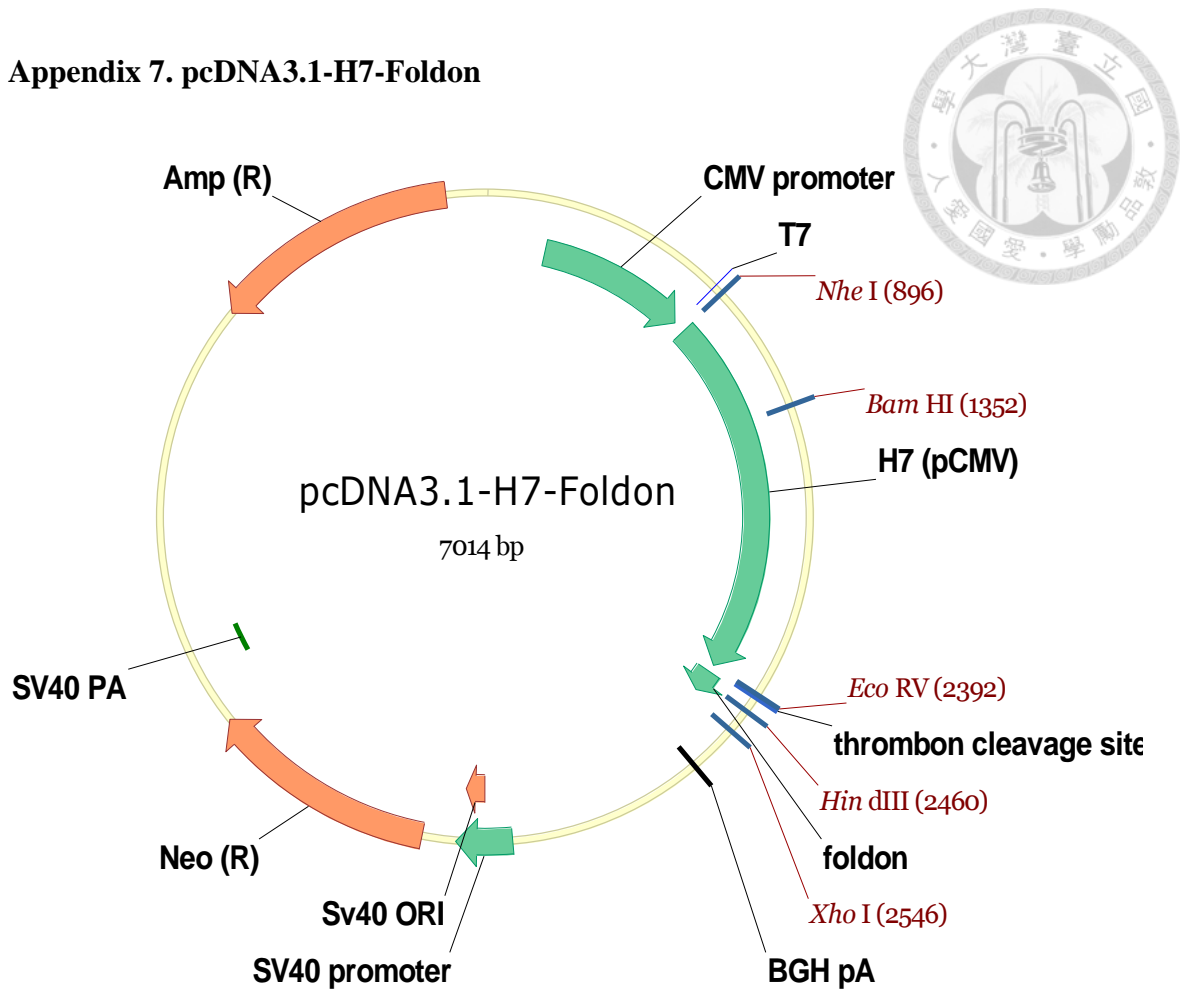
H7-5, which was composed of several important epitopes of the well-known broadly neutralizing antibodies, was amplified by PCR using TSJ435 and TSJ430 primers and pCMV-H7 (Sino Biological Inc.) template. PCR was performed at 62 °C for annealing for 40 cycles. The PCR products were then digested with KpnI and XhoI for subcloning into the corresponding sites of pSecTag2A vector.

Appendix 6. pSecTag2A-H7-6



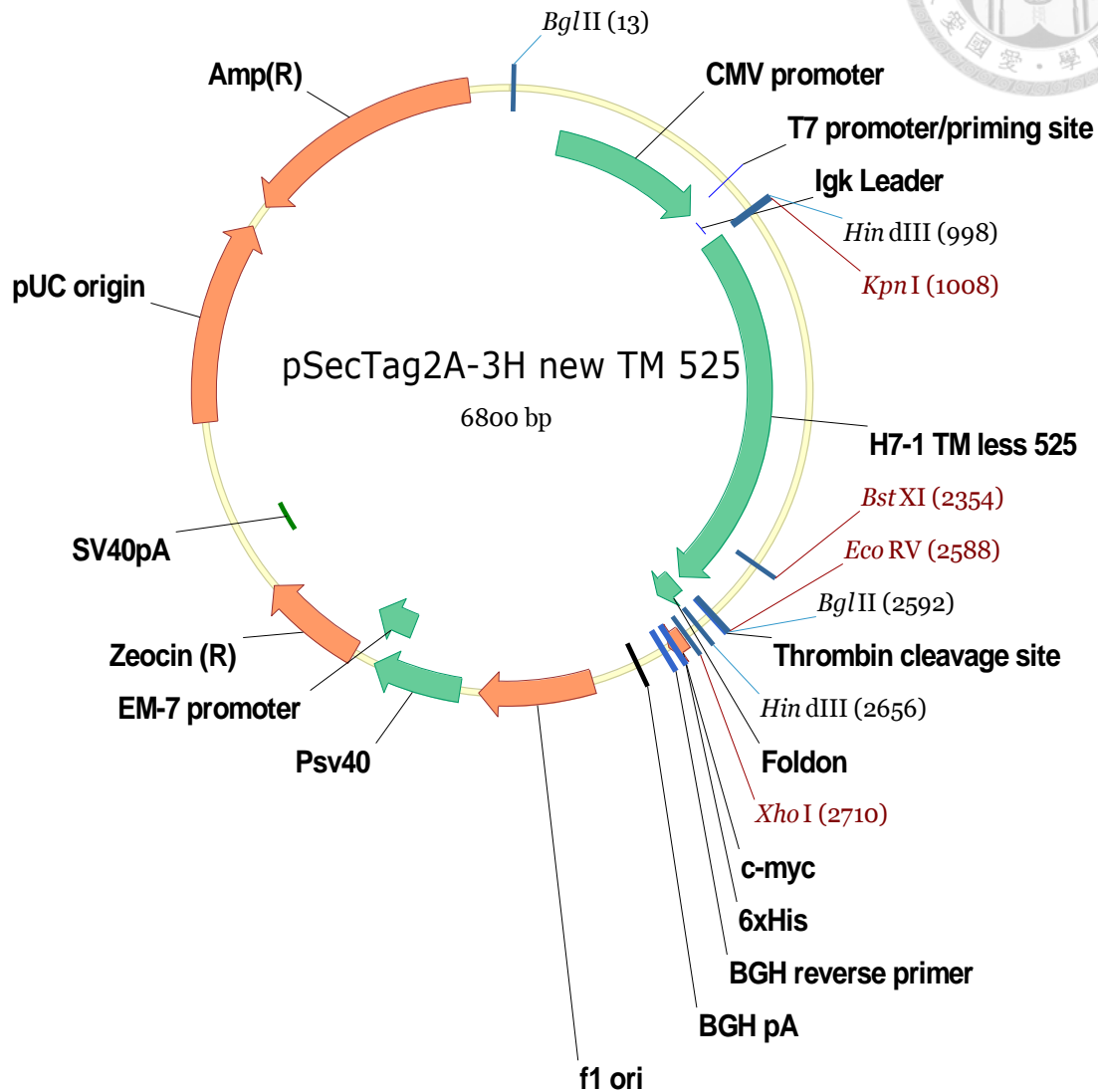
H7-6, which was composed of HA2, was amplified by PCR with TSJ435 and TSJ507 primers and pCMV-H7 (Sino Biological Inc.) template. PCR was performed at annealing temperature 62 °C for 40 cycles, followed by digestion with KpnI and XhoI. The purified H7-6 cDNAs were subcloned into KpnI and XhoI cloning sites of the pSecTag2A vector.

Appendix 7. pcDNA3.1-H7-Foldon



H7 without sequences of transmembrane domain was amplified by PCR with TSJ363 and TSJ394 primers containing NheI and EcoRV sites, respectively at a condition of annealing temperature 54 °C for 40 cycles. The pCMV-H7 (Sino Biological Inc.) was included as template. After digested with NheI and EcoRV, the purified H7 cDNAs were subcloned into the pcDNA3.1-H1-foldon vector to replace the H1 cDNA, resulting in formation of H7-foldon fusion proteins when expressed.

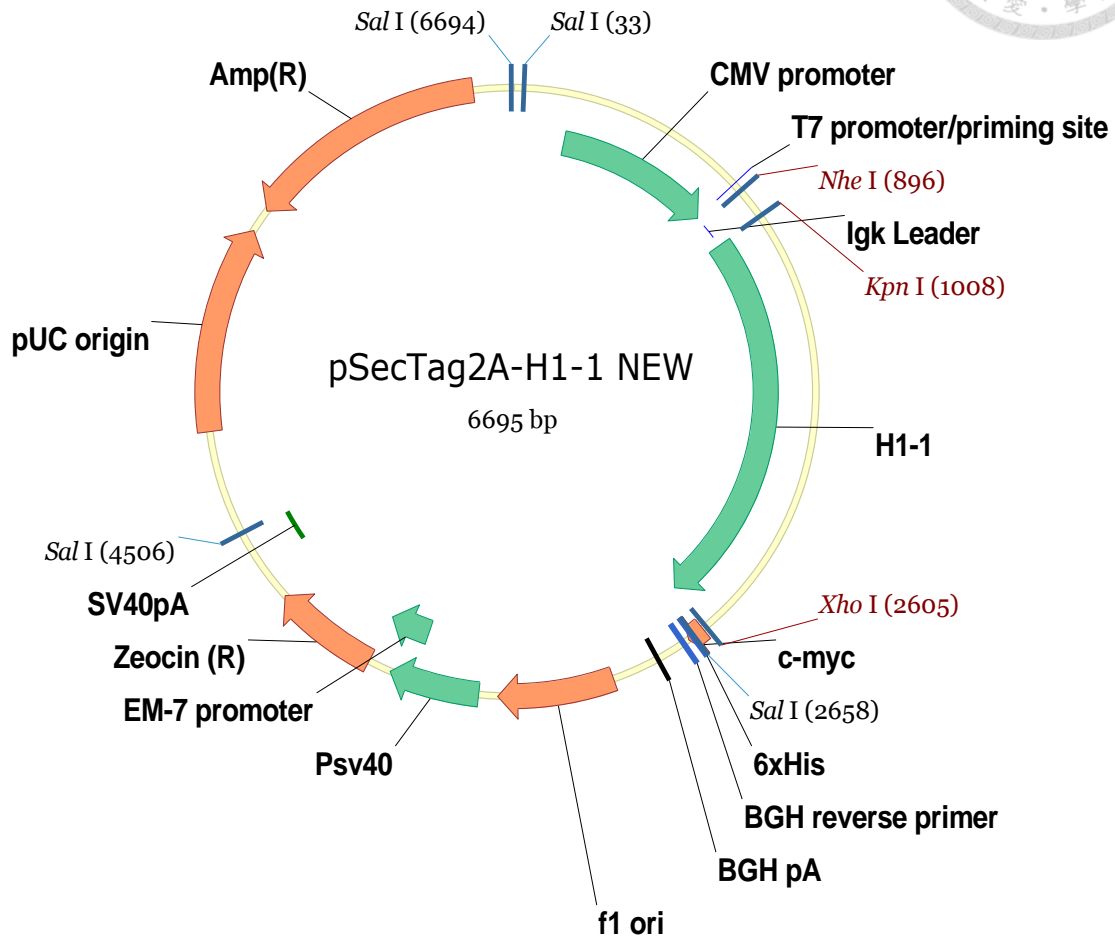
Appendix 8. pSecTag2A-3H



H7-foldon, which forms trimeric structure, was amplified by PCR with TSJ429 and TSJ452 primers containing KpnI and XhoI sites. PCR was performed at the condition of annealing temperature 62 °C for 40 cycles using pcDNA3.1-H7-Foldon as the template. After digested with both restriction enzymes, the H7-foldon cDNAs were subcloned into the pSecTag2A expression vector..

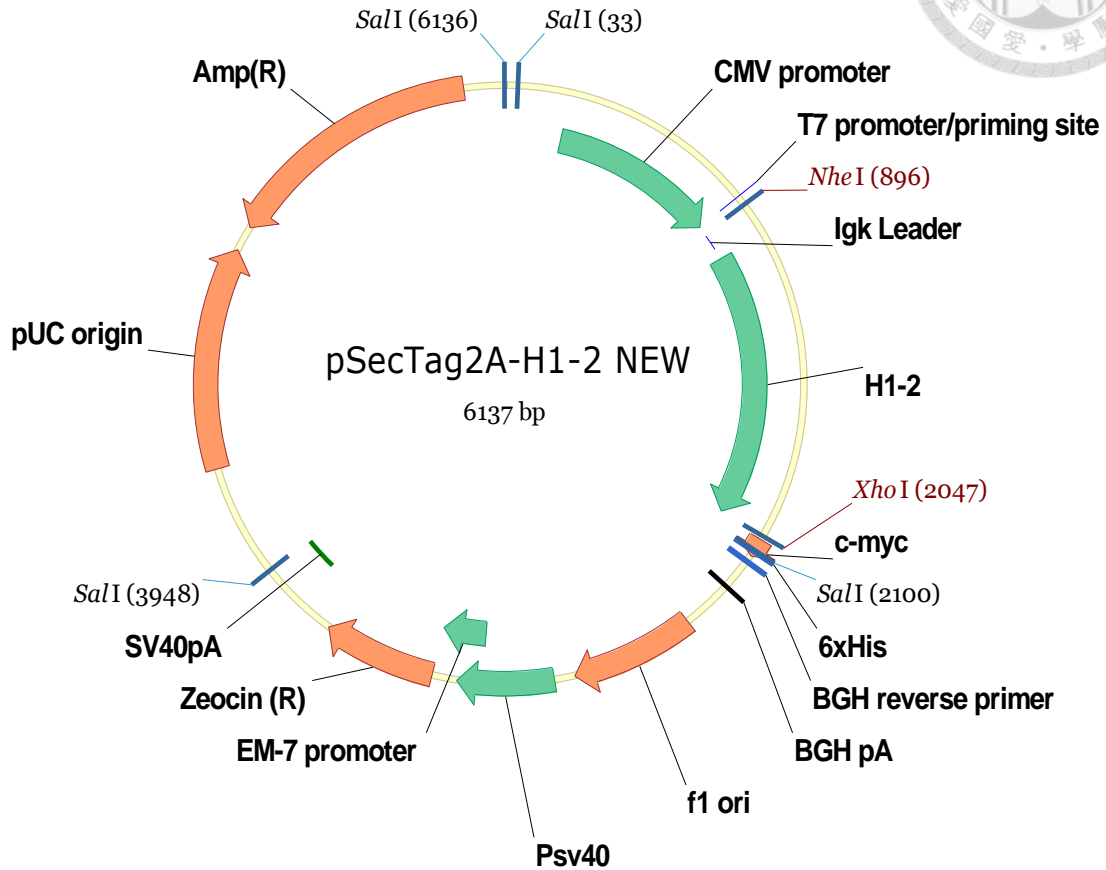


Appendix 9. pSecTag2A-H1-1



H1-1, which contains full-length H1 without transmembrane domain, was amplified by PCR with TSJ494 and TSJ495 primers and pCMVH1 (Sino Biological Inc.) template at annealing temperature 60 °C for 40 cycles. The PCR products of H1-1 were digested with KpnI and XhoI and subcloned into the corresponding sites in the pSecTag2A vector.

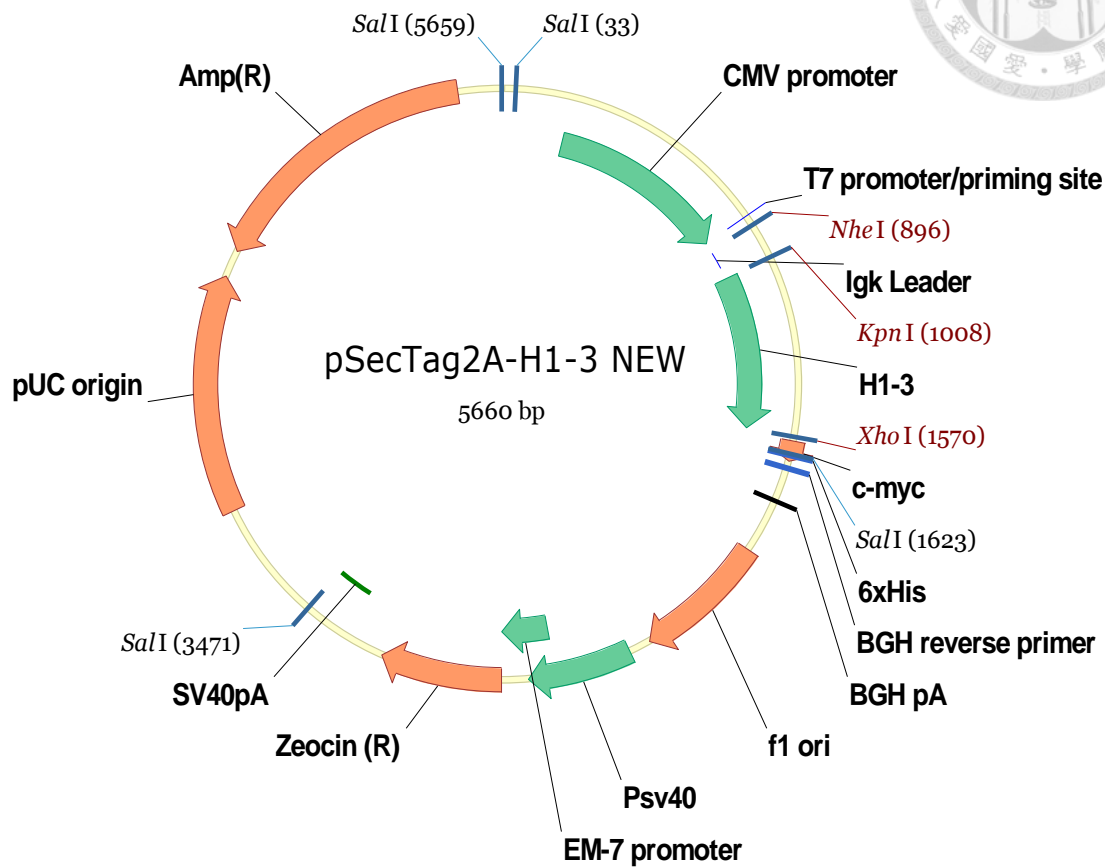
Appendix 10. pSecTag2A-H1-2



H1-2, which contains HA1 domain of H1, was amplified by PCR with TSJ494 and TSJ496 primers and pCMVH1 (Sino Biological Inc.) template at annealing temperature 60 °C for 40 cycles. The amplified H1-2 cDNAs were digested with KpnI and XhoI sites and subcloned into the pSecTag2A vector.

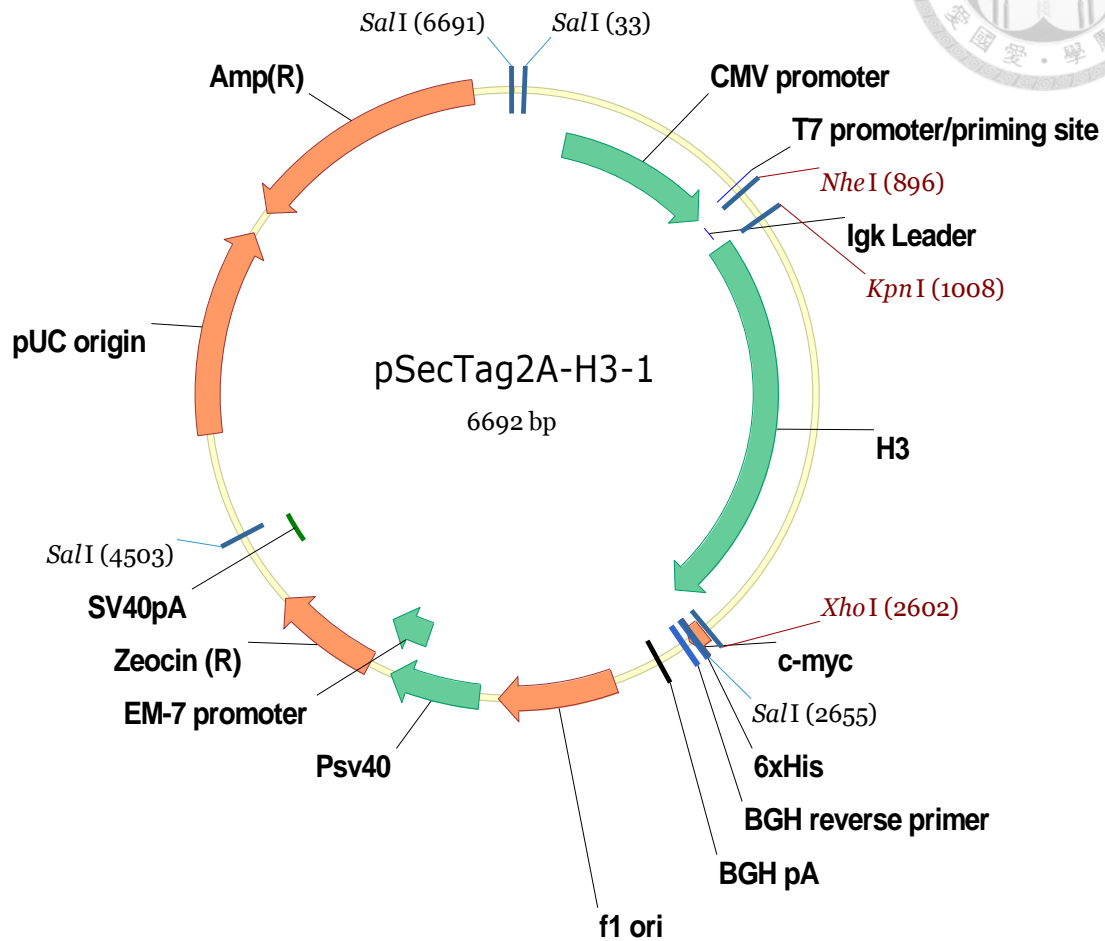


Appendix 11. pSecTag2A-H1-3



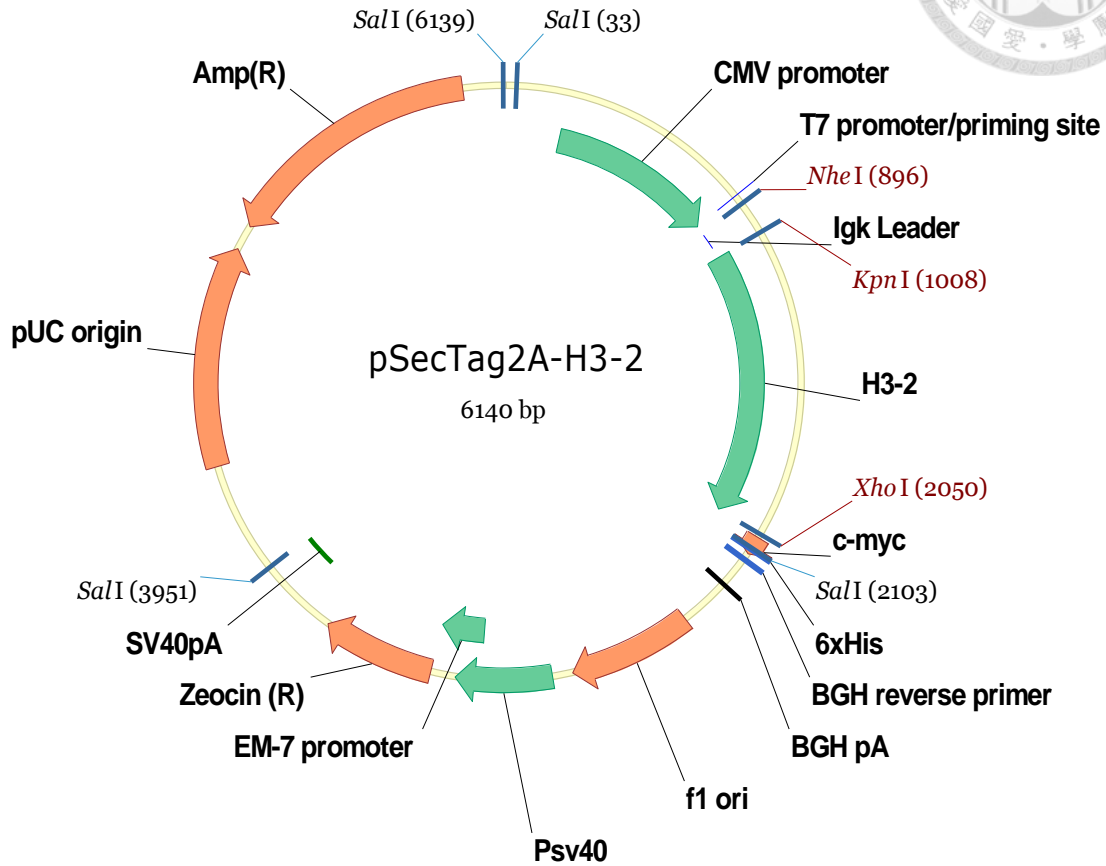
H1-3, which contained HA2domain of H1, was amplified by PCR with TSJ497 and TSJ496 primers containing KpnI and XhoI sites, respectively and pCMVH1 (Sino Biological Inc.) template. The PCR reaction was performed at annealing temperature 60 °C for 40 cycles using DNA polymerase (Phusion). After digestion, the H1-3 cDNAs were subcloned into KpnI and XhoI sites of the pSecTag2A vector.

Appendix 12. pSecTag2A-H3-1



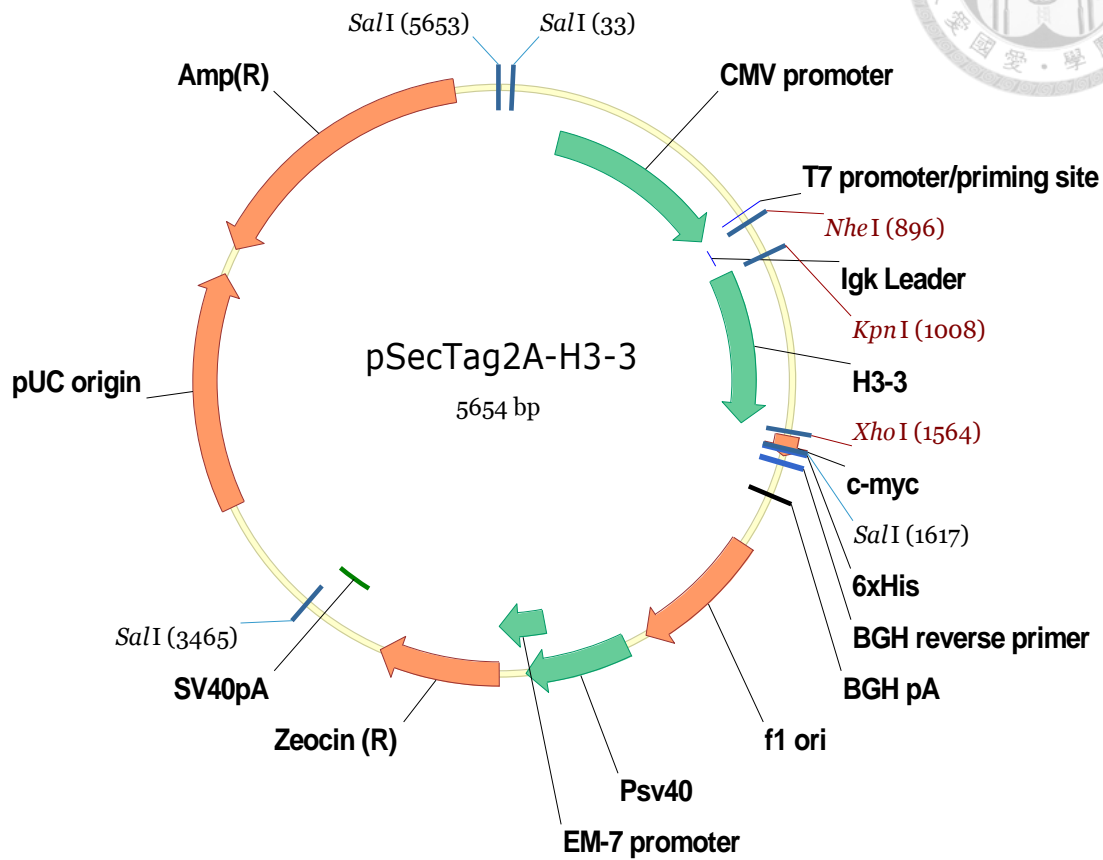
H3-1, which contains HA2 domain of H1, was amplified by PCR with TSJ486 and TSJ487 primers containing KpnI and XhoI sites, respectively and pCMVH3 (Sino Biological Inc.) template. The PCR was performed at the condition of annealing temperature 60 °C for 40 cycles. After digestion the H3-1 cDNAs were subcloned into the KpnI and XhoI sites of the pSecTag2A vector.

Appendix 13. pSecTag2A-H3-2



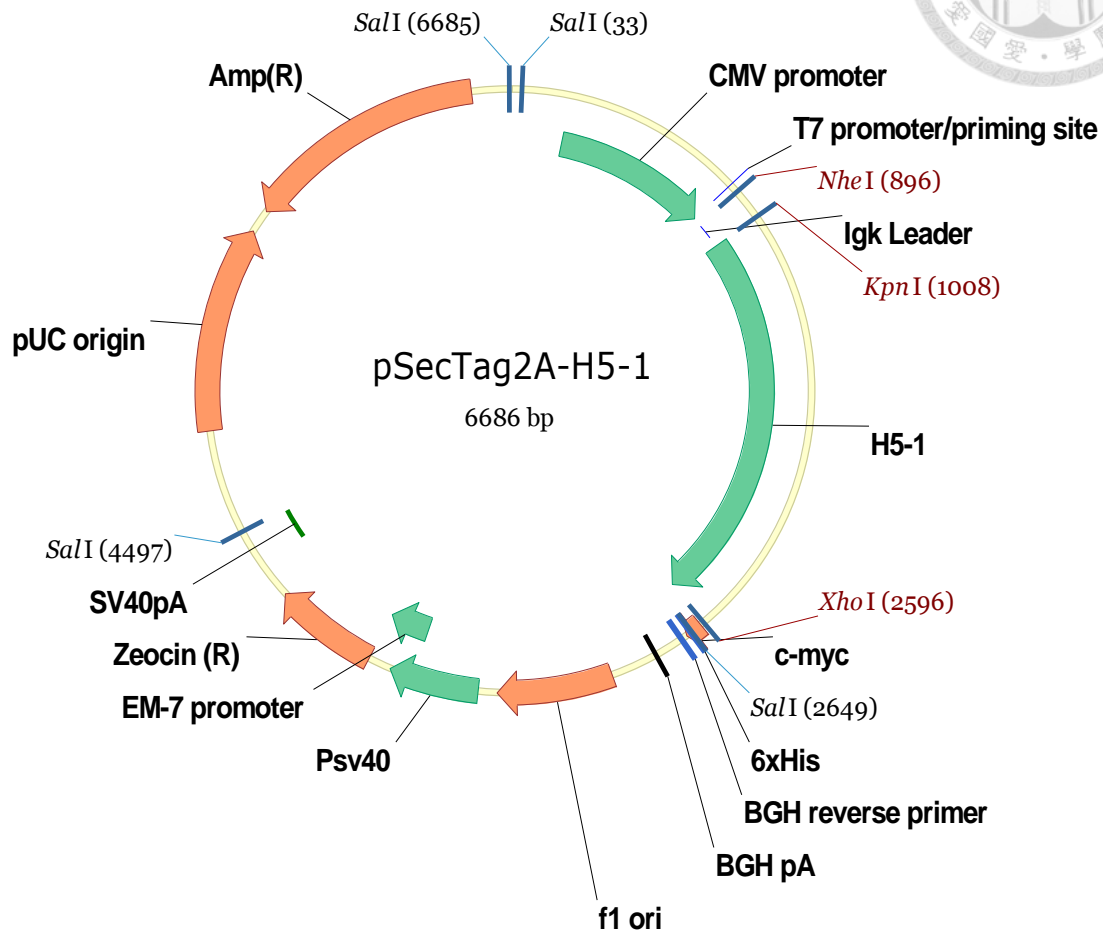
H3-2, which contained HA1 domain of H3, was amplified by PCR with TSJ486 and TSJ488 primers containing KpnI and XhoI sites, respectively and pCMVH3 (Sino Biological Inc.) template at the condition of annealing temperature 60 °C for 40 cycles. After digestion, the H3-2 cDNAs were subcloned into the KpnI and XhoI sites of the pSecTag2A vector.

Appendix 14. pSecTag2A-H3-3



H3-3, which contained HA2domain of H3, was amplified by PCR with TSJ489 and TSJ487 primers and pCMVH3 (Sino Biological Inc.) template. PCR was performed at annealing temperature 60 °C for 40 cycles. After digestion and purification, the H3-3 cDNAs were subcloned into the KpnI and XhoI sites of the pSecTag2A expression vector.

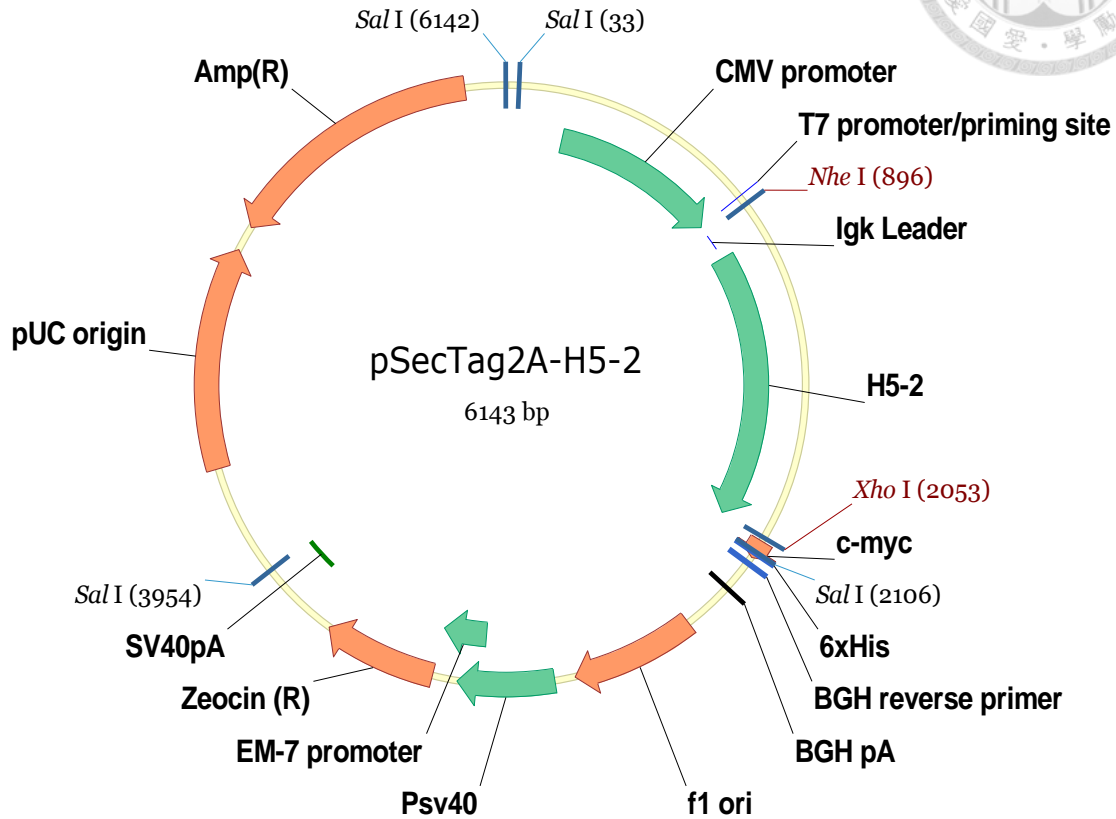
Appendix 15. pSecTag2A-H5-1



H5-1, which contained HA2domain of H3, was amplified by PCR with TSJ490 and TSJ491 primers containing KpnI and XhoI sites, respectively and pCMVH5 (Sino Biological Inc.) template. PCR was performed at the condition of annealing temperature 60 °C for 40 cycles using DNA polymerase (Phusion). After digestion the H5-1 cDNAs were subcloned into the KpnI and XhoI sites of the pSecTag2A vector.

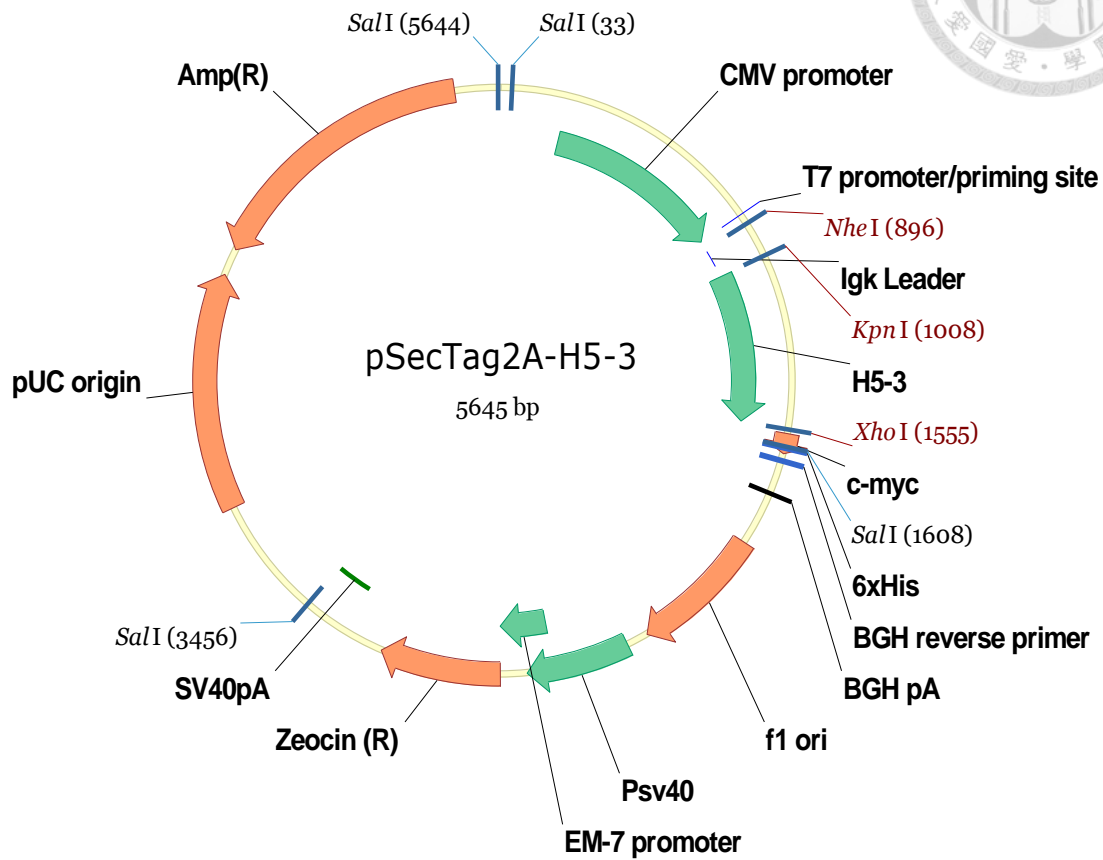


Appendix 16. pSecTag2A-H5-2



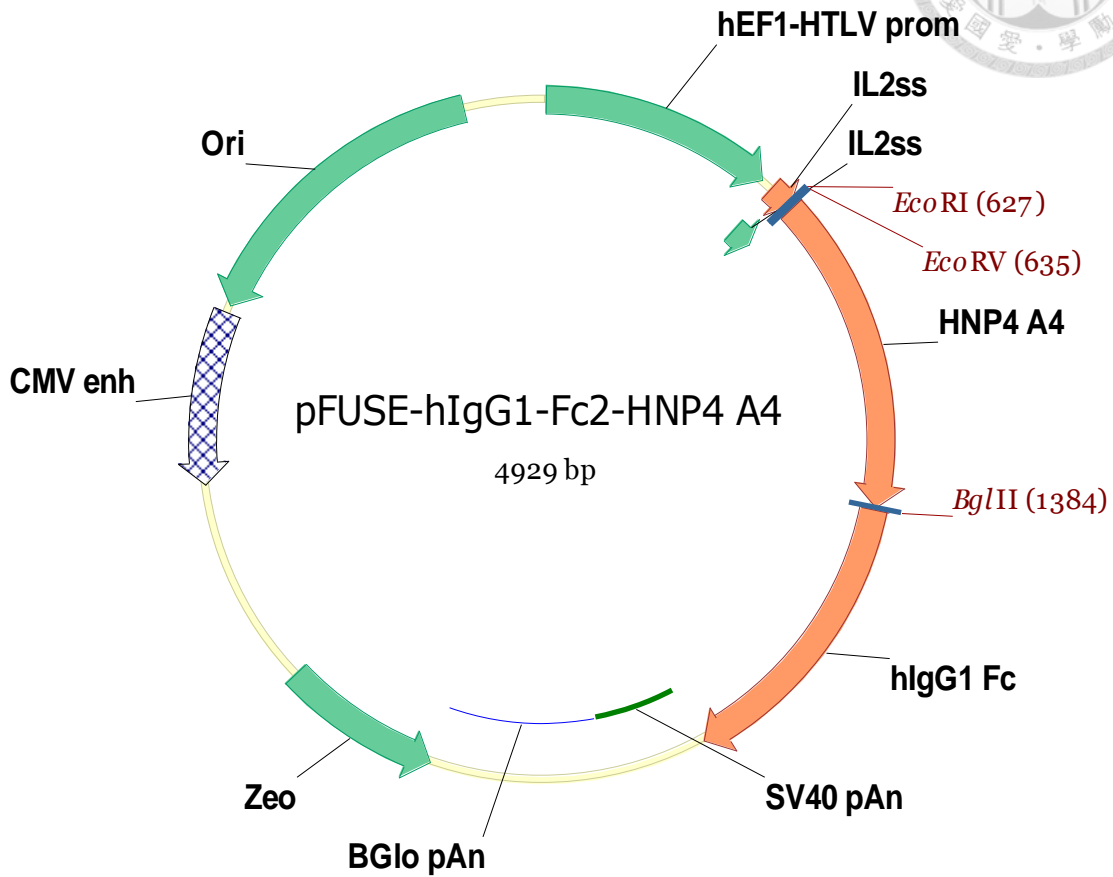
H5-2, which contained HA1 domain of H5, was amplified by PCR with TSJ490 and TSJ492 primers and pCMVH5 (Sino Biological Inc.) template. PCR was performed at the condition of annealing temperature 60 °C for 40 cycles using DNA polymerase (Phusion). After digestion with KpnI and XhoI, the H5-2 cDNAs were subcloned into the pSecTag2A vector.

Appendix 17. pSecTag2A-H5-3



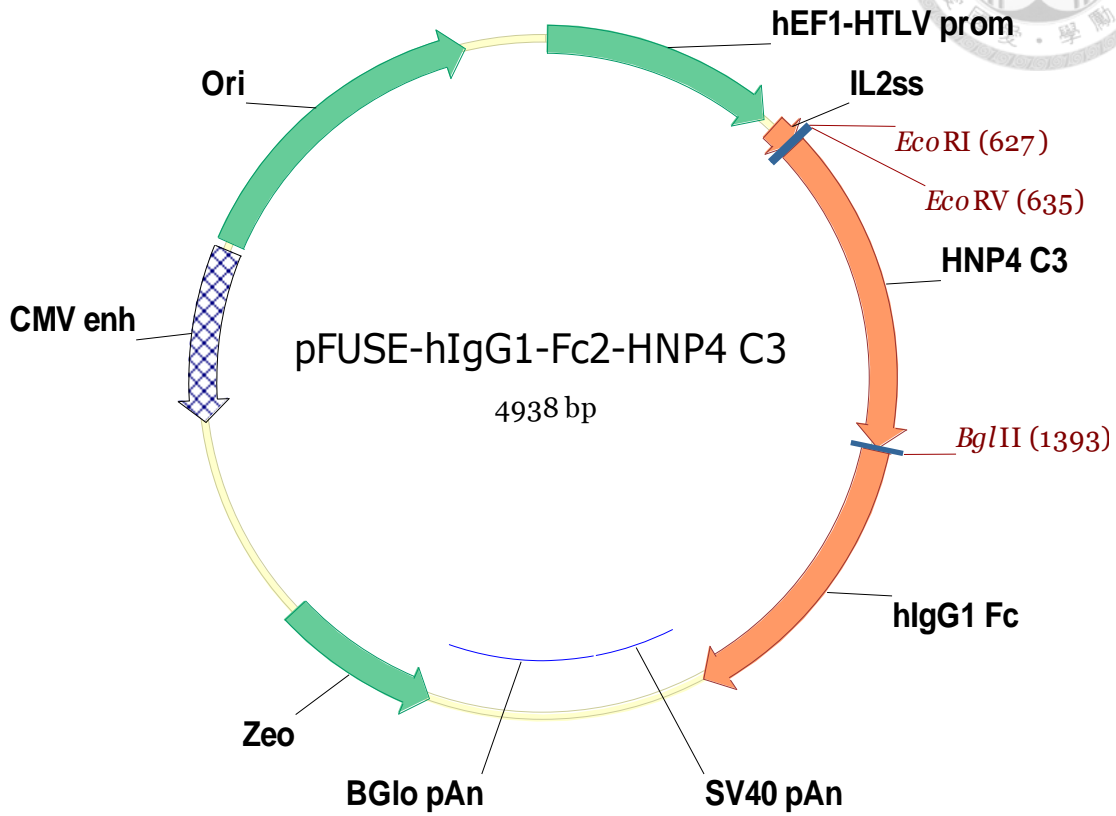
H5-3, which contained HA2 domain of H5, were amplified by PCR with TSJ492 and TSJ493 primers and pCMVH5 (Sino Biological Inc.) template. PCR was performed at the condition of annealing temperature 60 °C for 40 cycles using DNA polymerase (Phusion). After digestion with KpnI and XhoI, the H5-3 cDNAs were subcloned to the corresponding sites of the pSecTag2A vector.

Appendix 18. pFUSE-hIgG1-Fc2-HNP4 A4



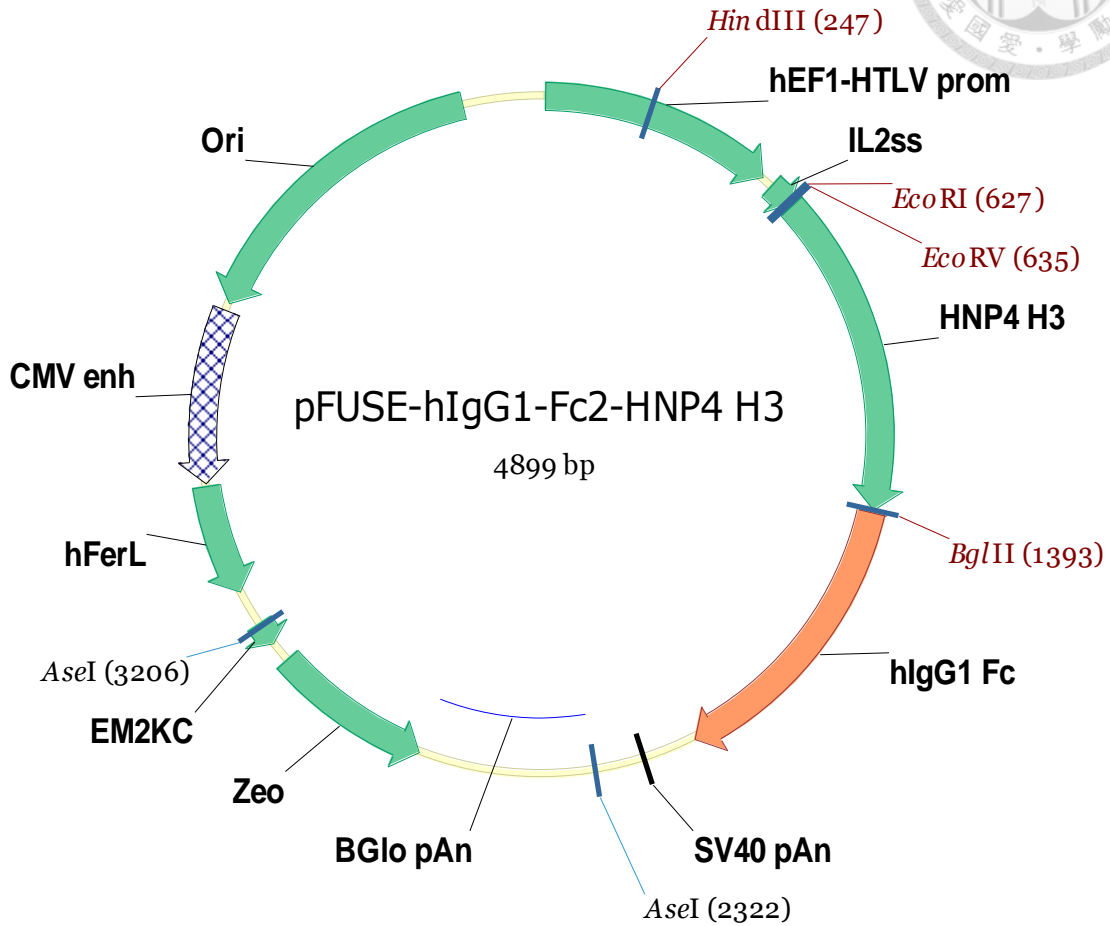
The synthesized heavy chain and light chain genes of HNP4-A4 scFV antibody were cut out with EcoRV and BglII, followed by purification and subcloning into the pFUSE-hIgG1-Fc2 plasmid containing the CH2 and CH3 domains of the human IgG heavy chain, the hinge region and the IL2 signal peptide.

Appendix 19. pFUSE-hIgG1-Fc2-HNP4 C3



The synthesized heavy chain and light chain genes of HNP4-C3 scFV antibody were digested with EcoRV and BglII and the purified inserts were subcloned into the pFUSE-hIgG1-Fc2 plasmid containing the CH2 and CH3 domains of the human IgG heavy chain, the hinge region and the IL2 signal peptide.

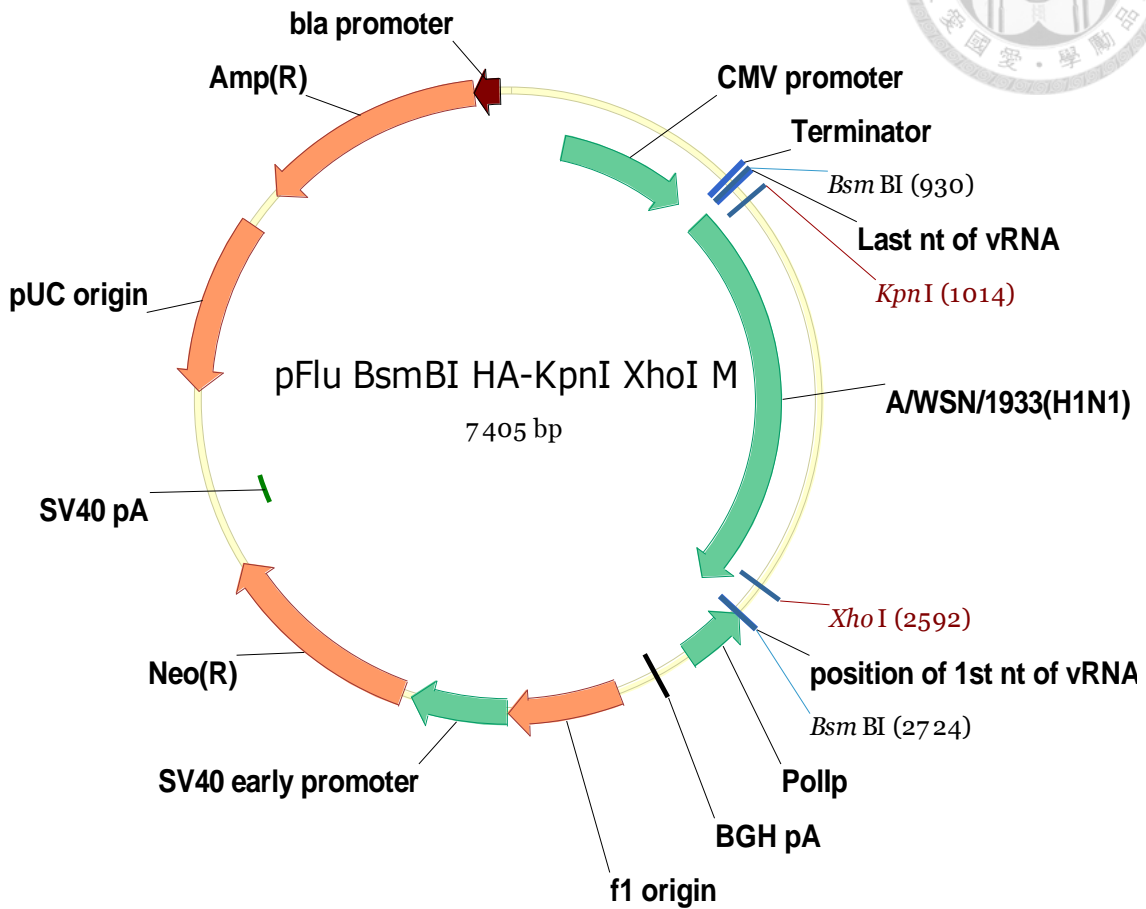
Appendix 20. pFUSE-hIgG1-Fc2-HNP4 H3



The synthesized heavy chain and light chain genes of HNP4-H4 scFV antibody were digested with EcoRV and BglII and the inserts were subcloned into the pFUSE-hIgG1-Fc2 plasmid containing the CH2 and CH3 domains of the human IgG heavy chain, the hinge region and the IL2 signal peptide.



Appendix 21. pFlu BsmBI HA-KpnI XhoI M



PCR primers were designed to create two restriction enzyme sites to fit in the coding region of A/WSN/33/H1N1 HA gene. At the end of the 5' packaging region (first 45 nucleotides of coding sequence) in front of coding region, KpnI restriction site was created with TSJ498 and TSJ499 primers for cloning. The pfu-X DNA polymerase (SolGent) was used for PCR reaction. By same token, XhoI restriction site was generated with TSJ500 and TSJ509 primers at the end of the 3' packaging region (last 80 nucleotides of coding sequence).



Table 3. Primers for cloning

Primers	Sequence of primer
TSJ363-HA-TM-less-3'	5'-GGATATCATATCATAGGTGTTATTTCTAA-3'
TSJ394-pc3HA-5'	5'-CAGATCTCGAGATGAACACTCAAATCCTG-3'
TSJ429-pCMV-H7-5'	5'-CGGTACCGATGAACACCCAGATTCTGG-3'
TSJ431-pCMV-H7-Stalk2-3'	5'-CCTCGAGATCCCCTACCCTTTGGAATC-3'
TSJ432-pCMV-H7-LBD-5'	5'-CGGTACCGTGTAGCAAGGGCAAGAGGA-3'
TSJ433-pCMV-H7-LBD-3'	5'-CCTCGAGAACAGTTGGCATCCACCTGG-3'
TSJ434-pCMV-H7-Stalk2-5'	5'-CGGTACCGTGTGAGGGAGACTGTTACC-3'
TSJ435-pCMV-H7-Stalk3-5'	5'-CGGTACCAGGACTGTTTGGAGCCATTG-3'
TSJ452-pst3H-3' XhoI	5'-ACTCGAGATCCCAGGAAAGTAGACAGCA
TSJ466-pFlu-H7-3'	5'-ACTCGAGTTAGATGCAGATTGTGCACCT-3'
TSJ486-pST-H3-TM less-5'	5'-TGGTACCTATGAAGACCATCATTGCCCT-3'
TSJ487-pST-H3-TM less-3'	5'-CCTCGAGTCCAGTCCTTGTAGCCAGAT
TSJ488-pST-H3-HA1-3'	5'-ACTCGAGTGCCCCTGGTCTGCTT-3'
TSJ489-pST-H3-HA2-5'	5'-TGGTACCTATCTTTGGAGCCATTGCTG-3'
TSJ490-pST-H5-TM less-5'	5'-TGGTACCTATGGAGAAGATTGTGCTGCT-3'
TSJ491-pST-H5-TM less-3'	5'-ACTCGAGTGCCAATGCTCTCCAATT-3'
TSJ492-pST-H5-HA1-3'	5'-ACTCGAGTTCCCCTTTTCTTGCGCCTA-3'
TSJ493-pST-H5-HA2-5'	5'-TGGTACCTCTGTTTGGAGCCATTGCT-3'
TSJ494-pST-H1-TM less-5'	5'-TGGTACCTATGAAGGCTATCCTGGTGG-3'
TSJ495-pST-H1-TM less-3'	5'-CCTCGAGTCAGGATCTGGTAAATCCTGG-3'
TSJ496-pST-H1-HA1-3'	5'-CCTCGAGTTCCCCTGCTCTGGATG-3'
TSJ497-pST-H1-HA2-5'	5'-TGGTACCTCTGTTTGGAGCCATTGCT-3'
TSJ498-pFlu-HA-kpnI M-5'	5-'CCTGTTATATGCATTGGTACCTACAGATGCA GACA-3'
TSJ499-pFlu-HA-kpn IM-3'	5'-TGTCTGCATCTGTAGGTACCAATGCATATAA CAGG-3'
TSJ500-pFlu-HA-XhoI M-5'	5'-TGTCGCCAGTTCACTCGAGCTTTTGGTCTCCC T-3'
TSJ507-H7 TM less 525-3'	5'-CCTCGAGTGATATCGATCACATCCTTGTAGC CAG-3'
TSJ509-pFlu-HA-XhoI M-3'	5'-AGGGAGACCAAAGCTCGAGTGAAGTGGCG ACAGTTGAGTAGA-3'



References

Barrett, D. M., Singh, N., Porter, D. L., Grupp, S. A., and June, C. H. (2014). Chimeric antigen receptor therapy for cancer. *Annual Review of Medicine* 65, 333-347.

Bauer, S., Adrian, N., Fischer, E., Kleber, S., Stenner, F., Wadle, A., Fadle, N., Zoellner, A., Bernhardt, R., Knuth, A., *et al.* (2006). Structure-activity profiles of Ab-derived TNF fusion proteins. *Journal of Immunology (Baltimore, Md : 1950)* 177, 2423-2430.

Bogusław, S., Krystyna, B.-S., and Ewelina, K. (2014). Introduction to molecular biology of influenza A viruses. *Acta Biochimica Polonica* 61, 397-401.

Boulo, S., Akarsu, H., Ruigrok, R. W. H., and Baudin, F. (2007). Nuclear traffic of influenza virus proteins and ribonucleoprotein complexes. *Virus Research* 124, 12-21.

Bouvier, N. M., and Lowen, A. C. (2010). Animal models for influenza virus pathogenesis and transmission. *Viruses* 2, 1530-1563.

Brahmer, J. R., Tykodi, S. S., Chow, L. Q., Hwu, W. J., Topalian, S. L., Hwu, P., Drake, C. G., Camacho, L. H., Kauh, J., Odunsi, K., *et al.* (2012). Safety and activity of anti-PD-L1 antibody in patients with advanced cancer. *The New England Journal of Medicine* 366, 2455-2465.

Braster, R., O'Toole, T., and van Egmond, M. (2014). Myeloid cells as effector cells for monoclonal antibody therapy of cancer. *Methods (San Diego, Calif)* 65, 28-37.

Burton, D. R. (2002). Antibodies, viruses and vaccines. *Nature Reviews Immunology* 2, 706-713.

Chiu, C., and Openshaw, P. J. (2015). Antiviral B cell and T cell immunity in the lungs. *Nature Immunology* 16, 18-26.

Chodorge, M., Züger, S., Stirnimann, C., Briand, C., Jermutus, L., Grütter, M. G., and Minter, R. R. (2012). A series of Fas receptor agonist antibodies that demonstrate an inverse correlation between affinity and potency. *Cell Death and Differentiation* 19, 1187-1195.

Corti, D., Voss, J., Gamblin, S. J., Codoni, G., Macagno, A., Jarrossay, D., Vachieri, S. G., Pinna, D., Minola, A., Vanzetta, F., *et al.* (2011). A neutralizing antibody selected from plasma cells that binds to group 1 and group 2 influenza A hemagglutinins. *Science* 333, 850-856.

Cuesta, Á. M., Sánchez-Martín, D., Sanz, L., Bonet, J., Compte, M., Kremer, L., Blanco,

F. J., Oliva, B., and Álvarez-Vallina, L. (2009). In Vivo Tumor targeting and imaging with engineered trivalent antibody fragments containing collagen-derived sequences. *PLOS ONE* 4, e5381.

Cuesta, Á. M., Sainz-Pastor, N., Bonet, J., Oliva, B., and Álvarez-Vallina, L. (2010). Multivalent antibodies: when design surpasses evolution. *Trends in Biotechnology* 28, 355-362.

Deyev, S. M., Waibel, R., Lebedenko, E. N., Schubiger, A. P., and Pluckthun, A. (2003). Design of multivalent complexes using the barnase*barstar module. *Nature Biotechnology* 21, 1486-1492.

Dolezal, O., Pearce, L. A., Lawrence, L. J., McCoy, A. J., Hudson, P. J., and Kortt, A. A. (2000). ScFv multimers of the anti-neuraminidase antibody NC10: shortening of the linker in single-chain Fv fragment assembled in V(L) to V(H) orientation drives the formation of dimers, trimers, tetramers and higher molecular mass multimers. *Protein Engineering* 13, 565-574.

Domingo, E., and Holland, J. J. (1997). RNA virus mutations and fitness for survival. *Annual Review of Microbiology* 51, 78-151.

Dreyfus, C., Laursen, N. S., Kwaks, T., Zuijdggest, D., Khayat, R., Ekiert, D. C., Lee, J. H., Metlagel, Z., Bujny, M. V., Jongeneelen, M., *et al.* (2012). Highly conserved protective epitopes on influenza B viruses. *Science* 337, 6.

Du, L., Zhao, G., Zhang, X., Liu, Z., Yu, H., Zheng, B. J., Zhou, Y., and Jiang, S. (2010). Development of a safe and convenient neutralization assay for rapid screening of influenza HA-specific neutralizing monoclonal antibodies. *Biochemical and Biophysical Research Communications* 397, 580-585.

Duan, Y., Gu, H., Chen, R., Zhao, Z., Zhang, L., Xing, L., Lai, C., Zhang, P., Li, Z., Zhang, K., *et al.* (2014). Response of mice and ferrets to a monovalent influenza A (H7N9) split vaccine. *PLOS ONE* 9, e99322.

Dunand, C. J., Leon, P. E., Kaur, K., Tan, G. S., Zheng, N. Y., Andrews, S., Huang, M., Qu, X., Huang, Y., Salgado-Ferrer, M., *et al.* (2015). Preexisting human antibodies neutralize recently emerged H7N9 influenza strains. *The Journal of Clinical Investigation*.

Ekiert, D. C., Bhabha, G., Elsliger, M. A., Friesen, R. H., Jongeneelen, M., Throsby, M., Goudsmit, J., and Wilson, I. A. (2009). Antibody recognition of a highly conserved



influenza virus epitope. *Science* 324, 246-251.

Ekiert, D. C., Friesen, R. H., Bhabha, G., Kwaks, T., Jongeneelen, M., Yu, W., Ophorst, C., Cox, F., Korse, H. J., Brandenburg, B., *et al.* (2011). A highly conserved neutralizing epitope on group 2 influenza A viruses. *Science* 333, 7.

Ekiert, D. C., Kashyap, A. K., Steel, J., Rubrum, A., Bhabha, G., Khayat, R., Lee, J. H., Dillon, M. A., O'Neil, R. E., Faynboym, A. M., *et al.* (2012). Cross-neutralization of influenza A viruses mediated by a single antibody loop. *Nature* 489, 526-532.

Fan, C. Y., Huang, C. C., Chiu, W. C., Lai, C. C., Liou, G. G., Li, H. C., and Chou, M. Y. (2008). Production of multivalent protein binders using a self-trimerizing collagen-like peptide scaffold. *FASEB journal : official publication of the Federation of American Societies for Experimental Biology* 22, 3795-3804.

Fouchier, R. A. M., Bestebroer, T. M., Herfst, S., Van Der Kemp, L., Rimmelzwaan, G. F., and Osterhaus, A. D. M. E. (2000). Detection of Influenza A Viruses from Different Species by PCR Amplification of Conserved Sequences in the Matrix Gene. *Journal of Clinical Microbiology* 38, 4096-4101.

Francis, T., Pearson, H. E., Salk, J. E., and Brown, P. N. (1944). Immunity in human subjects artificially infected with influenza virus, type B. *American Journal of Public Health and the Nations Health* 34, 317-334.

Fries, L. F., Smith, G. E., and Glenn, G. M. (2013). A recombinant viruslike particle influenza A (H7N9) vaccine. *The New England Journal of Medicine* 369, 2564-2566.

Friesen, R. H., Lee, P. S., Stoop, E. J., Hoffman, R. M., Ekiert, D. C., Bhabha, G., Yu, W., Juraszek, J., Koudstaal, W., Jongeneelen, M., *et al.* (2014). A common solution to group 2 influenza virus neutralization. *Proceedings of the National Academy of Sciences of the United States of America* 111, 445-450.

Fujii, I. (2004). Antibody affinity maturation by random mutagenesis. in *Antibody Engineering*, B.C. Lo, ed. (Humana Press), pp. 345-359.

Gao, R., Cao, B., Hu, Y., Feng, Z., Wang, D., Hu, W., Chen, J., Jie, Z., Qiu, H., Xu, K., *et al.* (2013). Human infection with a novel avian-origin influenza A (H7N9) virus. *New England Journal of Medicine* 368, 1888-1897.

Goldenberg, D. M., Rossi, E. A., Sharkey, R. M., McBride, W. J., and Chang, C. H. (2008). Multifunctional antibodies by the dock-and-lock method for improved cancer

imaging and therapy by pretargeting. *Journal of Nuclear Medicine* 49, 158-163.

Gould, L. H., Sui, J., Foellmer, H., Oliphant, T., Wang, T., Ledizet, M., Murakami, A., Noonan, K., Lambeth, C., Kar, K., *et al.* (2005). Protective and therapeutic capacity of human single-chain Fv-Fc fusion proteins against West Nile virus. *Journal of Virology* 79, 14606-14613.

Gravel, C., Elmgren, C., Muralidharan, A., Hashem, A. M., Jaentschke, B., Xu, K., Widdison, J., Arnold, K., Farnsworth, A., Rinfret, A., *et al.* (2015). Development and applications of universal H7 subtype-specific antibodies for the analysis of influenza H7N9 vaccines. *Vaccine* 33, 1129-1134.

Guo, Y., Rumschlag-Booms, E., Wang, J., Xiao, H., Yu, J., Wang, J., Guo, L., Gao, G. F., Cao, Y., Caffrey, M., and Rong, L. (2009). Analysis of hemagglutinin-mediated entry tropism of H5N1 avian influenza. *Virology Journal* 6, 39.

Harmsen, M. M., and De Haard, H. J. (2007). Properties, production, and applications of camelid single-domain antibody fragments. *Applied Microbiology and Biotechnology* 77, 13-22.

Hodi, F. S., O'Day, S. J., McDermott, D. F., Weber, R. W., Sosman, J. A., Haanen, J. B., Gonzalez, R., Robert, C., Schadendorf, D., Hassel, J. C., *et al.* (2010). Improved survival with ipilimumab in patients with metastatic melanoma. *The New England Journal of Medicine* 363, 711-723.

Hoffmann, E., Neumann, G., Kawaoka, Y., Hobom, G., and Webster, R. G. (2000). A DNA transfection system for generation of influenza A virus from eight plasmids. *Proceedings of the National Academy of Sciences of the United States of America* 97, 6108-6113.

Holliger, P., Prospero, T., and Winter, G. (1993). "Diabodies": small bivalent and bispecific antibody fragments. *Proceedings of the National Academy of Sciences of the United States of America* 90, 6444-6448.

Hu, S., Shively, L., Raubitschek, A., Sherman, M., Williams, L. E., Wong, J. Y., Shively, J. E., and Wu, A. M. (1996). Minibody: A novel engineered anti-carcinoembryonic antigen antibody fragment (single-chain Fv-CH3) which exhibits rapid, high-level targeting of xenografts. *Cancer Research* 56, 3055-3061.

Hudis, C. A. (2007). Trastuzumab — Mechanism of action and use in clinical practice. *New England Journal of Medicine* 357, 39-51.

Huhlov, A., and Chester, K. A. (2004). Engineered single chain antibody fragments for radioimmunotherapy. *The quarterly journal of nuclear medicine and molecular imaging* : official publication of the Italian Association of Nuclear Medicine (AIMN) [and] the International Association of Radiopharmacology (IAR), [and] Section of the So 48, 279-288.

Hust, M., Jostock, T., Menzel, C., Voedisch, B., Mohr, A., Brenneis, M., Kirsch, M. I., Meier, D., and Dubel, S. (2007). Single chain Fab (scFab) fragment. *BMC Biotechnology* 7, 14.

Kageyama, T., Fujisaki, S., Takashita, E., Xu, H., Yamada, S., Uchida, Y., Neumann, G., Saito, T., Kawaoka, Y., and Tashiro, M. (2013). Genetic analysis of novel avian A(H7N9) influenza viruses isolated from patients in China, February to April 2013. *Euro Surveill.*

Kanegae, Y., Sugita, S., Endo, A., Ishida, M., Senya, S., Osako, K., Nerome, K., and Oya, A. (1990). Evolutionary pattern of the hemagglutinin gene of influenza B viruses isolated in Japan: cocirculating lineages in the same epidemic season. *Journal of Virology* 64, 2860-2865.

Kashyap, A. K., Steel, J., Rubrum, A., Estelles, A., Briante, R., Ilyushina, N. A., Xu, L., Swale, R. E., Faynboym, A. M., Foreman, P. K., *et al.* (2010). Protection from the 2009 H1N1 pandemic influenza by an antibody from combinatorial survivor-based libraries. *PLOS pathogens* 6, e1000990.

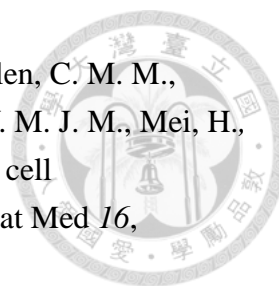
Kenneth, M. (2011). *Janeway's Immunobiology*.

Kipriyanov, S. M., Moldenhauer, G., Schuhmacher, J., Cochlovius, B., Von der Lieth, C. W., Matys, E. R., and Little, M. (1999). Bispecific tandem diabody for tumor therapy with improved antigen binding and pharmacokinetics. *Journal of Molecular Biology* 293, 41-56.

Klasse, P. J., and Sattentau, Q. J. (2002). Occupancy and mechanism in antibody-mediated neutralization of animal viruses. *The Journal of General Virology* 83, 2091-2108.

Kontermann, R. E. (2005). Recombinant bispecific antibodies for cancer therapy. *Acta Pharmacol Sin* 26, 1-9.

Krammer, F., and Palese, P. (2015). Advances in the development of influenza virus vaccines. *Nat Rev Drug Discov* 14, 167-182.



- Kwakkenbos, M. J., Diehl, S. A., Yasuda, E., Bakker, A. Q., van Geelen, C. M. M., Lukens, M. V., van Bleek, G. M., Widjojoatmodjo, M. N., Bogers, W. M. J. M., Mei, H., *et al.* (2010). Generation of stable monoclonal antibody-producing B cell receptor-positive human memory B cells by genetic programming. *Nat Med* *16*, 123-128.
- Lee, E. C., Liang, Q., Ali, H., Bayliss, L., Beasley, A., Bloomfield-Gerdes, T., Bonoli, L., Brown, R., Campbell, J., Carpenter, A., *et al.* (2014). Complete humanization of the mouse immunoglobulin loci enables efficient therapeutic antibody discovery. *Nat Biotech* *32*, 356-363.
- Leung, H.-C., Chan, C. C.-S., Poon, V. K.-M., Zhao, H.-J., Cheung, C.-Y., Ng, F., Huang, J.-D., and Zheng, B.-J. (2015). An H5N1-based matrix protein 2 ectodomain tetrameric peptide vaccine provides cross-protection against lethal infection with H7N9 influenza virus. *Emerging Microbes & Infections* *4*, e22.
- Li, Q., Zhou, L., Zhou, M., Chen, Z., Li, F., Wu, H., Xiang, N., Chen, E., Tang, F., Wang, D., *et al.* (2014). Epidemiology of human infections with avian influenza A(H7N9) virus in China. *The New England Journal of Medicine* *370*, 520-532.
- Li, S. L., Liang, S. J., Guo, N., Wu, A. M., and Fujita-Yamaguchi, Y. (2000). Single-chain antibodies against human insulin-like growth factor I receptor: expression, purification, and effect on tumor growth. *Cancer Immunology, Immunotherapy : CII* *49*, 243-252.
- Lima, A. B., Macedo, L. T., and Sasse, A. D. (2011). Addition of bevacizumab to chemotherapy in advanced non-small cell lung cancer: a systematic review and meta-analysis. *PLOS ONE* *6*, e22681.
- Liu, Y., Paquette, S. G., Zhang, L., Leon, A. J., Liu, W., Xiuming, W., Huang, L., Wu, S., Lin, P., Chen, W., *et al.* (2015). The third wave: H7N9 endemic reassortant viruses and patient clusters. *Journal of Infection in Developing Countries* *9*, 122-127.
- Loregian, A., Mercorelli, B., Nannetti, G., Compagnin, C., and Palu, G. (2014). Antiviral strategies against influenza virus: towards new therapeutic approaches. *Cellular and Molecular Life Sciences : CMLS* *71*, 3659-3683.
- Lu, J., Wu, J., Guan, D., Yi, L., Zeng, X., Zou, L., Liang, L., Ni, H., Zhang, X., Lin, J., and Ke, C. (2014). Genetic changes of reemerged influenza A(H7N9) viruses, China. *Emerging Infectious Diseases* *20*, 1582-1583.

Mallajosyula, V., Citron, M., Ferrara, F., Lu, X., Callahan, C., Heidecker, G. J., Sarma, S. P., Flynn, J. A., Temperton, N. J., Liang, X., and Varadarajan, R. (2014). Influenza hemagglutinin stem-fragment immunogen elicits broadly neutralizing antibodies and confers heterologous protection. *Proceedings of the National Academy of Sciences of the United States of America* *111*, 10.

Mallery, D. L., McEwan, W. A., Bidgood, S. R., Towers, G. J., Johnson, C. M., and James, L. C. (2010). Antibodies mediate intracellular immunity through tripartite motif-containing 21 (TRIM21). *Proceedings of the National Academy of Sciences of the United States of America* *107*, 19985-19990.

Marasco, W. A., and Sui, J. (2007). The growth and potential of human antiviral monoclonal antibody therapeutics. *Nature Biotechnology* *25*, 1421-1434.

Millman, A. J., Havers, F., Iuliano, A. D., Davis, C. T., Sar, B., Sovann, L., Chin, S., Corwin, A. L., Vongphrachanh, P., Douangneun, B., *et al.* (2015). Detecting spread of avian influenza A(H7N9) virus beyond China. *Emerging Infectious Diseases* *21*, 741-749.

Mok, C. K., Lee, H. H., Lestra, M., Nicholls, J. M., Chan, M. C., Sia, S. F., Zhu, H., Poon, L. L., Guan, Y., and Peiris, J. S. (2014). Amino acid substitutions in polymerase basic protein 2 gene contribute to the pathogenicity of the novel A/H7N9 influenza virus in mammalian hosts. *Journal of Virology* *88*, 3568-3576.

Molesti, E., Cattoli, G., Ferrara, F., Böttcher-Friebertshäuser, E., Terregino, C., and Temperton, N. (2013). The production and development of H7 Influenza virus pseudotypes for the study of humoral responses against avian viruses. *Journal of Molecular and Genetic Medicine* *7*, 6.

Pielak, R. M., Schnell, J. R., and Chou, J. J. (2009). Mechanism of drug inhibition and drug resistance of influenza A M2 channel. *Proceedings of the National Academy of Sciences of the United States of America* *106*, 7379-7384.

Rogers, G. N., Paulson, J. C., Daniels, R. S., Skehel, J. J., Wilson, I. A., and Wiley, D. C. (1983). Single amino acid substitutions in influenza haemagglutinin change receptor binding specificity. *Nature* *304*, 76-78.

Roopenian, D. C., and Akilesh, S. (2007). FcRn: the neonatal Fc receptor comes of age. *Nature Reviews Immunology* *7*, 715-725.

Rowe, T., Abernathy, R. A., Hu-Primmer, J., Thompson, W. W., Lu, X., Lim, W.,

Fukuda, K., Cox, N. J., and Katz, J. M. (1999). Detection of antibody to avian influenza A (H5N1) virus in human serum by using a combination of serologic assays. *Journal of Clinical Microbiology* 37, 937-943.

Rumschlag-Booms, E., and Rong, L. (2013). Influenza a virus entry: implications in virulence and future therapeutics. *Advances in Virology* 2013, 121924.

Sanz, L., Blanco, B., and Álvarez-Vallina, L. (2004). Antibodies and gene therapy: teaching old 'magic bullets' new tricks. *Trends in Immunology* 25, 85-91.

Schoonjans, R., Willems, A., Schoonooghe, S., Fiers, W., Grooten, J., and Mertens, N. (2000). Fab chains as an efficient heterodimerization scaffold for the production of recombinant bispecific and trispecific antibody derivatives. *Journal of Immunology (Baltimore, Md : 1950)* 165, 7050-7057.

Shi, J., Deng, G., Liu, P., Zhou, J., Guan, L., Li, W., Li, X., Guo, J., Wang, G., Fan, J., *et al.* (2013). Isolation and characterization of H7N9 viruses from live poultry markets - Implication of the source of current H7N9 infection in humans. *Chinese Science Bulletin*.

Smith, J. H., Nagy, T., Barber, J., Brooks, P., Tompkins, S. M., and Tripp, R. A. (2011). Aerosol inoculation with a sub-lethal influenza virus leads to exacerbated morbidity and pulmonary disease pathogenesis. *Viral Immunology* 24, 131-142.

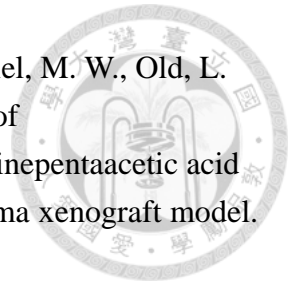
Smith, K., Garman, L., Wrammert, J., Zheng, N. Y., Capra, J. D., Ahmed, R., and Wilson, P. C. (2009). Rapid generation of fully human monoclonal antibodies specific to a vaccinating antigen. *Nature Protocols* 4, 372-384.

Smith, S. A., Zhou, Y., Olivarez, N. P., Broadwater, A. H., de Silva, A. M., and Crowe, J. E., Jr. (2012). Persistence of circulating memory B cell clones with potential for dengue virus disease enhancement for decades following infection. *Journal of Virology* 86, 2665-2675.

Subbarao, K., and Joseph, T. (2007). Scientific barriers to developing vaccines against avian influenza viruses. *Nature Reviews Immunology* 7, 267-278.

Sui, J., Hwang, W. C., Perez, S., Wei, G., Aird, D., Chen, L.-m., Santelli, E., Stec, B., Cadwell, G., Ali, M., *et al.* (2009). Structural and functional bases for broad-spectrum neutralization of avian and human influenza A viruses. *Nature Structural & Molecular Biology* 16, 265-273.

Tahtis, K., Lee, F.-T., Smyth, F. E., Power, B. E., Renner, C., Brechbiel, M. W., Old, L. J., Hudson, P. J., and Scott, A. M. (2001). Biodistribution properties of ¹¹¹Indium-labeled C-functionalized trans-cyclohexyl diethylenetriaminepentaacetic acid humanized 3S193 diabody and F(ab')₂ constructs in a breast carcinoma xenograft model. *Clinical Cancer Research* 7, 1061-1072.



Topp, M. S., Gokbuget, N., Stein, A. S., Zugmaier, G., O'Brien, S., Bargou, R. C., Dombret, H., Fielding, A. K., Heffner, L., Larson, R. A., *et al.* (2015). Safety and activity of blinatumomab for adult patients with relapsed or refractory B-precursor acute lymphoblastic leukaemia: a multicentre, single-arm, phase 2 study. *The Lancet Oncology* 16, 57-66.

Traggiai, E., Becker, S., Subbarao, K., Kolesnikova, L., Uematsu, Y., Gismondo, M. R., Murphy, B. R., Rappuoli, R., and Lanzavecchia, A. (2004). An efficient method to make human monoclonal antibodies from memory B cells: potent neutralization of SARS coronavirus. *Nat Med* 10, 871-875.

Wang, X., Katayama, A., Wang, Y., Yu, L., Favoino, E., Sakakura, K., Favole, A., Tsuchikawa, T., Silver, S., Watkins, S. C., *et al.* (2011). Functional characterization of an scFv-Fc antibody that immunotherapeutically targets the common cancer cell surface proteoglycan CSPG4. *Cancer Research* 71, 7410-7422.

Wu, Y., Bi, Y., Vavricka, C. J., Sun, X., Zhang, Y., Gao, F., Zhao, M., Xiao, H., Qin, C., He, J., *et al.* (2013). Characterization of two distinct neuraminidases from avian-origin human-infecting H7N9 influenza viruses. *Cell Res* 23, 1347-1355.

Wu, Y., Wu, Y., Tefsen, B., Shi, Y., and Gao, G. F. (2014). Bat-derived influenza-like viruses H17N10 and H18N11. *Trends in Microbiology* 22, 183-191.

Yen, H. L., Zhou, J., Choy, K. T., Sia, S. F., Teng, O., Ng, I. H., Fang, V. J., Hu, Y., Wang, W., Cowling, B. J., *et al.* (2014). The R292K mutation that confers resistance to neuraminidase inhibitors leads to competitive fitness loss of A/Shanghai/1/2013 (H7N9) influenza virus in ferrets. *The Journal of Infectious Diseases* 210, 1900-1908.

Zhirnov, O. P., Klenk, H. D., and Wright, P. F. (2011). Aprotinin and similar protease inhibitors as drugs against influenza. *Antiviral Research* 92, 27-36.